Assessing Spatial and Temporal Variation in Source Water Quality and Drinking Water Treatability Across a Gradient of Forest Harvest on Vancouver Island, BC

by

Alyssa Kathleen Bourgeois

A thesis submitted in partial fulfillment of the requirements for the degree of

Master of Science

in

Ecology

Department of Biological Sciences

University of Alberta

ABSTRACT

On Canada's Pacific Coast, forestry is integral to society. Although economically important, harvesting practices may alter source waters that originate in forested watersheds through changes in suspended solids (SS) and dissolved organic matter (DOM). Each of these metrics has the potential to degrade source water quality, which poses challenges for drinking water treatment. While harvest impacts on source waters are generally well understood, effects differ regionally due to variations in climate, topography, and soil characteristics. Research is therefore needed across different ecozones, and until now, few studies have focused on the Pacific Maritime. Within this ecozone, one question that remains is how the magnitude of change caused by recent forest harvest compares to the background spatiotemporal variation in source water quality, and how this impacts drinking water treatability. To assess these effects, I examined variation in stream water SS and DOM across different flow conditions in forested subwatersheds with contrasting forest harvest histories and diverse characteristics (e.g., topography, soil depth and clay content). This work was done on the east coast of Vancouver Island, British Columbia, in the Comox Lake watershed. Subwatersheds ranged greatly in size (0.21–214.08 km^2) and mean elevation (371–1366 m above sea level). Total annual precipitation in the watershed averaged 2193 mm yr^{-1} between 1981 and 2019. Streams were sampled from April 2019 to March 2020 across synoptic (thirty sites sampled four times), seasonal (ten sites sampled ten times), and storm (four sites; two storm events captured) sampling campaigns. Synoptic and seasonal sampling were conducted during stable baseflow conditions, while storm sampling targeted peak flows. Samples were analyzed for turbidity, total SS, DOM carbon concentration (DOM-[C]), and DOM composition to evaluate source water quality, as well as disinfection by-product formation potentials (DBP-FPs) to infer drinking water treatability. Targeted water quality monitoring revealed that recent forest harvest did not overwhelm

the background spatiotemporal variation of SS and DOM in a recovering landscape. Instead, storm event and seasonal changes in hydrology were the primary control on water quality (i.e., SS and DOM) and resultant DBP-FPs: each exhibited a greater change with seasonal and storm flows than across spatially distinct subwatersheds. This highlights that temporal (i.e., hydrologic) factors, rather than spatial ones (i.e., forest harvest and catchment characteristics), were key in driving variation in water quality and treatability. Temporally-driven changes in SS, DOM, and DBP-FPs were not amplified by forest harvest, which suggests weak anthropogenic influences on source waters in the region. Here, a muted response to recent harvesting may be attributed to forestry practices (i.e., slash removal) and the prevalence of second growth forests (i.e., historical harvest in this region). Although responses were subdued, water quality and treatability metrics did vary according to harvested area in the Comox Lake watershed; this highlights the necessity of evaluating the relative importance of forest harvest and flow conditions when assessing source waters. Overall, this study contributes to our understanding of spatiotemporal effects on SS, DOM, and DBP-FPs in forested Pacific Coast subwatersheds.

PREFACE

This thesis is the original work of Alyssa Kathleen Bourgeois. It is structured into four chapters: Chapter 1 provides a general introduction into the field of research and study region and briefly outlines research objectives, hypotheses, and significance; Chapters 2 and 3 are manuscripts that will be submitted for publication in the scientific literature (cited as below); and Chapter 4 offers general conclusions drawn from this research as well as future research directions.

The research presented in this thesis was a collaborative effort between Alyssa Bourgeois, Dr. Bill Floyd (Vancouver Island University), Drs. Suzanne Tank and David Olefeldt (University of Alberta), and Drs. Monica Emelko and Fariba Amiri (University of Waterloo). Given these collaborations, this thesis is written in the plural. Alyssa Bourgeois wrote the introductory and concluding chapters of this thesis, and was responsible for study design development, sample collection, data analysis, and manuscript composition for Chapters 2 and 3. Drs. Tank and Floyd oversaw this research, providing revisions on all thesis chapters and advice on storyline ideas, study design, and data analysis for Chapters 2 and 3. Dr. Olefeldt offered manuscript suggestions and guidance on study site selection for Chapter 2. Drs. Emelko and Amiri contributed manuscript comments and data analysis recommendations for Chapter 3.

Chapter 2

Bourgeois, A. K., Tank, S. E., Floyd, W. C., and Olefeldt, D. Spatial and seasonal dynamics of stream water quality in forested watersheds on Canada's Pacific Coast. In preparation for submission to *Journal of Geophysical Research: Biogeosciences*.

Chapter 3

Bourgeois, A. K., Tank, S. E., Floyd, W. C., Emelko, M. B., and Amiri, F. Hydrology overwhelms harvest history and landscape variation to control water quality and disinfection by-product formation potentials in forested Pacific Coast watersheds. In preparation for submission to *Environmental Science & Technology Water*.

ACKNOWLEDGMENTS

First and foremost, I would like to thank my supervisors, Drs. Suzanne Tank and Bill Floyd, for guiding me through my Master's research. Their continuous support, advice, and encouragement have not only elevated the caliber of my research, but have also nurtured my growth as a scientist. I am especially grateful to Suzanne, for inspiring me and exemplifying what a great scientist (and person) should be. I would also like to thank the final member of my committee, Dr. David Olefeldt, for his invaluable expertise provided at every stage of my degree, as well as Drs. Monica Emelko and Fariba Amiri for their insightful manuscript suggestions. Each of these scientists have enhanced my research skills and overall academic experience, and I am fortunate to have learned from them.

A special thank you to Sheetal Patel, whose assistance in the field and lab greatly enriched my Master's experience. Her good humour, quick wit, and entertaining stories were always appreciated. I also sincerely thank Dr. Chuck Bulmer for his guidance on calculating soil clay contents, as well as Zoe Norcross-Nu'u for introducing me to the area and sending me many water samples at my request. My gratitude also extends to Mosaic Forest Management Corp. for granting us land access, and the forWater Network, University of Alberta, and Government of Alberta for their financial support that made this research possible.

I am privileged to be a part of two lab groups that have been integral to my success over the past two years. An immense thank you to Emily Barrie, Sydney Huculak, Ryan Hutchins, Nikki van Klaveran, Joanna Li Yung Lung, Erin MacDonald, and Sarah Shakil at the University of Alberta for all of their methodological, statistical, and dating advice, and to Alison Bishop, Stewart Butler, and Alex Cebulski in the Coastal Hydrology Research Lab for their field assistance, programming expertise, and GIS knowledge. I am especially thankful to Emily for all of her help with statistics and continued friendship throughout my Master's degree.

My success would not have been possible without the unwavering support of my parents, Danielle and Gerry. I cannot thank them enough for everything that they have done for me. I would also like to thank my sister, Brooklyn, for acting as my sounding board and assisting me with syntax, as well as my other family and friends who have been there for me throughout this experience. Thank you all for believing in me. Last but certainly not least, I would like to thank my partner, Brendan, for his unconditional support (and for treating me to many desserts). Brendan, this journey was much more enjoyable with you by my side.

TABLE OF CONTENTS

LIST OF TABLES

LIST OF FIGURES

CH1: General Introduction

1.1 Drinking water source quality and treatability in forested watersheds

1.1.1 Water sourced from forested watersheds and drinking water treatment

Forested watersheds are critical sources of water supply. In healthy forest ecosystems, high quality stream water is produced through riparian processes that regulate stream sedimentation, organic matter transport, and peak flows (Berkowitz et al., 2014, Gartner et al., 2014). Maintaining source water quality in forested watersheds is important because two thirds of Canadian communities rely on forested catchments for their drinking water supplies (Natural Resources Canada, 2020b). While drinking water sources are typically high in quality across Canada (McKitrick et al., 2018), there has been a recent increase in water quality issues resulting from a range of forest disturbances (e.g., harvesting, wildfire, pests), climate change, and acid precipitation (Natural Resources Canada, 2020a). Each of these factors may diminish stream functioning (Erdogan et al., 2018), which in turn causes increasingly variable or degraded source water quality. This not only complicates water treatment processes, but also results in additional treatment and chemical costs (Chowdhury, 2018).

In Canada, drinking water is regarded as safe for human consumption if certain microbiological, chemical, and physical parameters are below designated limits (Health Canada, 2020). Each of these thresholds were established to reduce constituents that pose health risks, prevent diseases caused by harmful pathogens, and mitigate taste and odour issues (Delpla and Rodriguez, 2017, Richardson and Ternes, 2018). In order to meet drinking water quality guidelines, source waters often require treatment. Typically, conventional water treatment involves coagulation, flocculation, sedimentation, and filtration processes to remove solids and organics, with disinfection taking place thereafter (e.g., Emelko et al., 2011). Although providers continually monitor source waters to ensure appropriate water treatment, a plant's capacity may be overwhelmed by highly variable source water quality during extreme weather events (Emelko et al., 2011). It is therefore essential to investigate variation in source water quality, and how it relates to drinking water treatability for both current and future facilities.

1.1.2 Suspended solids and dissolved organic matter in drinking water sources

Drinking water sources naturally contain suspended solids (SS) and dissolved organic matter (DOM). While both are imperative in determining source water quality (e.g., Mbonimpa

et al., 2014, Warner and Saros, 2019), DOM is a particularly important water quality indicator because of its ability to have compositional variability. Through its composition, DOM provides information about potential source characteristics and reveals which DOM pools dominate in stream water (Hansen et al., 2016, Hood et al., 2006). Generally, streams in forested watersheds contain allochthonous, terrestrial DOM (Hood et al., 2006), although different DOM pools may arise depending on (1) levels of organic matter processing (e.g., microbial decay) and reactivity (Stubbins et al., 2010) and (2) dominant flow paths (e.g., between shallow and deeper groundwater sources) (Jacobs et al., 2017).

Given that SS and DOM are common in almost all source waters (Roberts and Inniss, 2014), each are of concern to drinking water utilities. Increases in SS, as indicated by turbidity or total SS (TSS), reduces the effectiveness of chlorination and ultraviolet irradiation (Weiler et al., 2010) and may cause boil water advisories in municipalities with unfiltered supplies (Barraclough et al., 2016). At the same time, increases in DOM carbon concentration (DOM-[C]), and especially DOM with a more aromatic composition (Chow et al., 2011, Delpla and Rodriguez, 2017), may result in higher disinfection by-product formation potentials (DBP-FPs) (Li et al., 2014). Some DBPs, including trihalomethanes (THMs) and haloacetic acids (HAAs), are produced through the reaction of DOM with chlorine disinfectants (Gonsier et al., 2014). At very high levels, these DBPs can have significant effects on human health including an increased risk of cancer, miscarriage, and birth defects (Richardson and Ternes, 2018). However, causal drinking water-related cancer risks from these DBPs remain uncertain, and are likely small when compared to other common environmental factors (Cotruvo and Amato, 2019, Hrudey, 2008). In practice, while it is globally recognized that the risks of inadequate disinfection far outweigh the risks created by DBPs, DBPs in treated drinking water are managed and regulated using a sensible, precautionary approach that contributes to overall water quality management (Cotruvo and Amato, 2019, Hrudey, 2008).

1.1.3 Catchment characteristics, forest harvest, and seasonal and storm event hydrology

Considering the importance of forested drinking water sources, many studies have independently examined the effects of catchment characteristics (e.g., Mzobe et al., 2020), forest harvest (e.g., Erdozain et al., 2018), and seasonal and storm event hydrology (e.g., Fellman et al., 2020, Parr et al., 2019) on source water quality. For example, prior research has found

considerable variation in source water SS and DOM based on naturally occurring catchment characteristics, including topography, soil type and depth, and forest cover (e.g., Awad et al., 2018, Coynel et al., 2005, Fellman et al., 2016, Mbonimpa et al., 2014). Broad gradients in each of these characteristics occur along the Pacific coast, and this variation may partly explain why some dominate in different watersheds. For instance, Fellmann et al. (2016) found catchment slope, elevation, size, and topographic wetness to be important characteristics driving water quality, while Oliver et al. (2017) suggested that wetland extent, catchment slope, soil depth, and lake presence were primary drivers. The diverse suite of catchment characteristics that may affect water quality, coupled with their broad variation across landscapes, underscores the need for communities to identify important local characteristics affecting the quality of their drinking water sources.

In addition to the effects of natural catchment variability, anthropogenic modification via forestry practices may also impact source water quality (e.g., Dai et al., 2001, Erdogan et al., 2018, Schelker et al., 2012). For instance, Erdozain et al. (2018) found elevated TSS, increased DOM-[C], and more humic DOM in subwatersheds with higher harvest intensities in temperate mixed forests. While these findings indicate that water quality deteriorates with increased forest harvest, other studies have shown improved or no change in water quality within temperate coniferous and boreal forests (e.g., Chow et al., 2011, Schelker et al., 2014). Evidently, water quality responses to forestry practices are varied across different landscape types, and may differ within ecozones such as the Pacific Maritime (e.g., Fellman et al., 2016, McSorley, 2020, Oliver et al., 2017). Temperate coniferous forests in this region with extensive clearcutting (Canadian Council of Forest Ministers, 2015, Hansen et al., 2013) may experience deteriorated source water quality through increases in soil erosion and leaching from woody debris and decomposed logs (e.g., Dai et al., 2001, Jordan, 2006); additional research is therefore needed in the Pacific Maritime to advance our understanding of forestry consequences on water sources.

Along with catchment characteristics and forest harvest, watershed hydrology also influences source water quality. Previous studies have documented variation in SS and DOM with changes in seasonal flow (Coch et al., 2020, Parr et al., 2019) and storm flow across individual events (Delpla and Rodriguez, 2017, Fellman et al., 2020). Although hydrology is often a key parameter modulating water quality, the extent of its influence depends on subwatershed connectivity (Parr et al., 2019), which is controlled by antecedent moisture

(Winkler et al., 2010). Saturated areas (e.g., saturated soil patches) typically generate lateral flow only if they are hydrologically connected to streams within a catchment (Levia et al., 2011); once hydrologic connectivity is achieved, newly activated flow paths can link disconnected sediment sources or DOM pools to the stream network (Dawson et al., 2008). Given that Canada's Pacific Coast is characterized by high to very high precipitation (Wang et al., 2016), this region provides an opportunity to investigate how hydrologic connectivity and associated changes in flow influence source water quality.

Although variation in water quality is governed by individual catchment characteristics, their modification by disturbances such as forest harvest, and seasonal and storm event hydrology, the relative importance of each of these factors is unknown. It is therefore critical to examine the impacts of current harvesting practices in conjunction with natural spatiotemporal attributes. While the effects of forest harvest (Levia et al., 2011) and natural spatiotemporal variation (Kreutzweiser et al., 2008) on source water quality have been well studied, most of this research has focused on discrete watersheds with specific characteristics. As a result, findings are not transferable to other catchments of interest, such as the Comox Lake watershed.

1.2 Source water considerations in the Comox Lake watershed

Comox Lake is the primary water supply for 45,000 residents in the Comox Valley Regional District (CVRD) (Comox Valley Regional District, 2016c). Along with providing drinking water to nearby communities, the lake is also used for recreational activities (e.g., swimming, boating, fishing), regulated for hydro-electric power, and represents important fish habitat (Comox Valley Regional District, 2016a). The health of Comox Lake depends on the surrounding watershed, the majority (67%) of which is privately-owned by forestry companies (Barraclough et al., 2016). The remainder of the watershed falls within a Class A Provincial Park (31%) or consists of municipal lands (2%) (Barraclough et al., 2016). Both anthropogenic activities and natural catchment characteristics affect stream waters draining into Comox Lake, which highlights the necessity for source water protection in the CVRD.

Ensuring safe, high-quality drinking water requires both the protection of the Comox Lake watershed, and the effective treatment of lake water. Presently, drinking water in the Comox Valley is unfiltered and only chlorinated before distribution to residents (Comox Valley Regional District, 2019a), although a new filtration plant that includes ultraviolet irradiation and

chlorination will soon be operational (Comox Valley Regional District, 2019b). This plant will help mitigate the risk of pathogens in drinking water while also reducing the frequency of turbidity-related boil water notices (Comox Valley Regional District, 2019a). According to the CVRD, turbidity is the main concern of drinking water authorities because this metric often does not meet provincial surface water treatment guidelines (Government of British Columbia, 2012) and thus results in recurrent multi-day boil water advisories. These advisories are typically caused by erosion of silty clay streambanks in the Perserverance subwatershed (Comox Valley Regional District, 2019a), but may also result from high-intensity harvesting (Erdogan et al., 2018) or the development of unpaved resource roads (Reid et al., 2016, van Meerveld et al., 2014), both of which increase sediment supply to streams. In order to provide safe drinking water, the CVRD continuously monitors and tests water for a suite of parameters (e.g., turbidity, pH, *E. coli*) throughout the water treatment process (Comox Valley Regional District, 2016c).

1.3 Research rationale, objectives, and hypotheses

The Comox Lake watershed has an extensive history of forest harvest, diverse landscape attributes, and experiences generally high precipitation as both rain and snow. These factors provide a valuable opportunity to compare stream water across a range of flow conditions in forested subwatersheds with varying harvest intensities and catchment characteristics. This work was designed to provide insight into how forest harvesting and background spatiotemporal variation impact source water quality (i.e., SS and DOM) and drinking water treatability (i.e., DBP-FPs) in a recovering landscape.

This thesis is formatted as two manuscript-style chapters with appendices. The first of these manuscripts (Chapter 2) assesses seasonal variation and identifies dominant spatial factors driving variation in stream water quality across subwatershed sites. The research objectives for Chapter 2 are to: (1) evaluate the impacts of seasonality and spatial variation in natural catchment characteristics on stream water quality; and (2) investigate forest harvesting effects on water quality across seasons and landscapes with diverse catchment characteristics. I hypothesized that: (1) stream water quality will exhibit natural spatiotemporal variation controlled by seasonality and catchment characteristics (e.g., topography, soil depth and clay content, forest cover); and (2) forest harvesting will overwhelm this background spatiotemporal variation. The second manuscript (Chapter 3) undertakes an in-depth look at four subwatershed

sites with differing harvest intensities to compare water quality and resultant DBP-FPs across storm event and stable baseflow conditions. The research objectives for Chapter 3 are to: (1) isolate leading DOM drivers of DBP-FPs; (2) examine how water quality and DBP-FPs vary between baseflow and stormflow; and (3) assess the joint influence of storm events and forest harvest on water quality and DBP-FPs. I hypothesized that: (1) DOM-[C] is the best predictor of DBP-FPs; (2) water quality will deteriorate (and result in higher DBP-FPs) in stormflow relative to baseflow; and (3) forest harvest will amplify the effects of storm events on water quality.

1.4 Significance

This research parses the effects of forestry, catchment characteristics, and hydrology to determine whether recent forest harvest in a recovering landscape overwhelms the background variability of SS and DOM, and how this affects water treatment. Knowledge gained through this study may enable practitioners in the CVRD to (1) establish forest management practices that ensure source water protection, and (2) develop water treatment strategies that ensure appropriate responses from utilities to changes in water quality. It is critical to implement these plans to effectively manage and protect community drinking water sources; improvements to forestry and water treatment practices may ameliorate water quality issues (Baillie and Neary, 2015, Gartner et al., 2014), which will positively impact communities dependent on forested landscapes for their water supplies. Since this research is taking place in collaboration with the CVRD drinking water authority, our findings have the potential to inform decision making and increase the efficiency of drinking water treatment, both of which will help ensure consistent, high quality drinking water in the Comox Lake watershed in future years.

CH2: Spatial and seasonal dynamics of stream water quality in forested watersheds on Canada's Pacific Coast

2.1 Introduction

Clean water sources are essential for societies and ecosystems worldwide. Typically, intact forest landscapes produce clean, high quality source waters through riparian processes that filter water and regulate suspended solids and organic matter transport (Berkowitz et al., 2014, Gartner et al., 2014). If these processes are diminished, degradation of source water quality can occur. This issue is particularly pertinent in British Columbia, as 86% of the population relies on source waters that originate in forested watersheds for their drinking water supplies (Government of British Columbia, 1996). Source waters across the province are generally high in quality (Pike et al., 2010), but may deteriorate if forestry practices alter hydrological flow paths and thus organic matter export and sediment load (Berkowitz et al., 2014, Erdogan et al., 2018). Considering the potential of forest harvest to impact hydrologic flow paths, the availability of organic matter, and sediment generation (e.g., Kreutzweiser et al., 2008, Reid et al., 2016, Tremblay et al., 2009), British Columbian communities are developing source water protection plans that emphasize the importance of maintaining high quality water sources (e.g., Barraclough et al., 2016).

Although there are many indicators of water quality, suspended solids (SS; i.e., turbidity and total suspended solids) and dissolved organic matter (DOM) are of key concern because they pose risks to drinking water treatability (e.g., Emelko et al., 2011, Ritson et al., 2014). Given that turbidity and DOM can change rapidly in source waters, both challenge water treatment: at high levels, turbidity interferes with drinking water disinfection (Chang et al., 1983, Pike et al., 2010, Weiler et al., 2010) while DOM enables the formation of possibly carcinogenic disinfection by-products (Delpla and Rodriguez, 2017, Li et al., 2014, Richardson and Ternes, 2018). Drinking water authorities are especially interested in DOM because of its ubiquity in source waters and role as a unique biogeochemical tracer (Fellman et al., 2010, Roberts and Inniss, 2014), which allows DOM compositional metrics to track the contribution of terrestrial and microbial pools to streamflow and also elucidate the chemical characteristics of each source (Hansen et al., 2016, Hood et al., 2006). While each of turbidity, DOM carbon concentration (DOM-[C]), and DOM composition directly affect water quality and hence treatability (Awad et al., 2018, Nkambule et al., 2011, Zhai et al., 2017), other metrics such as conductivity, cations (e.g., Ca^{2+}, Mg^{2+}), and

stable water isotopes (e.g., $\delta^{18}O$) provide insight into hydrological flow paths and water sources (Csank et al., 2019, Vidon et al., 2008), which indirectly impact water quality. It is therefore crucial to consider indicators of hydrology in addition to measures of water quality to thoroughly evaluate water sources.

Over recent decades, the desire for sustainable and effective management of catchment drinking water sources has prompted investigations into how the composition of surrounding watersheds impacts source water quality and treatability (e.g., Awad et al., 2018, Emelko et al., 2011). Numerous studies have found considerable variation in source water turbidity, DOM-[C], and DOM composition based on watershed area, geology, topography, soil type and depth, and forest cover (e.g., Fellman et al., 2016, McSorley, 2020, and Oliver et al., 2017 from the Pacific coast of North America). Universally-important catchment characteristics have been unidentifiable, however, because different watersheds have distinct landscape features that determine local source water quality. Superimposed on the effects of natural landscape variability, land disturbance via forest harvest may also fundamentally alter source water quality: while some studies have reported increased turbidity, DOM-[C], and more aromatic, high molecular weight DOM with forest harvesting (e.g., Berkowitz et al., 2014, Erdogan et al., 2018), other research has reported an opposite pattern or no effect (e.g., Chow et al., 2011, Schelker et al., 2014). As a result, there is a need for additional research that identifies linkages between landscape attributes and water quality indicators in diverse ecozones.

In addition to landscape attributes, source water quality is also affected by seasonal shifts in watershed hydrology (e.g., water table depth, catchment connectivity) and climate (e.g., temperature) (Jacobs et al., 2017, Oliver et al., 2017, Schelker et al., 2012). While climate regulates the seasonal production and availability of DOM (Chow et al., 2011, Oliver et al., 2017), hydrology controls turbidity, DOM-[C] export, and the extent of DOM source pools that are available for active transport to surface water networks (Coch et al., 2020, Parr et al., 2019). Due to the diverse hydroclimatic regimes that occur even within temperate biomes (e.g., Ohte and Tokuchi, 2011), seasonal effects on source water quality differ regionally. Research is therefore required to reveal the impacts of seasonal (i.e., hydroclimatic) conditions on turbidity, DOM-[C], and DOM composition within the Pacific Maritime (Erdogan et al., 2018). Examining seasonality in this ecozone may also augment our understanding of the role that catchment characteristics and forest harvest play in modulating source water quality (Jacobs et al., 2017).

In Canada, forested watersheds have been extensively clearcut through commercial logging practices (Canadian Council of Forest Ministers, 2015, Hansen et al., 2013). Past and contemporary harvesting both influence ecological processes that occur today, and this subsequently affects source water quality (Barraclough et al., 2016). While these connections have been noted in various ecozones across the country (e.g., Erdozain et al., 2018, Tremblay et al., 2009), results are not readily applicable to watersheds within temperate, high precipitation zones such as the Pacific Maritime. We therefore conducted our own investigation within the Comox Lake watershed, where local municipalities struggle with water quality issues (Comox Valley Regional District, 2019a) that may stem from current forestry practices. Due to widespread forest harvest, the Comox Lake watershed may experience degraded source water quality through changes in turbidity, DOM-[C], and DOM composition. Quantifying these shifts is pertinent to understanding regional forest harvest impacts on source waters.

Despite documented effects of forestry on source waters (e.g., Dai et al., 2001, Erdozain et al., 2018, Jordan, 2006, Schelker et al., 2012), it is unknown if recent forest harvesting overwhelms the background spatial and seasonal variation of stream water quality in recovering landscapes on Canada's Pacific Coast. Within this ecozone, research tends to focus on specific watersheds (e.g., McSorley, 2020, Mistick and Johnson, 2020). The applicability of these findings to other watersheds is limited because high variation exists among catchments. As a result, this prompted us to investigate source waters within the Comox Lake watershed. The first objective of this study was to uncover the effects of seasonality and natural catchment characteristics on stream water quality, using turbidity, DOM-[C] and DOM composition as water quality metrics. Superimposed on this, our second objective was to investigate the impact of forest harvest on water quality metrics across seasons and landscapes with diverse catchment characteristics. Ultimately, this research will: (1) identify important factors driving variation in stream water quality; and (2) reveal the effect of forestry on water quality in a watershed with similar characteristics to many other temperate coastal regions, where drinking water is sourced.

2.2 Methods

2.2.1 Study region

Situated on the east coast of Vancouver Island, the Comox Lake watershed (49°36'N, 125°10'W) is the main drinking water supply for 45,000 residents in the Comox Valley Regional

District (CVRD) (Comox Valley Regional District, 2016c) (Figure 2-1). All study sites (further described in section 2.2.2) are sub-basins within the Comox Lake watershed (461 km^2). Six main tributary streams drain 76% of the total watershed area; the largest tributary of Comox Lake, the Cruikshank River, drains 46% (214 km^2) (Comox Valley Regional District, 2016a). The lake itself is comprised of a single basin with a surface area of 21 km^2 and lies at an elevation of 136 m (Comox Valley Regional District, 2016b). Across the watershed, elevation ranges from 136 m to 2034 m, with a mean of 778 m (Figure 2-1B). The Comox, Moving, and Cliffe glaciers lie at high elevations (> 1300 m) in the western reaches of the watershed, covering an area of 3.8 km^2 (Schnorbus, 2018).

The hydroclimatic regime of the Comox Lake watershed is nival dominated hybrid to pluvial: rain is the primary driver of high flows in late autumn and early winter, and a spring freshet is associated with snowmelt from the western-most, higher elevation subwatersheds (W. C. Floyd, BC Ministry of Forests, Lands, Natural Resource Operations and Rural Development, personal communication, 7 July 2020). The watershed is classified as having a Mediterranean climate, with cool to warm summers and mild, wet winters (Beck et al., 2018). From 1981 to 2019, the mean annual temperature was 9.4ºC and total annual precipitation averaged 2193 mm yr^{-1} (Wang et al., 2016). Most precipitation (82%) occurs from 1 October to 31 March (1981–2019; Wang et al., 2016), resulting in increased stream flows through autumn and winter. We defined this as the "wet" period (see also Oliver et al., 2017). In spring (1 April to 30 June), stream flows increase with snowmelt in some subwatersheds and decline in others due to limited snow inputs. Regardless of this, all streams decrease in flow throughout summer (1 July to 30 September), with some streams becoming dry in late summer (Comox Valley Regional District, 2016a). We demarcated spring and summer as the "dry" period (Figure 2-2).

The Comox Lake watershed lies within coastal western hemlock, mountain hemlock, and coastal mountain-heather alpine biogeoclimatic zones (MacKinnon et al., 1992), and is characterized by steep terrain, shallow soils, and coniferous forest (Valentine, 1978). Soils are predominately well drained humo-ferric podzols and tree species primarily consist of Douglas fir (*Pseudotsuga menziesii*), western hemlock (*Tsuga heterophylla*), western redcedar (*Thuja plicata*), and mountain hemlock (*Tsuga mertensiana*) (Government of British Columbia, 2003, MacKinnon et al., 1992, Valentine, 1978). The watershed is also underlain by Cretaceous

sedimentary bedrock that has partly eroded to expose underlying amygdaloidal and pillow basalts formed during the Triassic period (Muller et al., 1965, Natural Resources Canada, 1957).

Land in the Comox Lake watershed is used for both recreational and industrial purposes (i.e., power generation and timber harvesting) (Barraclough et al., 2016, Epps, 2011). The Comox Lake and surrounding area is a popular recreational site with boating, swimming, camping, hunting, mountain biking, and hiking among other activities, many of which contribute to the local economy (Barraclough et al., 2016, Epps, 2011). Although a natural lake, the Comox outlet is regulated for hydro-electric power by BC Hydro (Comox Valley Regional District, 2019a). BC Hydro manages and operates the Comox Lake Dam and Puntledge River Diversion Dam; both were constructed in 1912 along with a powerhouse and penstocks to regulate flow (Barraclough et al., 2016, BC Hydro, 2020). In addition to use for power generation and as a drinking water source, the Comox Lake watershed is also extensively harvested. Two thirds of the watershed is privately managed with commercial logging (Barraclough et al., 2016) (Figure 2-1A and Table A1-1). Native old growth forest has been actively logged since 1888, resulting in clearcut areas extending throughout the watershed (Barraclough et al., 2016). A second pass of forest harvesting has been underway since the 1980s; presently, both mature second growth and old growth forests are harvested for timber. As a result, most forests on private land are currently second or third growth forest (< 250 years, median age: 47 years) (P. Jorgenson, Mosaic Forest Management Corp., personal communication, 8 December 2020). The other third of the watershed is comprised of municipal land holdings, privately owned lands, crown provincial land, and provincial parkland (Figure 2-1A and Table A1-1). The latter two land uses represent protected areas and cover 31.2% of the Comox Lake watershed. Protected areas mainly encompass old growth forest landscapes (> 250 years) along the western ridge of the watershed (Fong, 2019), although there are alpine and other non-forested areas such as high elevation bogs also in the region (Government of British Columbia, 2003). The majority of water produced in the watershed originates in these protected areas, which receive the most precipitation and drain eastward, towards the lake (Wang et al., 2016).

2.2.2 Sampling campaigns and sample collection

To assess how forest harvest, natural catchment characteristics, and seasonality affect stream water quality in the Comox Lake watershed, we conducted synoptic and seasonal

sampling campaigns. In the seasonal campaign, sampling targeted 10 subwatershed stream outlet sites from April 2019 to March 2020 (Figure 2-1B). During this period, stream water grab samples were collected every one to two months (with less frequent sampling due to snow covered access roads in winter) in conjunction with the CVRD's water quality monitoring program. In addition, a spatially-extensive sampling approach was used in the synoptic campaign, whereby samples were collected from 30 subwatershed sites (Figure 2-1B). Synoptic sites included the 10 seasonal sites described above, along with 20 additional sites chosen to span broad gradients of forested area, soil depth and clay content, and topography. These gradients captured the range of variability that exists across the Comox Lake watershed. Sites were sampled four times (approximately every three weeks) from 3 September to 28 November 2019 (i.e., beginning near the onset of the typical wet period). In both campaigns, sampling targeted stable non-stormflow conditions to allow for cross-sample comparison under similar hydrologic conditions. Only these "baseflow" (or "between-event") conditions were assessed in this study; storm events, which account for the majority of variation in SS and DOM (Coynel et al., 2005), were not considered. Sampling was also limited at some sites that were dry in the summer period (July–September).

We analyzed stream water for conductivity, cations (Ca^{2+}, K^{+}, Mg^{2+}, Na^{+}, and dissolved Fe [dFe]), and $\delta^{18}O$ to help identify sources of water and transport flow paths, as well as turbidity, DOM-[C], and DOM composition to evaluate water quality. Prior to stream water sample collection, all glassware and plastic were pre-rinsed with 18.2 MΩ (Milli-Q) water, acid-washed with 10% hydrochloric acid, and rinsed thoroughly again with Milli-Q. After acid-washing, glassware was muffled at 475ºC for 4-h and all clean supplies were carefully stored until transportation to stream sites or the field laboratory. At each stream site, specific conductance was measured *in situ* with a multiparameter probe (YSI Professional Plus). Grab samples were collected immediately below the stream surface (0–30 cm), above the deepest part of the channel, and were processed for cations, $\delta^{18}O$, turbidity, DOM-[C], and DOM composition as described below. Turbidity samples were collected in 50-mL HDPE bottles, while all other metrics were collected concurrently in 500-mL polycarbonate bottles. Bottles were pre-rinsed three times with sample water, filled, and capped without headspace. After collection, samples were stored in cool (4ºC) and dark conditions and transported to the laboratory.

In the laboratory, samples were filtered (Millipore Express PLUS Membrane 0.45-µm PES) immediately upon arrival (within 48 hours of collection). Samples collected for $\delta^{18}O$ were filtered into 2-mL glass vials and tightly capped without headspace, whereas samples for dissolved cations were filtered into 15-mL centrifuge tubes and preserved with 18% nitric acid (trace-metal grade, to a pH of < 2). Samples collected for DOM-[C] were filtered into pre-combusted 40-mL borosilicate vials and acidified to pH 2 using trace-metal grade hydrochloric acid (Vonk et al., 2015), and samples collected for DOM composition were filtered into 60-mL amber glass bottles. Following filtration and preservation, all samples were kept in the dark and refrigerated (4ºC) until analysis.

2.2.3 Stream water quality analyses

Samples were analyzed for $\delta^{18}O$ and cations at the University of Alberta's ISO-certified Biogeochemical Analytical Service Laboratory, whereby $\delta^{18}O$ was measured using a L2130-i analyzer (Picarro) and cations were quantified on an Inductively Coupled Plasma – Optical Emission Spectrometer (Thermo Scientific iCAP 6300). Samples for turbidity were measured directly with a portable turbidimeter (Hach 2100Q) in the field laboratory.

Analyses for DOM-[C] and DOM were also completed at the University of Alberta. We quantified DOM-[C] using a Shimadzu TOC-V CPH analyzer, retaining the mean of the best three of five sample injections that satisfied a coefficient of variance of < 2%. We evaluated DOM composition by measuring absorbance and fluorescence on an Aqualog spectrofluorometer (Horiba Scientific). Absorbance samples were scanned from 240–800 nm at 1-nm increments to derive two metrics that are commonly used to assess DOM aromaticity: the spectral slope coefficient from 275–295 nm ($S_{275\text{-}295}$) and specific ultraviolet absorbance at 254 nm ($SUVA_{254}$). $S_{275\text{-}295}$ was calculated over the range of 275–295 nm using a linear regression model that estimated the slope of the relationship between the logarithm of absorption coefficients and wavelengths (Helms et al., 2008) while $SUVA_{254}$ was computed as the decadic absorbance at 254 nm normalized for DOM-[C] (Weishaar et al., 2003). For accurate $SUVA_{254}$ calculations, dFe was measured (Poulin et al., 2014), but effects were considered to be negligible because concentrations were frequently below detection or less than 0.15 mg L^{-1} at all subwatershed sites.

In addition to evaluating DOM aromaticity, we identified dominant DOM compounds and distinguished between compounds with varying sources and reactivity via fluorescent excitation

emission matrix (EEM) spectra (Fellman et al., 2010, Stubbins et al., 2014). Fluorescence samples were scanned from 230–500 nm at 5-nm increments for excitation wavelengths and 300–600 nm at 2.33-nm increments for emission wavelengths. Raw EEMs were corrected for inner filter effects, underwent a Milli-Q blank subtraction, and were normalized to Raman units (Murphy et al., 2013). We analyzed EEMs with parallel factor (PARAFAC) analysis, which decomposes EEMs into individual fluorescence components and provides estimates of the relative contribution of each component to total DOM fluorescence (Lee et al., 2018). This analysis was performed in MATLAB (9.7.0) with the drEEM toolbox (0.5.1) following the procedure of Murphy et al. (2013). The final PARAFAC model was validated using random split-half analysis, and all components successfully matched published fluorescence components (similarity scores > 0.95 on both excitation and emission spectra) in the OpenFluor database (Murphy et al., 2013).

2.2.4 Catchment characteristics

To assess spatial controls on stream water quality, we calculated a series of catchment characteristics for each of the 30 forested subwatershed sites. Upstream subwatershed drainage areas were delineated for all 30 sites in the ArcGIS (10.7.1) ArcHydro toolbox using a digital elevation model (DEM) (23-m x 23-m) obtained from GeoGratis (Government of Canada, 2017) and flow accumulation analysis of the stream network (GeoBC, 2020). Following catchment delineation, data were acquired for topography, soil depth and clay content, and forest cover characteristics (described below).

Mean slope angle, elevation, and terrain roughness were calculated based on the GeoGratis DEM. Soil depth to bedrock data (250-m x 250-m) were acquired from SoilGrids, a soil mapping system based on global soil profiles and environmental covariates (i.e., climate, terrain, and land cover) (Hengl et al., 2017), and used to calculate mean soil thickness. Soil clay contents were calculated as depth-weighted averages based on total percent clay data documented in the Soils of British Columbia database (Government of Canada, 2013) or texture classes identified in reports 44 and 45 of the British Columbia Soil Survey (Government of Canada, 1980, Government of Canada, 1985). After calculating clay contents, values were assigned to soil polygons previously identified across the study region (Government of British Columbia, 2020b).

Percent harvested area for each year from 1985 to 2019 was calculated for all subwatersheds. Harvest data were acquired from Canada's National Forest Information System (1985–2015; Canadian Council of Forest Ministers, 2015) and the Global Forest Change dataset (2016–2019; Hansen et al., 2013). Areas harvested prior to 1985 were not included in this study because satellite imagery was either unusable (i.e., image resolution was too coarse) or unavailable (i.e., Landsat does not predate 1972). We therefore only assessed forest harvesting within the past 35 years and assumed that all forest not included in the "percent harvested area" category is greater than 35 years of age. After calculating harvested areas, we computed the flow path distance from the edge of the nearest harvested area to each subwatershed site (termed "cutblock distance to sampling sites"). We also evaluated forest cover, as the percentage of total subwatershed area, based on harvested areas and biogeoclimatic zones (MacKinnon et al., 1992) derived from a regional ecosystem classification map produced by the Ministry of Forests, Lands, Natural Resource Operations and Rural Development (Government of British Columbia, 2020a). This map was additionally used to identify and assign dominant biogeoclimatic zones to each subwatershed.

After data acquisition and spatial statistics, all catchment characteristics were spatially-averaged or summarized and a single value was assigned to each subwatershed site in ArcGIS.

2.2.5 Statistical analyses

2.2.5.1 Determining seasonal and spatial patterns in stream water quality

All statistical analyses were performed in R (4.0.2) (R Core Team, 2020). Prior to analyses, all variables were tested for normality (Shapiro–Wilk test) and linearity to determine whether data transformations were required, and the Pearson correlation coefficient was computed to measure the strength and direction of significant relationships between variables (packages *stats, GGally,* and *corrplot*) (R Core Team, 2020, Schloerke et al., 2020, Wei and Simko, 2017). For data analyses, cation concentrations below the detection limit (i.e., 53 Na^+ samples) were set to half the detection limit; 9% of all cation samples were below-detect (U.S. Environmental Protection Agency, 2000). All major cations (Ca^{2+}, K^+, Mg^{2+}, Na^+) were then summed as a molar total because they were co-correlated.

In order to assess seasonal variation in stream water quality, we computed the Mann–Whitney U test, created scatter plots, generated box plots, and conducted principal components

analyses (PCAs) (packages *stats*, *ggplot2* and *factoextra*) (Kassambara and Mundt, 2020, Oksanen et al., 2019, R Core Team, 2020, Wickham, 2016). To evaluate spatial water quality differences among subwatersheds, we applied the Kruskal–Wallis test, constructed box plots, and performed an indirect gradient analysis (IGA) (packages *stats*, *ggplot2*, *factoextra*, and *vegan*) (Kassambara and Mundt, 2020, Oksanen et al., 2019, R Core Team, 2020, Wickham, 2016). Importantly, IGA shows relationships between stream water quality and catchment characteristics by first ordinating the water quality dataset and then correlating the ordination scores with catchment characteristics (Legendre and Legendre, 2012). PARAFAC components were not included as water quality metrics in the IGA model because each component lacked internal variability (i.e., was non-normal and highly skewed).

2.2.5.2 Assessing seasonality in stream water quality with air temperature and precipitation

Linear mixed-effects models (LMMs) were used to evaluate the influence of air temperature and the antecedent precipitation index (API) on water quality (package *lme4*) (Bates et al., 2015). This analysis highlights stream water differences between wet and dry seasons by considering the variation explained by air temperature and API (fixed effects), while also accounting for variation explained by the nested structure of subwatersheds within parent watersheds (random effect) (Bolker et al., 2009). Prior to inclusion in LMMs, air temperature was computed as the mean of maximum daily temperature over eight days preceding sample collection, and API was calculated as:

$$\mathrm{API_t} = \mathrm{API_{t-1}C} + \mathrm{P_{\Delta t}}$$

where $\mathrm{API_t}$ is API (mm) at time t, $\mathrm{P_{\Delta t}}$ is precipitation (mm) occurring during the eight-day time interval between t-1 and t, and C is a common decay constant (Fedora and Beschta, 1989). Importantly, C is used to represent the "memory" of a watershed by decreasing the influence of past precipitation with time (Bousfield, 2008).

We constructed LMMs for a suite of water quality metrics, including conductivity, major cations, $\delta^{18}O$, turbidity, DOM-[C], $SUVA_{254}$, $S_{275\text{-}295}$, and PARAFAC components. All stream water parameters were log transformed (except $\delta^{18}O$) to improve normality while air temperature and API were standardized (i.e., data were centered around zero and scaled with respect to the standard deviation). Different LMMs were compared and selected using the Akaike information criterion for small sample sizes (AIC_C), and final model fits were determined using restricted

maximum likelihood. A one-way ANOVA was used to compute significance values for fixed effects, with relationships where $p < 0.1$ considered significant. In addition, R^2 values were calculated and reported for fixed effects alone (marginal R^2) as well as fixed and random effects (conditional R^2) (Nakagawa and Schielzeth, 2013). After finalizing LMMs, diagnostic tests were performed for all models to ensure that assumptions of residual normality, homogeneity, and multicollinearity were satisfied.

2.2.5.3 Evaluating relationships between water quality indicators and landscape attributes

Partial redundancy analysis (partial RDA) was used to analyze relationships between landscape attributes and water quality indicators (package *vegan*) (Oksanen et al., 2019). This analysis allowed us to examine the variation in water quality indicators that was explained by recent forest harvest and catchment characteristics in the presence of covariates (Legendre and Legendre, 2012). Water quality indicators in the partial RDA models included conductivity, turbidity, DOM-[C], and DOM compositional indices (i.e., $SUVA_{254}$, $S_{275\text{-}295}$, and PARAFAC components), while landscape attributes included subwatershed area, percent harvested area (from 2000–2009 and 2010–2019), cutblock distance to sampling sites, percent total forest cover, mean soil thickness, mean soil clay content, mean slope angle, mean terrain roughness, mean elevation, and dominant biogeoclimatic zone. Importantly, terrain roughness was highly correlated with mean catchment slope (0.986, $p < 0.001$) and was therefore not analyzed further. We also accounted for the following covariates in all models: time (month), air temperature, API, and subwatershed nesting (i.e., the 30 subwatershed sites were nested within 13 parent watersheds).

We undertook three partial RDA models to better identify spatial drivers of stream water quality, examining samples collected during (1) all sampling campaigns, (2) only the synoptic campaign, and (3) only the seasonal campaign. In each model, highly correlated ($r > 0.7$) or skewed (skewness > 2.0) variables were removed prior to analysis. In addition, all explanatory variables and quantitative covariates (i.e., air temperature and API) were standardized to have a mean of zero and standard deviation of one, qualitative variables (i.e., biogeoclimatic zone, time (month), and subwatershed nesting) were coded as dummy variables, and water quality indicators and landscape attributes were log transformed when required to improve normality. A backwards stepwise selection procedure was then performed to identify dominant attributes

driving variation in stream water quality. Final models were validated via diagnostic tests confirming that assumptions of residual normality and multicollinearity were satisfied, and the statistical significance of each model and their axes were tested by permutation tests (999 permutations) on the F-*ratio*.

2.3 Results

2.3.1 Forest harvesting and catchment characteristics

Across the Comox Lake watershed, total recently harvested area increased approximately 100-fold (from 0.34 km^2 to 33.41 km^2) between 1985 and 2009, with over half of all harvesting occurring in the Cruikshank parent watershed (Figures 2-1C and 2-3A). There was a parallel increase in relative harvested area (adjusted for catchment size) over this period (Figure 2-3B). Cumulative harvested areas ranged between 2–54% across subwatersheds; those on the high end of the spectrum often had low slopes and thick soils (Table 2-1). While subwatersheds had differing proportions of harvested area, they also varied in other catchment characteristics, including forest cover, slope angle, elevation, soil thickness, and soil clay content (Table 2-1). Forest was the dominant form of land cover, ranging from 13.9–92.5%, with much smaller proportions of lakes, wetlands, and rocky outcrops. Mean watershed slope fluctuated from 11.4–38.7º (median: 28.2º) whereas mean elevation above sea level varied from 371.2–1366.5 m (median: 799 m, compared to 138 m for Comox Lake). Mean soil thickness (1.02–2.39 m) and clay content (1.4–14.7%) also varied across the entire watershed, with the thickest soils and greatest clay contents typically occurring at low slopes and elevations.

2.3.2 Stream water quality in Comox Lake subwatersheds: an overall assessment

A biplot of DOM-[C] and conductivity indicated three clear seasonally-driven end-members. At peak DOM-[C], conductivity was low, indicating enhanced surficial flow paths (Figure 2-4A). At lower concentrations of DOM-[C], conductivity increased at some sites (reflecting deeper groundwater flow paths) and decreased at others (reflecting seasonal snow and glacial melt in areas with thin soils) (Figure 2-4A). Whilst increased surficial flow (represented by $\delta^{18}O$ enrichment) did correspond to elevated DOM-[C], $\delta^{18}O$ showed no correlation with stream water turbidity (Figure 2-4B). Changes in DOM-[C] were also reflected in DOM

character: with decreasing DOM-[C], $S_{275\text{-}295}$ increased while $SUVA_{254}$ decreased, representing a shift towards more aliphatic, low molecular weight DOM (Figure 2-4C).

Irrespective of these relationships, all subwatersheds displayed similar seasonal fluctuations in $\delta^{18}O$ and relatively low conductivity (53.8 ± 27.5 µS cm^{-1}, 46.5 ± 20.0 µS cm^{-1}; synoptic, seasonal campaigns) and major cation concentrations (287 ± 167 µmol L^{-1}, 255 ± 118 µmol L^{-1}) (Tables A1-2 and A1-3). Turbidity (1.20 ± 0.55 NTU, 0.96 ± 1.54 NTU) and DOM-[C] (0.81 ± 0.55 mg L^{-1}, 1.02 ± 0.62 mg L^{-1}) were also typically low across catchments, but increased by 1.5 to 3-fold following periods of rainfall in July and January (Tables A1-2 and A1-3). While constituent concentrations were low across subwatersheds, the composition of DOM (i.e., $S_{275\text{-}295}$ and $SUVA_{254}$) ranged broadly from values consistent with highly aromatic, high molecular weight material to those consistent with aliphatic, low molecular weight material (Tables A1-2 and A1-3).

Additional DOM composition analyses via PARAFAC analysis revealed a validated model with four distinct fluorescence components: two that are consistent with terrestrial humic-like material (C1 and C2), and two consistent with a microbial protein-like DOM source (C3 and C4) (Figure A1-1). Across Comox Lake subwatersheds, the overall DOM pool is more terrestrial (C1 and C2; 69.4%) than microbial (C3 and C4; 30.6%) and is comprised primarily of component C1, followed by C2, C3, and finally C4 (Table 2-2). Notably, terrestrial and microbial fractions of the DOM pool were not readily altered by changes in DOM-[C] (Figure A1-2). Comparisons to the OpenFluor database revealed that components C1 and C2 (similarity scores > 0.98) most closely resemble peaks A and C, which are ubiquitous in aquatic environments and signify aromatic DOM that may be enriched in fulvic acids (Table 2-2). In comparison, components C3 and C4 (similarity scores > 0.95) both resemble peak T, which is linked to aquatic productivity and associated with tryptophan-like, more aliphatic DOM that may be enriched in amino acids (Table 2-2).

2.3.3 Spatial variation in stream water quality

Our IGA model indicated clear differences in stream water quality among subwatershed sites, which were associated with variation in landscape attributes (Figure 2-5). The first axis (PC1) explained 51% of cross-site variation, and was strongly correlated with DOM-[C], $SUVA_{254}$, and $S_{275\text{-}295}$; greater DOM-[C] and a more aromatic DOM composition (i.e., increased

$SUVA_{254}$ and decreased $S_{275\text{-}295}$) occurred in catchments with higher soil clay contents and a greater harvest intensity. The second axis (PC2) explained 22% of cross-site variation, and was strongly associated with turbidity, reflecting increased concentrations in smaller catchments at high elevations with steep slopes, thin soils, and little forest cover. In addition, turbidity concentrations rose with increasing distance from harvested areas. Forest harvest was inversely related to elevation (-0.587, $p < 0.001$) and slope (-0.384, $p < 0.05$), which suggests that harvest intensity increases at low slopes and elevations.

Both PC1 and PC2 were also affected by climate; biogeoclimatic zones plotted along both axes, revealing varying influences on stream water quality (Figure 2-5). For example, higher turbidity sites were more likely to be associated with the coastal western hemlock moist maritime montane zone (BGZ^3) but not the coastal western hemlock very dry maritime eastern zone (BGZ^2). DOM-[C] exhibited a similar pattern in different biogeoclimatic zones; high concentration sites were more related to the coastal western hemlock very dry maritime western zone (BGZ^1) and less to the mountain hemlock moist maritime windward zone (BGZ^4). Simultaneously, increasing DOM aromaticity and molecular weight were positively associated with BGZ^1 and BGZ^3 and negatively associated with BGZ^2 and BGZ^4, though to varying degrees.

Results of the partial RDA models revealed that soil clay content (models A, B, and C), BGZ^4 (models B and C), and elevation (model C) best predicted variation in stream water quality. Together, these three characteristics explained the largest proportion of the variance (1–5%) in the water quality matrix, although none of the three models were able to adequately explain the variance in stream water quality (Table A1-4). The remainder of the variance was attributed to subwatershed nesting, time (month), air temperature, and API (26–47%) or was left unexplained (48–70%) (Table A1-4). Evidently, seasonal and subwatershed nesting parameters were more important than landscape attributes in explaining the variance in stream water quality.

2.3.4 Seasonal variation in stream water quality

As a result of the variation introduced by July and January storm events in our seasonal dataset, bulk comparisons between wet and dry season baseflow (e.g., using Mann–Whitney U tests) were unable to elucidate seasonal shifts in mean values for stream water quality ($p > 0.05$; data not shown). However, PCAs indicated an overall shift in conductivity, major cations, and

$\delta^{18}O$ between wet and dry seasons, and a greater range of values for turbidity, DOM-[C], and DOM composition during the dry season when compared to the wet season (Figure A1-3). Given the clear and repeatable seasonality of these water quality metrics, we further investigated the effects of air temperature and API on each metric.

Across wet and dry periods, $\delta^{18}O$ was inversely related to air temperature (b = -0.185, p < 0.001) whereas major cations were positively related (b = 0.114, p < 0.001) (Table A1-5). Major cations were also negatively related to API (b = -0.084, p < 0.05) (Table A1-5). Evidently, major cations and $\delta^{18}O$ significantly differed between the wet and dry period: in the former, $\delta^{18}O$ became more enriched and major cations declined, while in the latter $\delta^{18}O$ became more depleted and major cations increased (Figure 2-6). Despite a strong correlation between major cations and conductivity (R^2 = 0.96), there were no significant relationships between conductivity and air temperature or API (Table A1-5). This may be ascribed to the number of samples analyzed; major cations and $\delta^{18}O$ were measured five times in the dry period and three times in the wet, whilst conductivity was measured five times in each period.

Significant water quality changes were also observed between wet and dry periods for DOM-[C], $SUVA_{254}$, and PARAFAC components (C1–C4) (Table A1-5). DOM-[C] was negatively related (b = -0.092, p < 0.1) while $SUVA_{254}$ was positively related (b = 0.055, p < 0.05) to air temperature. C1 and C2 (C1: b = -0.108, p < 0.01; C2: b = -0.155, p < 0.01) displayed an inverse relationship to API, whereas C3 and C4 (C3: b = 0.147, p < 0.05; C4: b = 0.034, p < 0.05) were directly proportional. In contrast, there were no significant effects of air temperature or API on turbidity or $S_{275\text{-}295}$ (Table A1-5). Although $S_{275\text{-}295}$ did not show clear relationships with air temperature or API, this metric did exhibit a synchronous pattern to other measures of DOM composition.

Given significant API and temperature-driven differences in DOM-[C], $SUVA_{254}$, and PARAFAC components (C1–C4), we focused on patterns in these six metrics, comparing a constrained set of baseflow values from late-summer (August–September; dry season) to those from mid-autumn (October–November; wet season). While the former period represents extremely low baseflow conditions, the latter represents higher baseflows immediately following rewetting. In general, DOM-[C] varied with hydrological condition: concentrations were lowest in late-summer and increased upon initial rewetting early in the wet season (Mann–Whitney U test, p = 0.0475) (Figure 2-6). DOM composition also differed between these two periods, with a

higher contribution of humic-like DOM in the late dry season (increased C1 and C2), and a greater contribution of protein-like DOM at the onset of the wet season (increased C3 and C4) (Mann–Whitney U tests, $p < 0.01$) (Figure 2-7). Finally, a seasonal transition also existed with elevated DOM aromaticity (increased $SUVA_{254}$) in late-summer and reduced aromaticity (decreased $SUVA_{254}$) following rewetting (Mann–Whitney U test, $p = 0.0484$) (Figure 2-6).

2.4 Discussion

Here, we compare the relative importance of seasonality, catchment characteristics, and forest harvest on stream water quality in Comox Lake subwatersheds. Although forestry is common in the region, the effects of recent forest harvest were minor when compared to the background spatial and seasonal variation of turbidity, DOM-[C], and DOM composition. Water quality metrics varied across space according to natural catchment characteristics (e.g., soil clay content, elevation), though subwatershed sites generally displayed low turbidity, little DOM-[C], and a DOM composition with variable aromaticity, molecular weight, and humification. In addition to spatial variation in stream water quality, DOM-[C] and DOM composition also exhibited seasonal variation. In the wet season, DOM-[C] increased and the DOM pool shifted towards a more aliphatic, low molecular weight, and protein-like composition; an inverse pattern was observed during the dry season. Overall, this study underscores stream water quality variation during stable non-stormflow conditions in forested catchments with various landscape attributes and, in particular, contributes to our understanding of key factors (i.e., seasonal importance of temperature and antecedent moisture) for driving variation in stream water quality within the Pacific Maritime ecozone.

2.4.1 Overall evaluation of stream water quality in Comox Lake subwatersheds

Baseflow stream water quality in Comox Lake subwatersheds was consistent with several other studies conducted in forested regions. In particular, turbidity was similar to or lower than other streams in temperate watersheds with active forest harvesting (Erdogan et al., 2018, Jordan, 2006). DOM-[C] was typical for streams or rivers draining forested watersheds with shallow soils and limited wetlands; comparably low concentrations have been found in actively managed forests in tropical (Jacobs et al., 2017), subtropical (Bao et al., 2019), and temperate ecozones (Mistick and Johnson, 2020). During stable non-stormflow conditions, neither DOM-[C] (total

organic carbon < 4 mg L^{-1}) nor turbidity (< 5 NTU) exceeded regional guidelines established for safe drinking water (Government of British Columbia, 2001) or freshwater aquatic life (Government of British Columbia, 2019). Measures of $S_{275-295}$ and $SUVA_{254}$ exhibited broad variability analogous to temperate streams draining forested watersheds in the coastal mountains (Werner et al., 2019), interior mountains (Lee and Lajtha, 2016), and icefields (Fellman et al., 2016). This variation may possibly be linked to changes in seasonal flow paths that delivered different DOM pools to stream water (further discussed in section 2.4.3). Finally, PARAFAC components, which were similar to streams draining tropical (C1 and C3), subarctic (C2) and temperate (C4) forested watersheds (García et al., 2019, Osburn et al., 2018, Wu et al., 2020, Yamashita et al., 2011), indicated that the DOM pool was principally derived from terrestrial plant or soil organic matter, rather than from in situ microbial activity. Although the compositional metrics discussed here provide insight into possible sources of DOM, DOM composition likely had a negligible effect on overall stream water quality due to limited DOM-[C] in stream water.

2.4.2 Spatial dynamics and drivers of stream water quality

Spatial variation in baseflow stream water quality was driven by numerous landscape attributes, including biogeoclimatic zones, catchment area, soil thickness and clay content, slope angle, elevation, forest cover, and harvested area. While clear relationships emerged between these attributes and water quality indicators, only soil clay content, elevation, and the occurrence of the mountain hemlock biogeoclimatic zone (i.e., BGZ^4) significantly predicted stream water quality. Despite their significance, however, these three characteristics did not explain a considerable proportion of the variance in stream water quality (< 6%), and were instead overwhelmed by seasonality and subwatershed nesting parameters (26–47%). Our findings were consistent with previous studies examining spatial variability in stream water quality during stable flow conditions (e.g., Jacobs et al., 2017, Oliver et al., 2017) that show that water quality depends on a combination of landscape attributes. Although landscape attributes were associated with some water quality metrics in subwatersheds, there were ultimately no dominant attributes driving variation in stream water quality, which differs substantially from other research (e.g., Jones et al., 2019).

Elevation, soil clay content, and BGZ^4 have been previously implicated as important controls on turbidity, DOM-[C], and DOM composition in forested watersheds. A rise in elevation reduces soil organic carbon content, decreases hydrologic connectivity, and enhances sediment particle detachment (Kreutzweiser et al., 2008, Mbonimpa et al., 2014, Parry et al., 2015), while an increase in soil clay content leads to greater absorption of DOM onto clay mineral surfaces and elevates fine soil particle suspension in stream water (Groeneveld et al., 2020, Hur and Jung, 2008). Therefore, with increased elevation and soil clay content, turbidity increases, DOM-[C] decreases, and the DOM pool shifts towards a more aliphatic, low molecular weight, and protein-like composition (Awad et al., 2018, Hutchins et al., 2019, Mbonimpa et al., 2014, Nkambule et al., 2011). All of these relationships were observed across Comox Lake subwatersheds, with the exception of decreased DOM-[C] and more aliphatic, protein-like DOM with increased soil clay. This lack of relationship with DOM-[C] and DOM composition may have occurred because stream pH (7–8) limited DOM absorption to clay (Groeneveld et al., 2020), which would weaken soil clay content effects on DOM. Alongside elevation and soil clay content, BGZ^4 (mountain hemlock biogeoclimatic zones) also experienced a significant shift in water quality. In this zone, less productive forests at subalpine elevations result in decreased organic matter and greater detachment of sediment particles (Meidinger and Pojar, 1991, Mbonimpa et al., 2014), which in turn increases turbidity, decreases DOM-[C], and alters the DOM pool to become more aliphatic, low molecular weight, and protein-like. Each of these changes were noted in BGZ^4 within the Comox Lake watershed.

Although we were able to elucidate landscape controls on stream water quality, hydrologic (i.e., seasonal) controls appeared to exert a dominant influence across Comox Lake subwatersheds (e.g., Figures 2-6, 2-7 and Table A1-5).

2.4.3 Seasonal dynamics and drivers of stream water quality

Previous research has found that the seasonality of stream water quality is primarily controlled by precipitation, discharge, and soil moisture, all of which influence hydrologic connectivity (Jacobs et al., 2017, Schelker et al., 2012). Typically, connectivity increases in the wet season with frequent storm events, and this results in elevated DOM fluxes (e.g., Coynel et al., 2005). At the same time, greater discharge during this period allows for increased SS fluxes via channel bank erosion (e.g., Smith and Dragovich, 2009). Hydrologic connectivity also

determines which source waters and transport flow paths dominate between wet and dry periods (Parr et al., 2019). In the wet period, consistently shallow surficial flow paths prevailed across the Comox Lake watershed, as shown by concurrent changes in conductivity, major cations, and $\delta^{18}O$. Comparably, these metrics indicated greater variation in source waters and flow paths during the dry period, with stream water originating from surficial snow and glacial melt as well as from deeper groundwater sources.

The importance of seasonal dynamics on stream water quality was emphasized by significant linkages between seasonal (air temperature and API) and water quality (DOM-[C], $SUVA_{254}$, and PARAFAC components) metrics in Comox Lake subwatersheds. On an annual basis, DOM-[C] decreased slightly under non-stormflow conditions in the dry period and increased through the wet period. Fluctuations in DOM-[C] are likely related to hydrology (i.e., DOM-[C] is transport limited). Prior studies suggest that (1) DOM-[C] is readily mobilized in soils with a high API (Werner et al., 2019) and is thus rapidly flushed to streams during periods of high flow (Oliver et al., 2017), and (2) a positive correlation often exists between DOM-[C] and discharge (Schelker et al., 2012), particularly in mineral soils where shallower flow paths increase interactions with organic matter. Therefore, a combination of hydrological factors likely contributes to increased DOM-[C] during the wet period. The composition of DOM (i.e., $SUVA_{254}$ and PARAFAC components) also shifted seasonally; periods of low flow produced a DOM pool with a more aromatic, high molecular weight, and humic-like composition. During the dry period, deeper groundwater sources may contribute more to stream water DOM than surficial flow (Zheng et al., 2018). In contrast, a more aliphatic, low molecular weight, and protein-like DOM composition was observed during the wet season. As hydrologic connectivity increased with greater antecedent precipitation in this period, additional flow paths may have linked disconnected DOM pools in deeper soil horizons to the stream network (Werner et al., 2019). A shift thus occurred to a differing DOM (i.e., more microbial) pool during high flow periods that overrode the low flow DOM signal. While most stream water quality indicators varied between the wet and dry period, mean values for turbidity did not; this is likely due to the dependence of sediments on storm events to mobilize (Hood et al., 2006, Mbonimpa et al., 2014).

In general, these findings add nuance to our understanding of seasonal variation in stream water quality across forested watersheds. Most prior research has documented (1) decreased

DOM-[C] and a higher contribution of more aromatic, high molecular weight, and humic-like DOM in the wet season, and (2) increased DOM-[C] and aliphatic, low molecular weight, and protein-like DOM in the dry season (Bao et al., 2019, Lee and Lajtha, 2016, Parr et al., 2019, Schelker et al., 2012). Our results, showing a contrasting seasonal pattern in Comox Lake subwatersheds, may have occurred because DOM-[C] was transport limited in the region. Due to its dependence on hydrology, DOM-[C] export likely increases in the wet season as storm events flush DOM to the stream network (e.g., Fellman et al., 2020, Hood et al., 2006, Vidon et al., 2008). Following each event, DOM-[C] decreases but has the potential to remain elevated when compared to the dry period. In addition to hydrology, glacial source waters may also explain seasonal patterns: glaciers, which contribute more to stream flows during the dry period, result in decreased DOM-[C] with variable aromaticity (Csank et al., 2019). Further research that investigates glacial source waters and DOM-[C] mobility is warranted to provide additional insight into the seasonal pattern observed here.

Comparisons between studies further reveal how different regions regulate stream water DOM-[C] and DOM composition, and highlight the importance of hydrology as a primary mechanism driving seasonal changes in stream water quality. For example, Jones et al. (2019) found that a considerable proportion of the variance in stream water quality was explained by precipitation and soil moisture. This finding aligns with our research, which shows that hydrological factors (e.g., antecedent precipitation) were more important than landscape attributes in explaining the variation in stream water quality. Overall, hydrology is a key factor regulating stream water quality in forested subwatersheds on Canada's Pacific Coast.

2.4.4 Forest harvest intensity and effects on stream water quality

We investigated forest harvesting over the past 35 years in the Comox Lake watershed. While the aerial extent of harvested areas grew substantially between 1985 and 2019, increases were disproportionate between studied subwatersheds. This may be linked to the high degree of forest harvesting that usually occurs in low-elevation subwatersheds (Erdozain et al., 2018). In the Comox Lake watershed, highly productive forests at low elevations (Meidinger and Pojar, 1991) were the focus of early logging in the first half of twentieth century (Barraclough et al., 2016). These low-elevation areas now contain mature second growth forests that have been actively harvested since the 1980s (Barraclough et al., 2016). Despite differences in harvested

area relative to elevation, the overall magnitude of forest harvest in the Comox Lake watershed was typical of actively managed watersheds on the southern coast of British Columbia (Canadian Council of Forest Ministers, 2015, Hansen et al., 2013).

While recent forest harvesting was ubiquitous across our study subwatersheds, its effects were less than the background seasonal and spatial variation of stream water quality. Spatial patterns were similar to other studies showing elevated turbidity, increased DOM-[C], and more aromatic, high molecular weight, and humic-like DOM in subwatersheds with a higher proportion of harvested area (Berkowitz et al., 2014, Erdogan et al., 2018, Erdozain et al., 2018, Lee et al., 2019, Lee and Lajtha, 2016, Schelker et al., 2012). Despite these observed relationships, spatial patterns were insignificant in Comox lake subwatersheds, signifying that baseflow stream water quality was not substantially altered by an increase in current forest harvest. Given that the overall effect of forest harvest was small, it is not surprising that water quality metrics lacked pronounced responses to harvesting in the wet season (i.e., when increased hydrologic connectivity linked additional harvested areas to streams).

Ultimately, the extent and magnitude of forestry impacts on stream water quality will depend on the hydrological connectivity (Coch et al., 2020, Kreutzweiser et al., 2008) of resource roads, landslides, and harvested areas to the stream network (Erdogan et al., 2018, Jordan, 2006, Reid et al., 2016, van Meerveld et al., 2014). Previous research has shown that when harvested areas are hydrologically linked to streams, changes in flow paths and runoff amplify the effects of forest harvest on stream water quality (Dai et al., 2001, Schelker et al., 2012). For example, subwatersheds in northern Sweden experienced a 90% increase in DOM-[C] due to enhanced water fluxes following clearcutting (Schelker et al., 2012). Given that forestry can modify flow pathways and increase peak flows (Wright et al., 1990), the sediment supply to streams may also increase following harvesting (Erdogan et al., 2018).

As hydrologic connectivity increases with enhanced rainfall in the future (Wang et al., 2016), currently minor impacts of forest harvest on stream water quality may become more important across Comox Lake subwatersheds. Since this study did not evaluate extreme rain or rain-on-snow events, it is critical for future research to assess these events and associated changes in water quality (Comox Valley Regional District, 2019b). In turn, this will enhance our understanding of forest harvest effects on stream water quality under different hydrologic conditions with enhanced flow.

2.4.5 Conclusions

This study investigated the spatial and seasonal variation of stream water quality in forested subwatersheds with different landscape attributes. Subwatersheds showed clear stream water quality differences in response to catchment characteristics and harvest intensities, but these relationships were muted when compared to the water quality changes associated with seasonal variations in hydrology and temperature. While many metrics (i.e., DOM-[C], $SUVA_{254}$, and PARAFAC components) varied seasonally, these fluctuations did not intensify in subwatersheds with greater proportions of harvested area. Overall, this research provides insight into the underlying factors (e.g., seasonal flows) that drive variation in water quality on Canada's Pacific Coast.

Although our findings indicate that the background spatiotemporal variability of stream water quality was not overwhelmed by forest harvest, this study only considers areas harvested within the past 35 years. As a result, our findings are confounded by historical harvest practices in the region; this regenerating landscape will take decades, if not centuries, to fully recover. This study also did not identify specific hydrologic factors driving water quality or assess water quality responses to stormflow. Further research should therefore (1) specifically quantify the influence of key hydrological factors (e.g., discharge, antecedent soil moisture) on stream water quality, and (2) examine water quality fluctuations with changes in flow (e.g., during storm events). Given that hydrology was a key variable driving variation in stream water quality, it is also necessary to evaluate water quality changes as hydroclimatic regimes shift over the long-term. Paired with other studies examining the effects of forest harvest on stream water quality, this work confirms the need to locally assess source waters while considering the composition of surrounding subwatersheds for the most accurate evaluation of source water quality.

2.5 Tables

Table 2-1. Catchment characteristics (parent watershed, area, slope, elevation, soil thickness, clay content, and forest cover) and harvested areas (1985-2019) for the 30 subwatershed sites in the Comox Lake watershed. Note that areas harvested between 1985 and 2019 were not included in percent forest cover.

Site	*Parent watershed	Area (km^2)	Mean slope (º Angle)	Mean elevation (m)	Mean soil thickness (m)	Mean clay content (% Soil)	Forest cover (% Area)	Harvest 1985-89 (% Area)	Harvest 1990-99 (% Area)	Harvest 2000-09 (% Area)	Harvest 2010-19 (% Area)
BAU†	1	2.2	29.1	862.2	1.17	3.46	85.3	0	0	13.1	1.6
BEC	2	17.3	27.1	957.8	1.30	4.82	53.5	0	3.7	6.8	0.3
BOC	3	9.2	26.3	801.7	1.71	9.11	85.0	0	0.2	2.5	10.0
CCC†	4	2.4	29.8	857.6	1.35	5.12	52.2	0	16.9	17.2	0.9
CK2†	4	88.8	28.3	1038.9	1.34	3.99	63.2	0	0.5	5.7	5.2
CKR	4	214.1	28.6	562.6	1.78	3.43	51.3	0	1.0	7.4	4.3
COC†	4	13.9	38.7	1053.5	1.47	2.24	39.2	0	0	1.1	2.9
CPC†	4	41.5	28.8	625.5	1.73	4.15	54.3	0	1.7	9.1	5.4
CRC†	4	4.8	23.6	945.0	1.53	5.92	74.5	0	0	14.0	11.5
DAC†	4	8.8	37.0	977.9	1.48	4.42	67.8	0	0	1.6	0
ERC†	4	76.8	28.1	1098.7	1.28	4.06	63.8	0	0.5	2.8	4.0
GGC	5	3.5	31.4	500.7	2.00	3.24	13.9	0	2.8	23.8	10.4
HAC†	6	1.0	29.1	737.3	1.24	2.57	76.8	0	0.1	8.5	14.6
HEC†	9	2.6	24.2	796.5	1.54	3.57	80.3	0	2.7	1.9	15.1
HTC†	8	1.4	17.7	526.1	1.46	3.62	71.9	0	0	12.3	15.9
IDC†	4	61.1	36.6	921.6	1.50	2.75	34.8	0	0	5.0	2.5
MOC†	4	29.8	24.2	1083.4	1.29	4.20	72.4	0	0	2.7	3.8
PC2†	7	5.6	32.9	917.9	1.38	3.70	54.5	2.1	1.5	4.8	1.1
PEC	7	7.3	33.8	585.9	1.77	3.80	45.9	2.9	1.4	4.7	5.0
PV2†	8	6.9	11.4	379.2	1.81	14.66	45.8	0	9.6	23.9	20.7
PVC	8	20.5	17.3	406.4	1.49	4.31	61.1	0.3	5.2	18.0	15.2
REC†	4	29.8	34.7	1246.4	1.31	1.42	17.4	0	0	2.9	0.7
TMT	10	1.9	16.0	371.2	1.71	4.26	67.9	0	0	11.9	22.7
TO2†	9	3.6	24.7	952.3	1.10	4.07	67.3	0	0	28.1	4.6
TOC	9	21.9	25.2	532.1	1.65	3.79	72.0	0	1.0	18.4	8.6
TRC†	8	3.7	14.1	711.3	2.39	3.13	92.5	0	0	2.8	4.7
UPR	12	81.8	32.1	774.3	1.68	3.61	71.5	0	0.8	8.0	3.8
UT1	11	1.0	28.0	653.5	1.64	3.76	59.6	0	0	12.3	27.7
WAC†	13	0.2	29.7	775.1	1.84	4.01	74.0	0	11.7	9.2	7.3
WHC†	4	7.7	26.4	1366.4	1.02	2.29	32.0	0	0	0	2.4

* Numbers correspond to parent watersheds indicated in Figure 2-1.

† Synoptic watershed sites.

Table 2-2. Properties of the four fluorescence components identified using PARAFAC analysis, including excitation (Ex.) and emission (Em.) peak values, percent composition, similarity scores, potential component characteristics, and related references for similar components. The OpenFluor database was used to obtain information on similarity scores and component characteristics (Murphy et al., 2013).

Component	Ex. (nm)	Em. (nm)	% composition*	Similarity score†	Potential characteristics	References
C1	310	418	45.9 ± 11.7 (5.8–58.7)	0.99	Peak A and C; terrestrial humic-like; enriched in fulvic acids	Amaral et al. 2016 (C1)
				0.99	Peak C; enriched in fulvic acids	Yamashita et al. 2011 (C1)
				0.99	Terrestrial humic-like; ubiquitous in aquatic environments	Garcia et al. 2015 (C1)
C2	240/370	488	23.5 ± 8.0 (1.4–35.7)	0.99	Terrestrial humic-like	Peleato et al. 2017 (C3)
				0.99	Humic-like	Chen et al. 2018 (C4)
				0.99	Peak A and C; ubiquitous in aquatic environments; signifies more aromatic DOM	Podgorski et al. 2018 (C6)
C3	270	297	16.2 ± 10.3 (0–79.9)	0.97	Protein tryptophan-like; enriched in amino acids	Cawley et al. 2012 (C5)
				0.97	Protein tannin-like	Romero et al. 2017 (C4)
				0.96	Protein-like; signifies more aliphatic DOM; linked to aquatic productivity	Gonçalves-Araujo et al. 2016 (C3)
C4	285	347	14.4 ± 15.2 (0–91.0)	0.98	Protein tryptophan-like	Murphy et al. 2011 (C5)
				0.98	Peak T	Wünsch et al. 2018 (C4)
				0.97	Peak T; protein tryptophan-like	Yamashita et al. 2011 (C5)

* Mean ± standard deviation (min-max) calculated from all samples.

† 70 studies were identified with at least one component similarity score > 0.95. Studies with the highest similarity scores (> 0.95) were chosen for comparison.

2.6 Figures

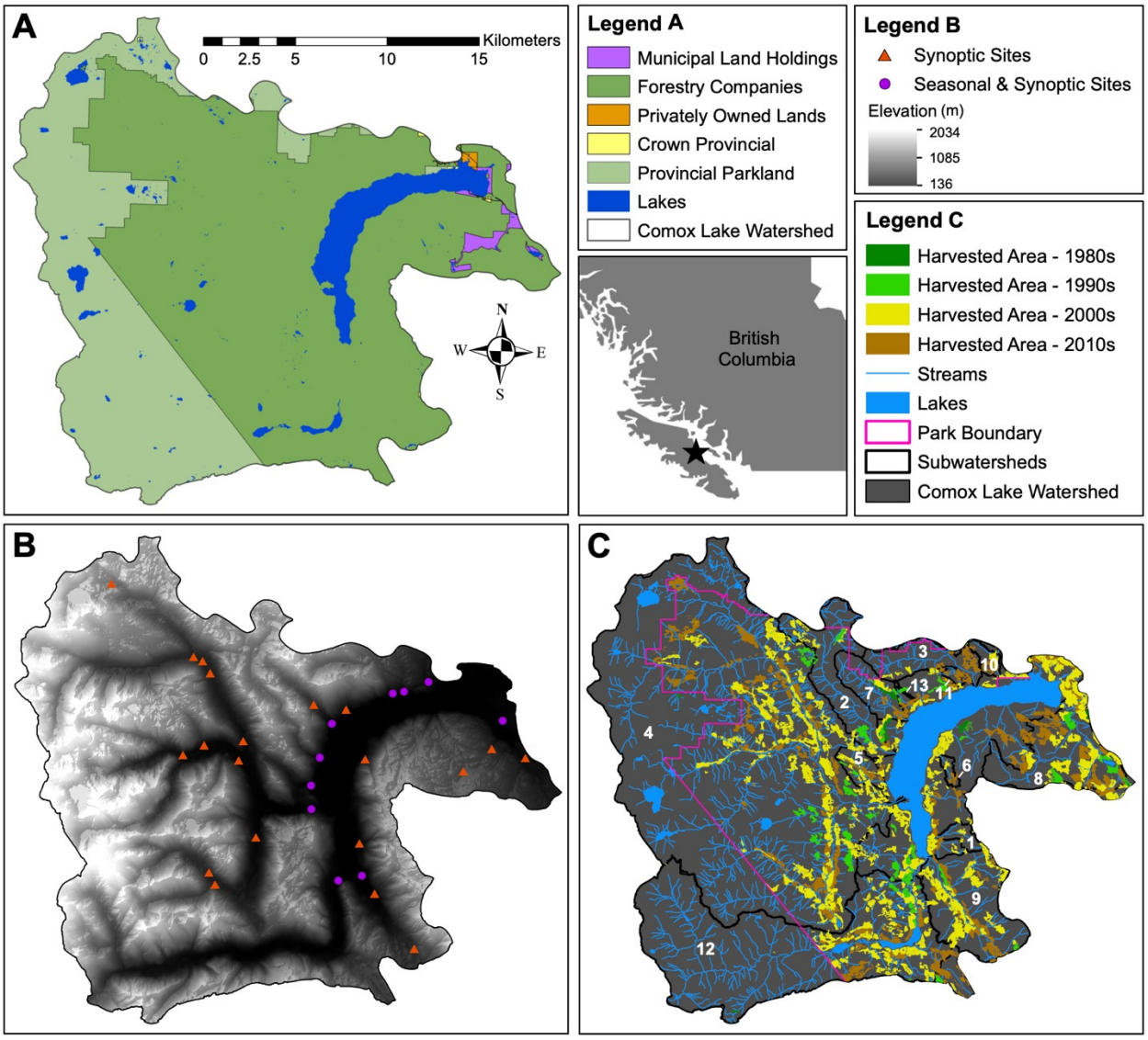

Figure 2-1. Maps of the Comox Lake watershed showing (A) land ownership, (B) elevation and study sites, and (C) harvested areas, streams, and other relevant features. In map (B), study sites were coded by campaign: synoptic sampling was performed at triangular orange locations, while both synoptic and seasonal sampling were conducted at circular purple locations. In map (C), parent watersheds were numbered as follows: 1 = Beaufort (BAU), 2 = Beech (BEC), 3 = Boston (BOC), 4 = Cruikshank (CKR), 5 = Ginger Goodwin (GGC), 6 = Harding (HAC), 7 = Pearce (PEC), 8 = Perserverance (PVC), 9 = Toma (TOC), 10 = Tomato (TMT), 11 = Unnamed (UT1), 12 = Upper Puntledge (UPR), and 13 = Wattaway (WAC). All 30 study sites were nested within these 13 parent watersheds.

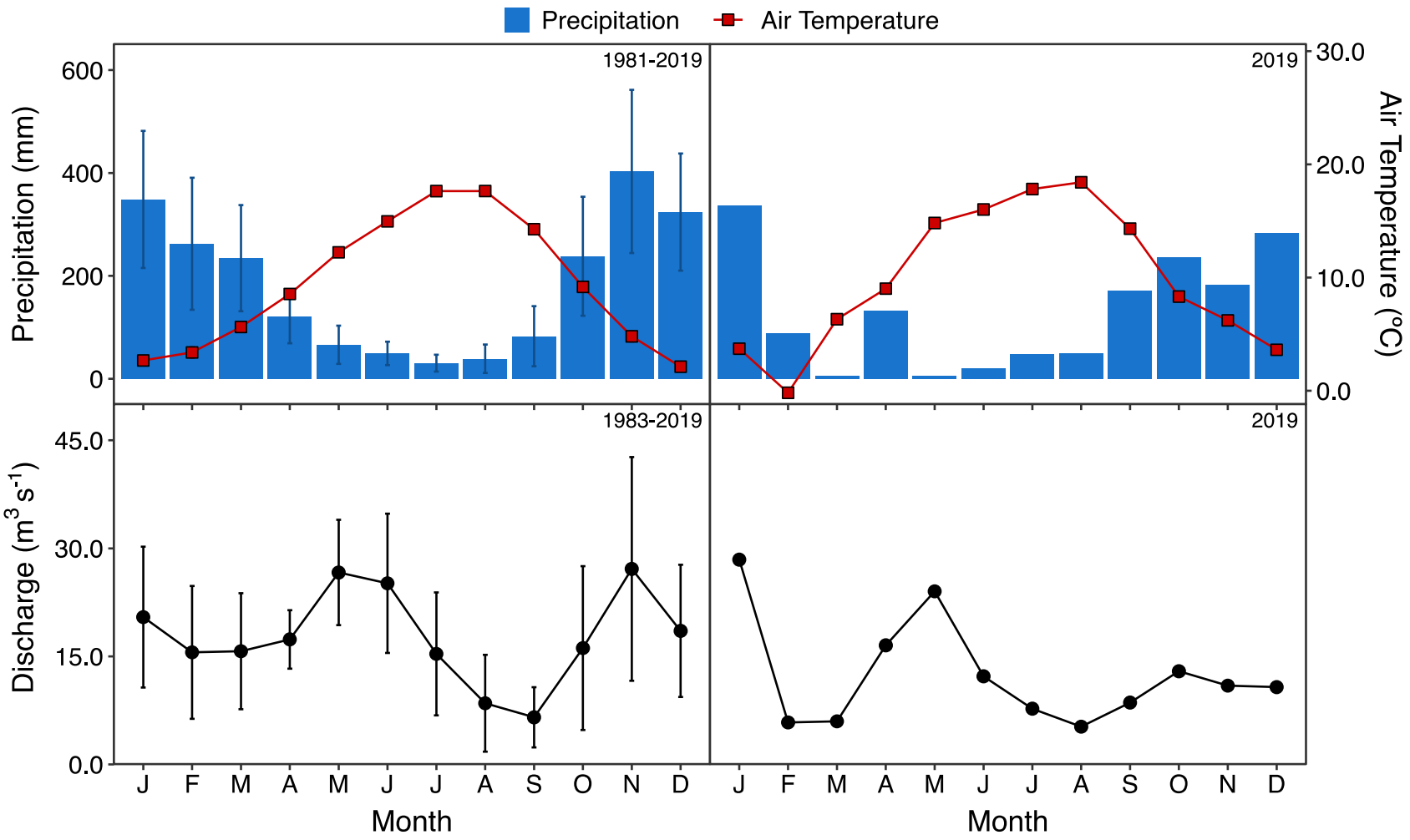

Figure 2-2. Comparisons of climatograms (1981–2019 to 2019) and Cruikshank River discharge (1983–2019 to 2019). Mean monthly discharge (m^3 s^{-1}) data were obtained from an Environment Canada hydrometric station located on the Cruikshank River, while precipitation (mm) and air temperature (ºC) data were acquired from Wang et al. (2016) (http://www.climatewna.com) at Comox Lake (49°36'N, 125°10'W). Note that the Comox Lake represents one microclimate in the Comox Lake watershed, and that different microclimates arise across the watershed due to variable topography.

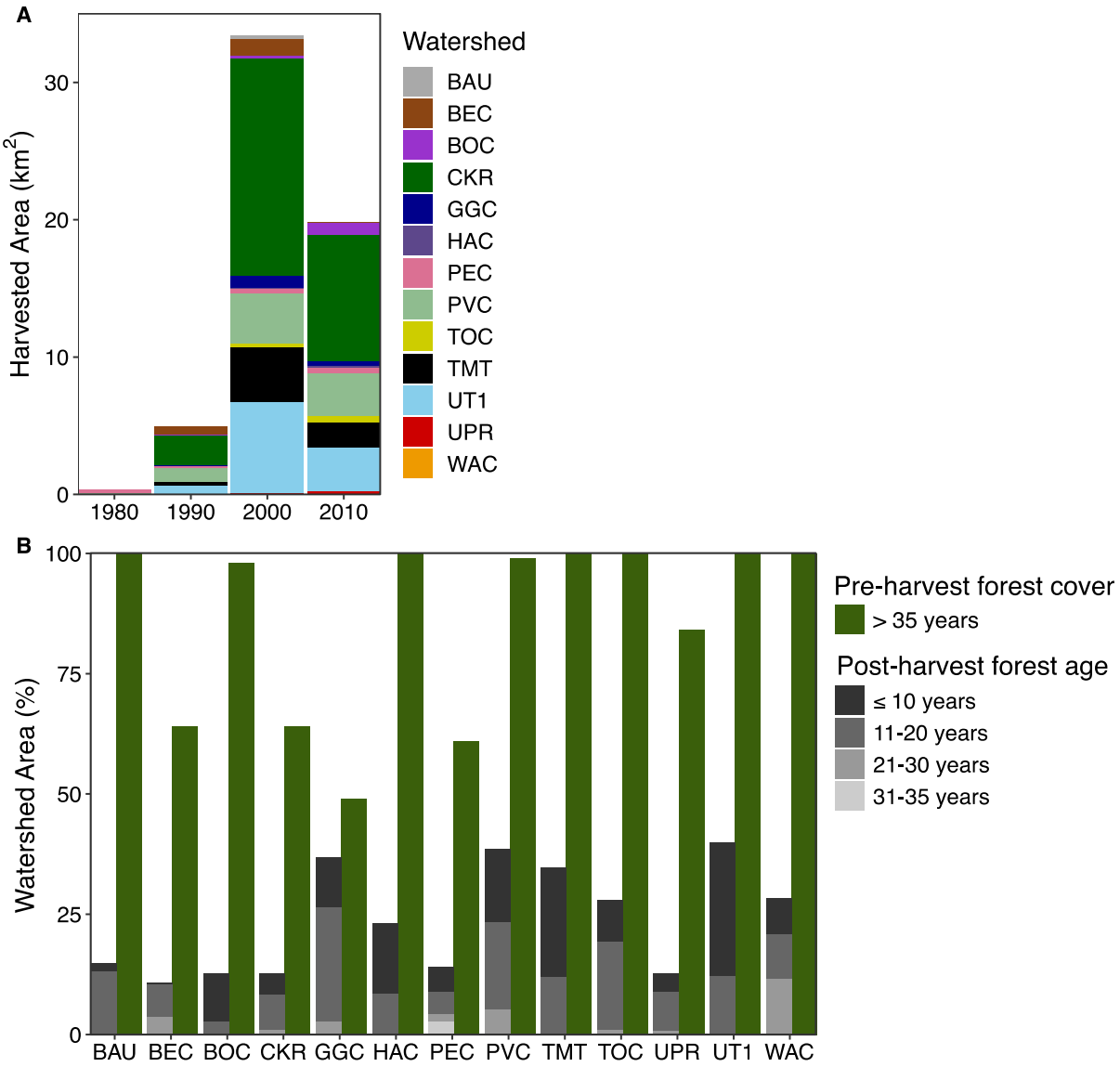

Figure 2-3. Forest harvesting from 1985–2019 showing (A) decadal bins of total harvested area in km^2, and (B) relative pre-harvest forest cover and harvested area age for the 13 parent watersheds. Within each parent watershed, the difference between pre-harvest cover (green bars) and post-harvest age (grey shaded bars) indicates the percentage of the watershed that is forested, but has not been harvested since 1985.

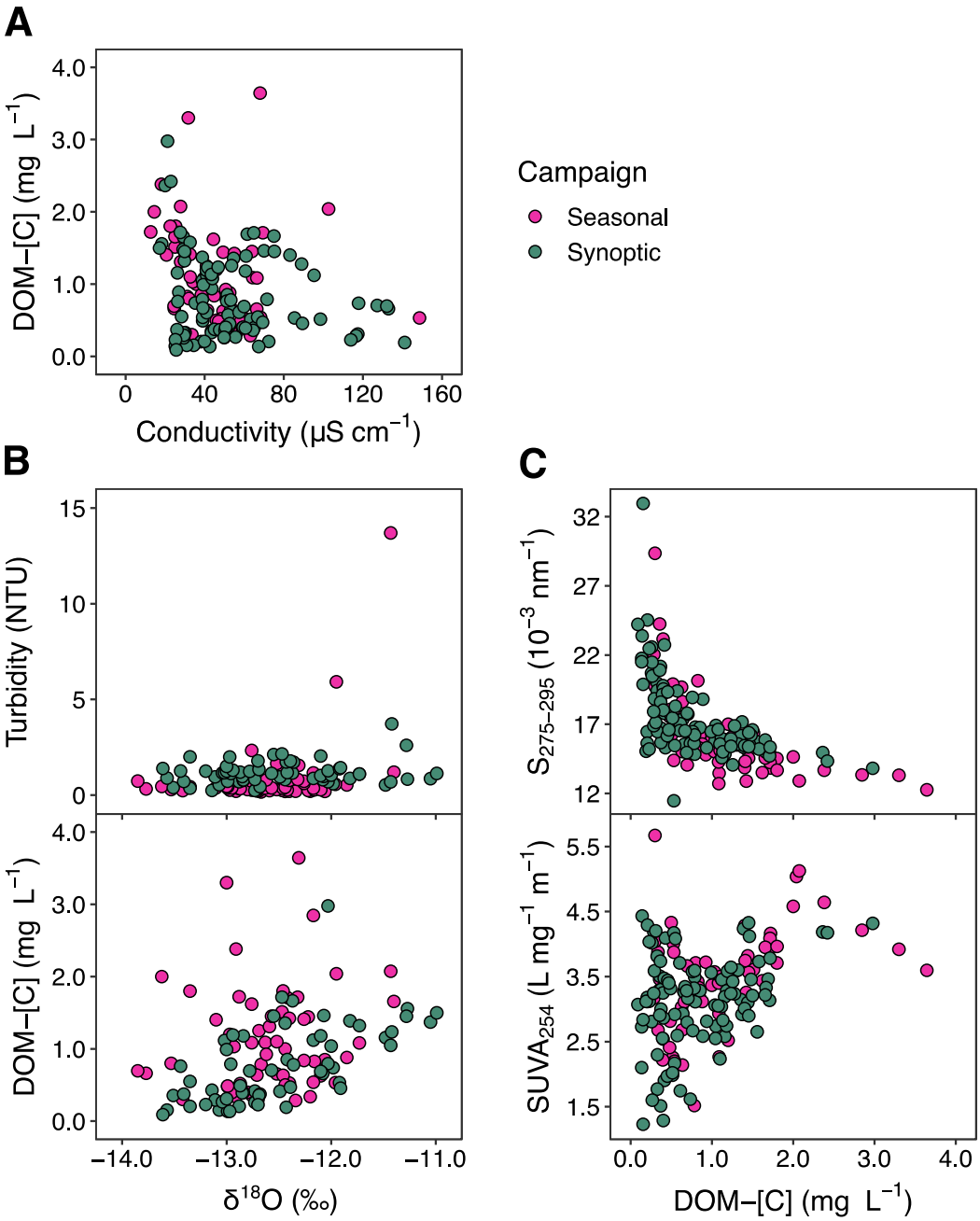

Figure 2-4. Biplots showing (A) DOM-[C] (mg L^{-1}) versus conductivity (µS cm^{-1}), (B) turbidity (NTU) and DOM-[C] (mg L^{-1}) versus $\delta^{18}O$ (‰), and (C) $S_{275-295}$ (10^{-3} nm^{-1}) and $SUVA_{254}$ (L mg^{-1} m^{-1}) versus DOM-[C] (mg L^{-1}) for stream water collected across Comox Lake subwatersheds during the seasonal and synoptic sampling campaigns. Note that 36 samples overlap between the two campaigns; these samples were all coded as "synoptic".

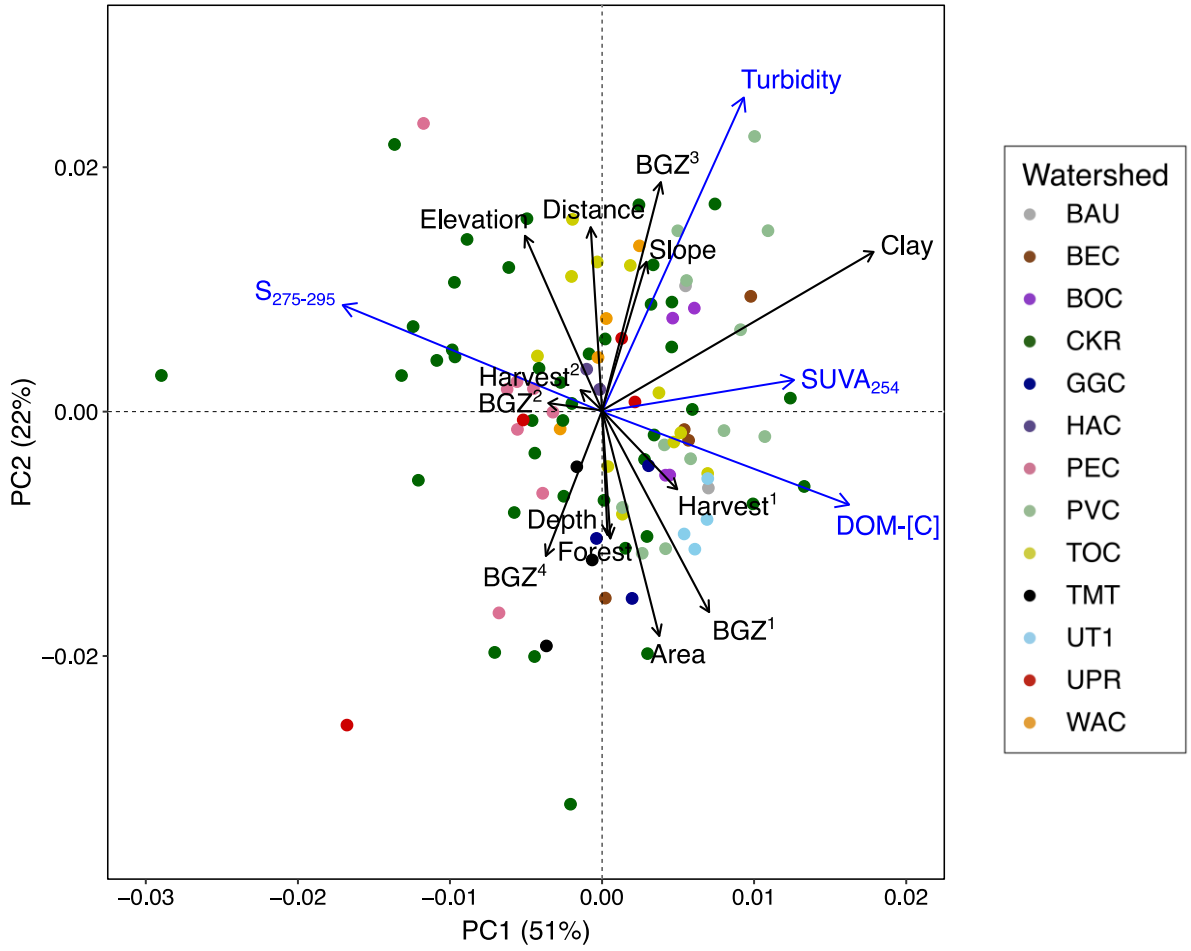

Figure 2-5. Indirect gradient analysis biplot of standardized landscape attributes and log-transformed water quality data for stream water samples collected during the synoptic campaign. Axis 1 and 2 explain 51% and 22% of the variance in stream water quality, respectively. Landscape attribute abbreviations are as follows: forest harvesting in the 2000s (Harvest^{1}), forest harvesting in the 2010s (Harvest^{2}), cutblock distance to sampling sites (Distance), forest cover (Forest), soil depth (Depth), soil clay content (Clay), slope angle (Slope), elevation (Elevation), and subwatershed area (Area). In addition, the four biogeoclimatic zones are abbreviated as: coastal western hemlock very dry maritime western (BGZ^{1}), coastal western hemlock very dry maritime eastern (BGZ^{2}), coastal western hemlock moist maritime montane (BGZ^{3}), and mountain hemlock moist maritime windward (BGZ^{4}).

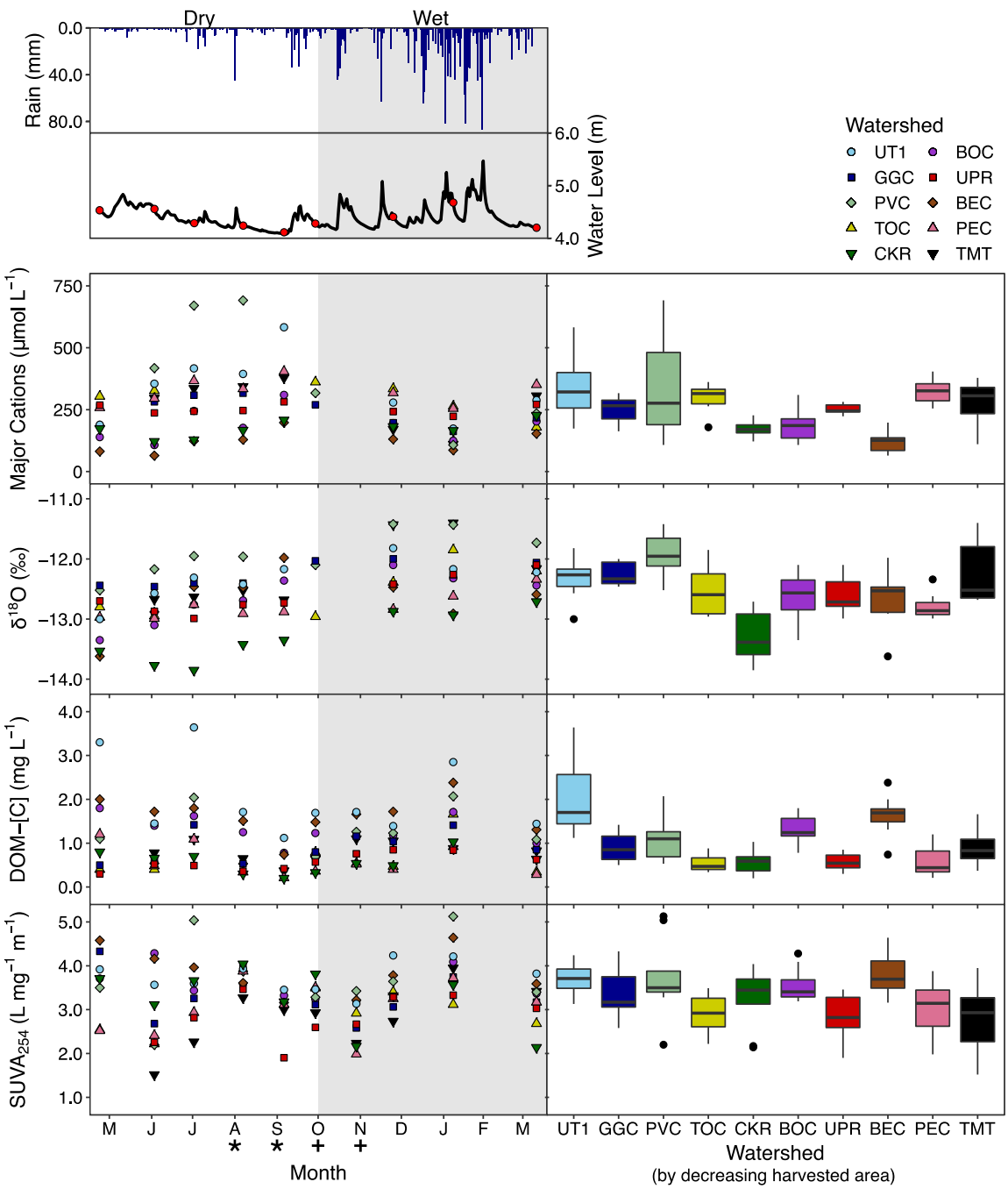

Figure 2-6. Seasonal (scatter plots, by month) and spatial (box plots, by watershed) patterns in major cations (µmol L^{-1}), $\delta^{18}O$ (‰), DOM-[C] (mg L^{-1}), and $SUVA_{254}$ (L mg^{-1} m^{-1}) for stream water collected across Comox Lake subwatersheds during the seasonal sampling campaign. Daily precipitation, water level (obtained from an Environment Canada hydrometric station on the Cruikshank River), and sampling dates (red circles) are shown in the top panel. The unshaded area indicates the dry period (24 April 2019 to 30 September 2019), while the wet period (1 October 2019 to 11 March 2020) is shown by grey shading. Symbols on the x-axis (August–September = *; October–November = +) represent months compared for Mann–Whitney U tests.

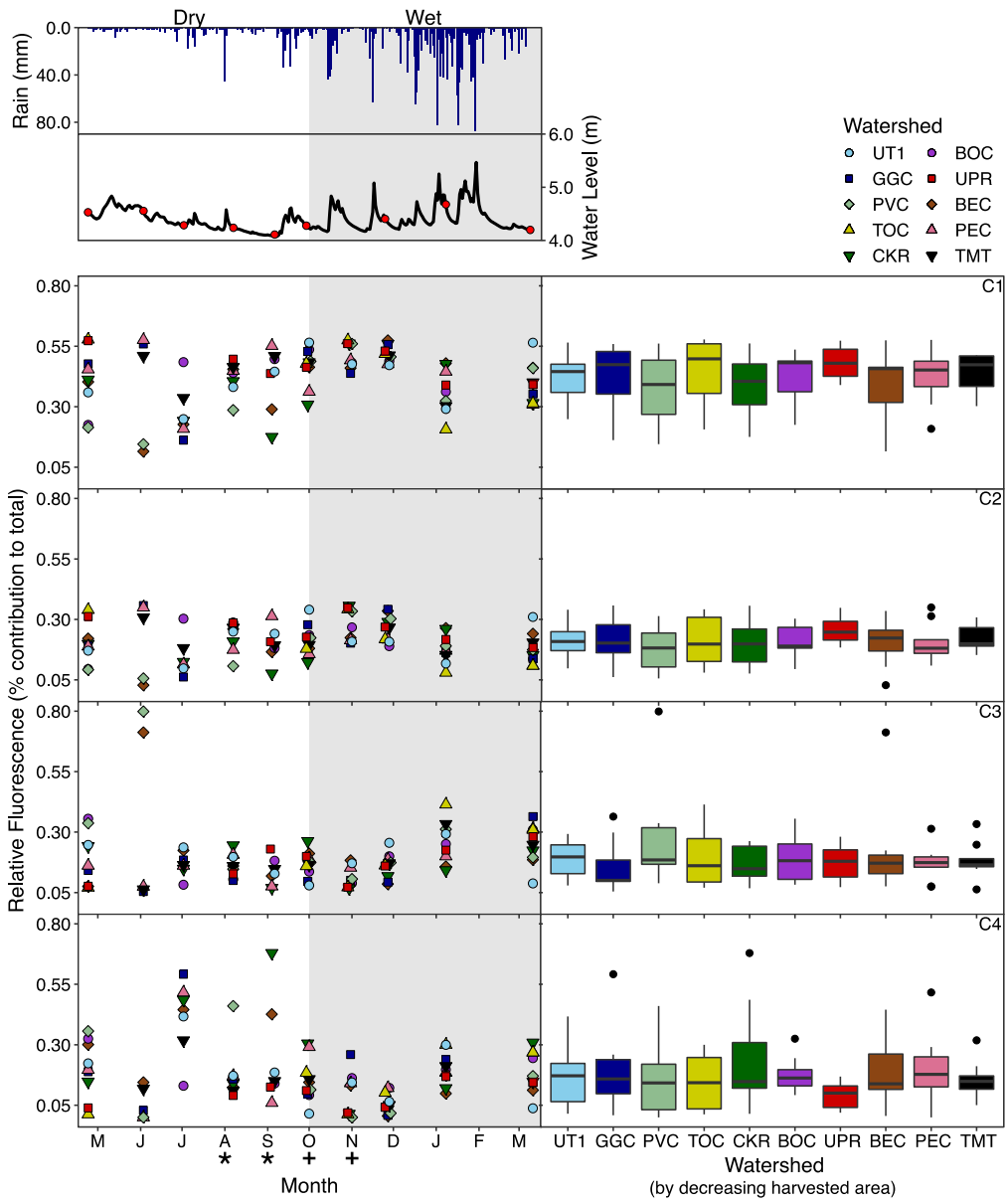

Figure 2-7. Seasonal (scatter plots, by month) and spatial (box plots, by watershed) patterns in relative fluorescence for stream water collected across Comox Lake subwatersheds during the seasonal sampling campaign. Parallel factor (PARAFAC) analysis was used to determine percent contribution of the four DOM components (C1–C4). Boxes comprise the 25th to 75th percentile, and whiskers represent the 5th and 95th percentile. Daily precipitation, water level (obtained from an Environment Canada hydrometric station on the Cruikshank River), and sampling dates (red circles) are shown in the top panel. The unshaded area indicates the dry period (24 April 2019 to 30 September 2019), while the wet period (1 October 2019 to 11 March 2020) is shown by grey shading. Symbols on the x-axis (August–September = *; October–November = +) represent months compared for Mann–Whitney U tests.

CH3: Hydrology overwhelms harvest history and landscape variation to control water quality and disinfection by-product formation potentials in forested Pacific Coast watersheds

3.1 Introduction

Suspended solids (SS) and dissolved organic matter (DOM) are ubiquitous in surface water supplies used as drinking sources (Roberts and Inniss, 2014). The pervasiveness of these parameters is not only useful for indicating the effects of land use changes and climate on water quality (Erdogan et al., 2018, Emelko et al., 2011), but they are also critically important for drinking water treatment (Zhai et al., 2017, Emelko et al., 2011, Ritson et al., 2014). Studies investigating the impacts of forest harvest and storm events on source waters rarely seek to determine the relative importance of each of these factors on water quality, and seldom consider drinking water treatability (Awad et al., 2018, Lee et al., 2018).

The efficiency of water treatment is often challenged by turbidity, total suspended solids (TSS), DOM carbon concentration (DOM-[C]), and DOM composition (Chang et al., 1983, Delpla and Rodriguez, 2017, Emelko et al., 2011, MWH, 2005, Pike et al., 2010). DOM is especially salient to drinking water providers because it drives infrastructure needs and chemical coagulant dosing requirements, and acts as the principal precursor in the formation of disinfection by-products (DBPs) (Li et al., 2014, Emelko et al., 2011). Trihalomethanes (THMs) and haloacetic acids (HAAs) are two regulated groups of DBPs that are produced through the reaction of DOM with chlorine disinfectants (Gonsior et al., 2014). High concentrations of aromatic DOM may increase the potential for DBP formation in water treatment plants (Richardson and Ternes, 2018, Zhai et al., 2017). Identifying key DOM drivers of DBPs is therefore critical to, and may help inform, drinking water treatment and management practices.

Typically, undisturbed forested watersheds regulate DOM export and sediment yield to produce high quality source waters (Berkowitz et al., 2014). With forest harvesting, water quality may deteriorate due to changes in hydrological flow paths and biogeochemical processes (Erdozain et al., 2018, Jordan, 2006, Kreutzweiser et al., 2008). Previous studies have shown that both harvest intensity (Schelker et al., 2014) and hydrologic connectivity (Erdogan et al., 2018) act concurrently to impact water quality in temperate forested watersheds; for example, clear cutting usually increases turbidity, TSS, and DOM-[C], but this effect may be dampened under conditions of low hydrologic connectivity (Schelker et al., 2012). Considering harvest history in

conjunction with variations in hydrology (e.g., the occurrence of storm events) is thus essential when assessing water quality and resultant DBP formation.

Storm event-driven changes in water quality are generally well understood (e.g., Coynel et al., 2005, Fellman et al., 2020, Hood et al., 2006), with emerging research further exploring effects on DBPs (e.g., Delpla and Rodriguez, 2017). However, responses can be complex because of regional variation in seasonal temperatures, antecedent moisture conditions, and hydroclimatic regimes (Bao et al., 2019, Fellman et al., 2020, Mistick and Johnson, 2020). While some prior studies have demonstrated that landscape attributes (e.g., land cover composition) determine water quality responses to rainfall events (e.g., Coch et al., 2019, Warner and Saros, 2019), others have reported that the magnitude and timing of rainfall are primary controls on water quality (e.g., Mistick and Johnson, 2020, Vidon et al., 2008). As a result, there is a need for additional research that considers differences in storm responses between diverse subwatersheds and consequent impacts on source waters.

Similar to storm events, the effects of forestry on source waters have been well studied (e.g., Dai et al., 2001, Erdozain et al., 2018, Jordan, 2006, Schelker et al., 2012). However, little of this research has focused on the interaction of forest harvest and storm events on water quality and treatability. Given the extensive history of forest harvest (Canadian Council of Forest Ministers, 2015, Hansen et al., 2013), high precipitation as rain and snow (Schnorbus, 2018), and propensity for intense storm events (Mistick and Johnson, 2020) on Canada's Pacific Coast, the Comox Lake watershed is well-suited for exploring variation in water quality and resultant DBPs across storm and baseflow conditions in subwatersheds with varying harvest intensities. In this study, we evaluated water quality (i.e., turbidity, TSS, DOM-[C], and spectral characteristics to inform DOM composition) and DBPs (i.e., THM formation potential (THM-FP) and HAA formation potential (HAA-FP)) in relation to forest harvest, storm events, and baseflow across four subwatershed sites. Stable water isotopes ($\delta^{18}O$) and major cation concentrations were also assessed to provide information on water sources and hydrologic flow paths. Within the Pacific Maritime ecozone, our objectives were to: (1) identify leading DOM drivers of DBP formation potentials; (2) investigate changes in water quality and DBPs under contrasting flow conditions; and (3) examine the combined effect of forest harvest and storm events on water quality and DBP formation potentials.

3.2 Methods

3.2.1 Study region

Similar to much of British Columbia (Government of British Columbia, 1996), the Comox Valley Regional District (CVRD) relies heavily on source waters that originate in forested watersheds. Within the region, 45,000 residents depend on the Comox Lake watershed for drinking water (Comox Valley Regional District, 2019a). The CVRD's drinking water supply is currently unfiltered and only chlorinated; however, a new filtration plant with ultraviolet irradiation and chlorination is being constructed to eliminate the need for turbidity-related boil water notices (Comox Valley Regional District, 2019b). Treatability of Comox Lake water is directly dependent on the water quality of inflowing tributary streams, which markedly declines during high rainfall events (Comox Valley Regional District, 2019b). Elevated turbidity levels in the lake during these events may interfere with chlorination and increase the risk of microbial contamination (Lechevallier et al., 1981, National Academies of Sciences, Engineering, and Medicine, 2018). The importance of Comox Lake as a forested drinking water source in a region characteristic of much of the Pacific coast prompted us to investigate four tributary streams in the watershed (Figure 3-1A).

The Comox Lake region is classified as having a nival dominated hybrid to pluvial hydroclimatic regime, indicating that the watershed experiences both rain and snow (W. C. Floyd, BC Ministry of Forests, Lands, Natural Resource Operations and Rural Development, personal communication, 7 July 2020). Mild, wet winters and cool to warm, dry summers characterize the local climate (Beck et al., 2018). The majority of precipitation occurs in autumn and winter, and is substantially reduced in spring and summer (Figure 2-2 and Table A2-1). Consequently, stream flows typically decline during warmer months and increase in cooler months. Annual peak flows generally occur from September through January and are often associated with atmospheric rivers (Sharma and Déry, 2020a, Sharma and Déry, 2020b). A snowmelt freshet can also appear in early to late spring in some high elevation subwatersheds (W. C. Floyd, 7 July 2020) that experience up to 58% of annual precipitation as snow (Table A2-1).

The Comox Lake watershed is typified by thick bedrock, shallow soils, and temperate rainforest. Bedrock is comprised mainly of Cretaceous sedimentary shale, sandstone, and conglomerate as well as Triassic igneous basalts (Muller et al., 1965, Natural Resources Canada,

1957), whilst soils are primarily characterized by well drained humo-ferric podzols (Valentine, 1978). Temperate rainforest trees overlay the entire watershed and predominantly consist of Douglas fir (*Pseudotsuga menziesii*), western hemlock (*Tsuga heterophylla*), western redcedar (*Thuja plicata*), and mountain hemlock (*Tsuga mertensiana*) (Government of British Columbia, 2003, MacKinnon et al., 1992). While the age of forests has significantly decreased with replanting after harvest (median age: 47 years, compared to old growth forests > 250 years), the composition of tree species has not substantially changed (P. Jorgenson, Mosaic Forest Management Corp., personal communication, 8 December 2020). For example, a private forestry company has replanted 76% of its land base with Douglas fir and a mix of western redcedar, western white pine (*Pinus monticola*), and yellow cypress (*Cupressus nootkatensis*) at high elevations (P. Jorgenson, 7 January 2021). Hemlock, maple (*Acer* spp.), and alder (*Alnus* spp.) may also grow in forest stands, depending on the occurrence of pre-harvest species and site conditions (P. Jorgenson, 7 January 2021).

Forest harvest represents the main anthropogenic land use in the Comox Lake watershed, which has resulted in extensive clearcut areas and a network of roads across subwatersheds. Timber harvesting of native old growth rainforest commenced in 1888 (Barraclough et al., 2016). A second pass of harvesting that began in the 1980s is now underway, whereby old growth and mature second growth forests are actively logged (Barraclough et al., 2016). Presently, 67% of the watershed is privately owned and operated by forestry companies, while municipal land holdings, privately owned lands, crown provincial land, and provincial parkland constitute the remaining 33% (Barraclough et al., 2016).

Four study sites (the Perserverance, Toma, Boston, and Moat subwatersheds) were selected to encapsulate variation in soils and forest harvest throughout the Comox Lake watershed. Recently, highest relative harvest occurred in the Perserverance and Toma subwatersheds, while harvest was relatively low in Boston and Moat (Table 3-1). In addition, the Boston and Perserverance subwatersheds had thicker soils (1.7–1.8 m) with higher clay contents (9–15%) whereas Moat and Toma were characterized by thin soils with reduced soil clay content (Table 3-1). Given these characteristics, we categorized our study subwatersheds as low harvest–shallow soil (LH-SS; Moat), low harvest–deep soil (LH-DS; Boston), high harvest–shallow soil (HH-SS; Toma), and high harvest–deep soil (HH-DS; Perserverance). Importantly, the headwaters of LH-SS and LH-DS originate in protected parkland and HH-DS has a small

reservoir (0.17 km^2 of 6.93 km^2 watershed area) located in its headwaters. HH-DS is also known for significant erosion of silty clay streambanks, which often result in elevated turbidity levels (Comox Valley Regional District, 2019a). Details on other catchment characteristics, including area, slope, elevation, and forest cover, are provided in Table 3-1 (refer to section 2.2.4 for a description on derivation of catchment characteristics).

3.2.2 Rainfall data

15-minute rainfall data were obtained from four hydrometric stations located throughout the Comox Lake watershed (Figure 3-1A). A different station was chosen for each study site based on site proximity; HH-DS was located 0.01 km from the nearest hydrometric station, LH-DS was 3.1 km, HH-SS was 5.1 km, and LH-SS was 9.9 km. Rainfall was variable across sites, as they were situated in contrasting topographies. A tipping bucket rain gauge was used to measure rainfall, which comprised 99% of precipitation during the monitoring period (September to mid-December; Wang et al., 2016).

3.2.3 Sampling campaigns and sample collection

Between 6 November and 14 December, 2019, high-frequency storm sampling was performed when rainfall events were forecasted to be greater than 25 mm in 24-hr. Storm water samples were collected via portable autosamplers (ISCO 6712) to represent the rising limb, peak, and falling limb of the storm hydrograph. Stream water levels were measured with a pressure transducer and recorded at 5-minute intervals on a CR300 Campbell Scientific data logger. During the monitoring period, we captured two storm events: one from 16–19 November and another from 5–9 December. Grab samples were also collected four times (approximately every three weeks from 3 September to 28 November, 2019) as stream water levels declined between periods of rainfall (Figure 3-1B). These "baseflow" (or "between-event") conditions were determined based on real-time water level data acquired from the "Cruikshank River Near the Mouth" hydrometric station (Figure 3-1A).

All storm and baseflow samples were processed for analysis of turbidity, TSS, DOM-[C], and spectral characteristics to inform DOM composition. Baseflow samples, and storm samples from the 5–9 December storm event, were also analyzed for cations (Ca^{2+}, K^{+}, Mg^{2+}, Na^{+}, and dissolved Fe [dFe]), $\delta^{18}O$, and DBPs. Prior to sample collection, all bottles and supplies were

acid-washed and rinsed with 18.2 MΩ (Milli-Q) water (refer to section 2.2.2 for additional details). At each site, storm water samples were automatically collected at the surface (20–50 cm) near the stream bank in 1-L polypropylene bottles, which were retrieved and capped with headspace within 24-hr of collection by the autosampler. Baseflow grab samples were collected immediately below the stream surface (0–30 cm) above the thalweg, and capped without headspace after a triplicate stream water rinse using polycarbonate (cations, $\delta^{18}O$, DOM-[C], and DOM composition) and high-density polyethylene (turbidity, TSS, and DBPs) bottles.

Following collection, unfiltered samples for DBPs were stored in the dark at 4ºC and shipped overnight to the University of Waterloo for analysis. All other samples were placed in a cool (4ºC) and dark environment and transported within 24-hr to the field laboratory. Upon arrival, samples for dissolved cations, $\delta^{18}O$, DOM-[C], and DOM composition were filtered (Millipore Express PLUS Membrane 0.45-µm PES). Cation and DOM-[C] samples were preserved to a pH of < 2 with trace-metal grade HNO_3 or HCl, respectively. Samples for TSS were filtered with pre-weighed filters (Whatman 0.7 µm GF/F), using a maximum of 1-L of sample water. After processing, TSS filters were frozen (-20ºC) while turbidity, cation, $\delta^{18}O$, DOM-[C], and DOM composition samples were stored in cool (4ºC) and dark conditions until analysis.

3.2.4 Stream water quality analyses

Filters used for TSS analysis were dried in an oven at 60ºC for 24-h and subsequently weighed to determine concentrations. Cations were analyzed on an Inductively Coupled Plasma – Optical Emission Spectrometer (Thermo Scientific iCAP 6300). Turbidity and DOM-[C] were measured using a portable turbidimeter (Hach 2100Q) and TOC-V analyzer (Shimadzu), respectively. $\delta^{18}O$ was quantified on a L2130-i analyzer (Picarro). Fluorescence and absorbance were measured on an Aqualog spectrofluorometer (Horiba Scientific) and used to calculate DOM compositional indices. Specifically, fluorescent excitation-emission matrices (EEMs) were input into parallel factor (PARAFAC) analysis to determine individual components (Murphy et al., 2013), while absorbance was used to compute the spectral slope coefficient from 275–295 nm ($S_{275\text{-}295}$), Napierian absorbance at 254 nm (a_{254}), and specific ultraviolet absorbance at 254 nm ($SUVA_{254}$) (Helms et al., 2008, Weishaar et al., 2003). To ensure accurate $SUVA_{254}$ values, we measured dFe (Poulin et al., 2014), which was always less than 0.11 mg L^{-1} and often below

detection, indicating negligible effects on $SUVA_{254}$. Additional information on laboratory measurements, calculation of DOM compositional metrics, and PARAFAC analysis is provided in section 2.2.3.

3.2.5 Analysis of true disinfection by-product formation potentials (DBP-FPs)

True DBP formation potentials (DBP-FPs) were evaluated using Standard Method 5710 B (APHA, AWWA, WEF, 2017). While other formation potential tests such as uniform formation conditions reflect DBP status within drinking water distribution systems (Summers et al., 1996), the true FP test assesses complete reactivity of DBP precursors and allows for cross-site comparisons. To determine DBP-FPs, sample chlorine demand was first evaluated. 250-mL of each sample was hyper-chlorinated with NaOCl at a concentration of 100 mg L^{-1} Cl_2 and then stored in the dark at room temperature (25ºC); residual chlorine was measured after 24-h. Chlorine demand was calculated by subtracting residual chlorine from the initial chlorine concentration. Three other 250-mL sub-samples were chlorinated thereafter, with doses equal to the chlorine demand plus 3, 5, and 7 mg L^{-1} Cl_2, and stored at room temperature (25ºC) in the dark for seven days. Chlorine residuals were then assessed again, and samples with residuals between 3 and 5 mg L^{-1} Cl_2 were preserved with Na_2SO_3 (for analysis of THMs) or NH_4Cl (HAAs) and analyzed by SGS Canada Inc. (Lakefield, Ontario).

Four THMs (trichloromethane (TCM), bromodichloromethane (BDCM), dibromochloromethane (DBCM), and tribromomethane (TBM)) and five HAAs (trichloroacetic acid (TCAA), dichloroacetic acid (DCAA), monochloroacetic acid (MCAA), monobromoacetic acid (MBAA), and dibromoacetic acid (DBAA)) were evaluated. For analysis of HAAs, 20-mL samples were acidified with concentrated H_2SO_4 to a pH of < 2. Afterwards, 15-g of Na_2SO_4 salt and 4-mL of MtBE were added to each sample. Samples were then shaken to transfer HAAs from the aqueous phase to MtBE. MtBE extracts were subsequently derivatized (methylated) with the addition of 10% H_2SO_4 in methanol, heated, and finally neutralized by the addition of saturated Na_2CO_3. Neutralized extracts were then separated from the aqueous phase and stored in cool (4ºC) conditions until analysis. Alongside HAAs analyses, a purge and trap concentrator was used to extract THMs from whole water samples; extracts were then kept at 4ºC until analysis. At the time of analysis, both THMs and HAAs extracts were measured on a gas

chromatograph with a mass spectrometer detector to derive true THM and HAA formation potentials.

3.2.6 Statistical analyses

3.2.6.1 Determining water quality and DBP-FPs patterns with baseflow and stormflow

All statistical analyses were conducted using R (4.0.2). Variables were assessed for linearity and normality (Shapiro–Wilk test) before analysis to determine whether data transformations were required (packages *stats* and *GGally*) (R Core Team, 2020, Schloerke et al., 2020). To evaluate water quality and DBP-FPs during stormflow and baseflow conditions, box plots and scatterplots were produced and the Mann–Whitney U test was computed (packages *stats*, *ggplot2*, and *factoextra*) (R Core Team, 2020, Wickham, 2016, Kassambara and Mundt, 2020). Baseflow and stormflow samples were grouped for Mann–Whitney U tests, two-way ANOVAs (further described in section 3.2.6.2), and multiple linear regression (3.2.6.3), where baseflow samples included those collected monthly during stable conditions, the first sample of the November 16–19 storm event, and the first two samples of the December 5–9 event, and stormflow samples included those remaining from the two storm events. Early "storm" samples classified as baseflow represented pre-event conditions (i.e., stream water levels had not yet risen in response to rainfall). Major cations (Ca^{2+}, K^{+}, Mg^{2+}, Na^{+}) were co-correlated and thus summed as a molar total for data analyses.

3.2.6.2 Comparing water quality and DBP-FPs across sites and flow condition

Two-way ANOVAs were used to simultaneously compare the effect of site and flow condition (i.e., baseflow versus stormflow) on water quality and DBP-FPs (package *stats*) (R Core Team, 2020). Individual ANOVAs were constructed for major cations, $\delta^{18}O$, turbidity, TSS, DOM-[C], $SUVA_{254}$, $S_{275\text{-}295}$, PARAFAC components, total THM-FP (TTHM-FP), and total HAA-FP (THAA-FP). When necessary, metrics were log transformed to improve data conformation to normality. A 5% significance level ($\alpha = 0.05$) was used to evaluate both main effects (i.e., site and flow condition) and interaction effects. Post-hoc site comparisons were assessed using Tukey honestly significant difference tests. After finalizing ANOVAs, diagnostic tests were performed to ensure that assumptions of residual normality and homogeneity were satisfied.

3.2.6.3 Assessing relationships between water quality indicators and DBP-FPs

Multiple linear regression (MLR) models were used to examine the influence of water quality indicators on DBP-FPs (package *stats*) (R Core Team, 2020, Zuur et al., 2007). Independent MLR models were created for both TTHM-FP and THAA-FP. In each model, water quality indicators included DOM-[C], a_{254}, $SUVA_{254}$, and $S_{275\text{-}295}$, which were all tested for independence, multicollinearity ($r > 0.7$), and skewness (> 2.0). Given that a_{254} was highly correlated with DOM-[C] (0.901, $p < 0.001$), this metric was not analyzed further. To improve model fits, TTHM-FP and THAA-FP were log transformed while water quality indicators were standardized (i.e., data were scaled to establish the mean and standard deviation at zero and one, respectively) and log transformed when required. Significance values for water quality indicators were computed via one-way ANOVAs, using $\alpha = 0.05$. Post-estimation diagnostics were also performed to verify that the statistical assumptions of normality, homogeneity, and multicollinearity were fulfilled. Although MLR models could be expanded upon by creating nonlinear regression models (as a nonlinear correlation exists between DOM-[C], $SUVA_{254}$, $S_{275\text{-}295}$, and DBP-FPs), this analysis was beyond the scope of our study.

3.3 Results

3.3.1 Weather and storm dynamics

Relative to the climate normal (9.4ºC, 2193 mm yr^{-1}), the Comox Lake watershed was warmer (9.9ºC) and experienced less precipitation (1512 mm yr^{-1}) in 2019 (Pacific Climate Impacts Consortium, 2019, Wang et al., 2016). Although dry conditions persisted throughout the year, with seasonal rainfall ranging from 154 mm (spring) to 681 mm (autumn), we were able to capture two storm events in autumn 2019 (Figure 3-1B). Rainfall during the 16–19 November (5–9 December) events ranged between 28.8–82.2 mm (14.2–35.2 mm) across the watershed, resulting in a rise in stream water level at each subwatershed site, with greatest increases observed at LH-DS (43 cm, 19 cm; November, December events), followed by LH-SS (41 cm, 10 cm), HH-DS (34 cm, 9 cm), and HH-SS (28 cm, 8 cm) (Table 3-1). Stage measurements also revealed that sites responded quickly to rainfall, with steep rising limbs and a quick return to baseflow conditions after peak stormflow (e.g., Figures 3-2 and 3-3).

3.3.2 Variation in water quality across sites during baseflow and storm events

All water quality metrics except for PARAFAC components displayed a significant flow condition effect, indicating that baseflow and stormflow water quality were different from one another. Subwatersheds displayed more depleted $\delta^{18}O$ ($F_{1,23} = 9.528$, $p < 0.01$) and higher major cation concentrations ($F_{1,23} = 9.814$, $p < 0.01$) under stable baseflow conditions than during storm events (Figure 3-3 and Tables A2-2, A2-3). In high flow conditions, turbidity ($F_{1,87} = 36.215$, $p < 0.001$), TSS ($F_{1,87} = 30.404$, $p < 0.001$), and DOM-[C] ($F_{1,86} = 114.666$, $p < 0.001$) increased across sites when compared to baseflow (Figures 3-2, 3-3 and Tables A2-2, A2-3, A2-4). Notably, TSS (turbidity) peaked at 120.3 mg L^{-1} (82.7 NTU) during the November event, reflecting a 93-fold (32-fold) increase relative to baseflow. Changes in DOM-[C] were also accompanied by a shift towards more aromatic, high molecular weight DOM ($SUVA_{254}$: $F_{1,86} = 51.574$, $p < 0.001$; $S_{275\text{-}295}$: $F_{1,87} = 56.202$, $p < 0.001$) during storms (Figures 3-2, 3-3 and Tables A2-2, A2-3, A2-4). Despite this, none of the PARAFAC components identified changed significantly with flow. Four PARAFAC components comprised the DOM pool: the first two (C1 and C2) were indicative of terrestrial humic-like material, while the second two (C3 and C4) were consistent with a microbial protein-like origin (Figure A2-1). The DOM compositional signature was mainly composed of C1 and C2 during both baseflow (79.8%) and stormflow (81.9%) (Figure A2-2). Additional information on PARAFAC components, including potential DOM characteristics, can be found in section 2.3.2.

To further investigate flow-driven changes in stream water quality, we examined hysteresis patterns and compared variation between stormflow and baseflow within individual subwatershed sites for those metrics with a significant flow condition effect (Table A2-5). While only a couple of sites (two or less) showed significant increases in TSS and $SUVA_{254}$ with peak flow, three or more sites displayed significant changes in turbidity, DOM-[C], and $S_{275\text{-}295}$ (Table A2-5). We therefore focused on patterns in these three metrics: turbidity and DOM-[C] displayed clockwise to no hysteresis during storm events, with higher concentrations on the rising limb of the hydrograph, whereas $S_{275\text{-}295}$ showed counter-clockwise hysteresis with increased values on the falling limb (Figure 3-4). When comparing the storm event in December to November, increases in stream water level and resultant water quality changes and hysteresis were much smaller (Figures 3-2 and 3-3). During both events, however, changes in turbidity, DOM-[C], and

$S_{275\text{-}295}$ prevailed across all sites, with none of the four subwatershed types displaying stronger effects on overall water quality when compared to each other.

As opposed to the differences observed between baseflow and stormflow, DOM quantity and quality exhibited little variation across subwatershed sites. Under both flow conditions, there were no significant differences amongst sites for DOM-[C], $SUVA_{254}$, $S_{275\text{-}295}$, or PARAFAC components. In contrast, turbidity ($F_{3,87} = 25.152$, $p < 0.001$) and TSS ($F_{3,87} = 14.446$, $p < 0.001$) concentrations were significantly elevated at HH-DS relative to the three other sites. There was no significant interaction effect between site and flow condition for any of the parameters examined, indicating similar water quality responses to differing flow across sites.

3.3.3 Variation in DBP-FPs across sites during baseflow and storm events

Across all study sites, we identified two THMs (BDCM and TCM) and two HAAs (DCAA and TCAA); all other DBPs (TBM, DBCM, MCAA, MBAA, and DBAA) were below the detection limit. TTHM-FP and THAA-FP both exhibited a significant flow condition effect, with greater concentrations during stormflow (TTHM-FP: $F_{1,31} = 11.926$, $p < 0.01$; THAA-FP: $F_{1,31} = 10.386$, $p < 0.01$) than during baseflow (Figure 3-3 and Tables A2-2, A2-3). While all sites showed increases in TTHM-FP and THAA-FP with peak flow, these were only significant in a few subwatersheds; however, the lack of significant relationships may be attributed to low statistical power (Table A2-5). TTHM-FP and THAA-FP also exhibited clockwise to no hysteresis during storm events, with higher concentrations on the rising limb of the hydrograph (Figure 3-4). Whilst baseflow and stormflow DBP-FPs were different from one another, TTHM-FP and THAA-FP did not significantly vary among subwatershed sites. Site comparisons revealed strong impacts on DBP-FPs with no differentiation based on subwatershed type. Furthermore, no significant interaction effects were found between site and flow condition, which suggests that TTHM-FP and THAA-FP similarly changed across sites in response to varying flow.

3.3.4 Linkages between DBP-FPs and water quality

True DBP-FPs were directly linked to water quality. Formation potentials increased with elevated DOM-[C] ($R^2 = 0.57$, $R^2 = 0.62$; TTHM-FP, THAA-FP) and more aromatic, high molecular weight DOM ($SUVA_{254}$: $R^2 = 0.16$, $R^2 = 0.20$; $S_{275\text{-}295}$: $R^2 = 0.06$, $R^2 = 0.09$) (Figure

A2-3). In particular, TTHM-FP was directly proportional to DOM-[C] ($b = 0.405$, $p < 0.001$) and $S_{275\text{-}295}$ ($b = 0.133$, $p < 0.05$), while THAA-FP was positively correlated with DOM-[C] ($b = 0.380$, $p < 0.001$) and $SUVA_{254}$ ($b = 0.105$, $p < 0.1$) (Table A2-6). Reasonably strong explanatory capabilities and good fits (i.e., high adjusted-R^2 values and low RMSE values) were observed for both TTHM-FP and THAA-FP models.

3.4 Discussion

3.4.1 Hydro-meteorological impacts on water sources, flow paths, and stream responses

The Comox Lake watershed experienced anomalously warm and dry conditions in 2019, which produced occasional high-flow storm events and extended low-flow baseflows throughout the study period. Changes in major cations and $\delta^{18}O$ indicated that surficial flow paths became more prominent with rainfall while baseflows were more strongly derived from groundwater sources connected to streams by deeper flow paths. Stream responses at each site appeared to be affected by antecedent moisture, which typically increases through autumn in this region as forest soils become progressively saturated due to the occurrence of autumn rains (Schnorbus, 2018). With increasingly saturated soils, a more rapid and greater flow response may have been generated that quickly discharged a high proportion of storm water into streams (Winkler et al., 2010). Although significant stream water quality responses were observed when comparing stormflow to baseflow, the magnitude of change was variable between events. More intense storms (e.g., the November event) generated stronger stream water quality and DBP-FPs responses, which aligns with the findings of other research. For example, Mistick and Johnson (2020) found that larger and faster rates of change in DOM-[C] occurred during periods of high rainfall. It is therefore critical to assess rainfall magnitude when evaluating flow-driven changes in stream water quality and DBP-FPs.

3.4.2 Key DOM drivers of DBP-FPs

The key driver of DBP-FPs was DOM-[C]. While DOM-[C] strongly predicted TTHM-FP and THAA-FP, compositional measures (i.e., $SUVA_{254}$ and $S_{275\text{-}295}$) were weaker predictors that moderated the DOM-[C] response. Nevertheless, DBP-FPs mimicked changes in both DOM-[C] and DOM composition across Comox Lake subwatersheds. Given that DOM-[C] was highly correlated with a_{254}, aromaticity also plays a role in determining DBP-FPs; DOM-[C] may

simply overwhelm the effects of DOM composition in MLR models. Constructing a model with a_{254}, which is indicative of both concentration and aromaticity, is therefore warranted to ascertain if a_{254} supersedes DOM-[C] as a key driver. Other studies have similarly noted strong DOM influences on DBP-FPs, with key metrics such as DOM-[C] yielding higher TTHM-FP and THAA-FP in drinking water (Chow et al., 2011, Chowdhury, 2018, Richardson and Ternes, 2018). Simple parameters such as DOM-[C] (or a_{254}) may therefore remain the most informative metrics for evaluating variation in DBP-FPs within forested subwatersheds. It is also important to note that chlorinated DBP-FPs prevailed across subwatershed sites; brominated TTHM-FP and THAA-FP, which are more toxic than chlorinated ones (Richardson and Ternes, 2018), likely did not form in the Comox Lake watershed due to low bromide concentrations (< detection limit of 0.02 mg L^{-1}; data not shown) across all of our sampling dates.

3.4.3 Water quality and DBP-FPs dynamics in storm and baseflow

Under stable baseflow conditions, low constituent concentrations occurred in stream water; turbidity (< 5 NTU) and DOM-[C] (total organic carbon < 4 mg L^{-1}) did not exceed thresholds instituted for treatment of raw (i.e., untreated) water (Government of British Columbia, 2001). Each of these constituents increased during storm events (especially with high-magnitude rainfall), and occasionally passed thresholds of concern. Stormflow turbidity values peaked at 82.7 NTU; rapid increases in turbidity can limit the efficiency of chlorination processes designed to remove pathogens (Lechevallier et al., 1981). This underscores the need to control the sediment source or construct a filtration plant that will be readily able to reduce turbidity to acceptable levels of 5 NTU or less (preferably less than 1 NTU) (Health Canada, 2020, National Academies of Sciences, Engineering, and Medicine, 2018). Also during storm events, DOM-[C] surpassed the 4 mg L^{-1} threshold for a short period of time, peaking at 4.62 mg L^{-1}. An increase in stream water DOM-[C] is of concern to drinking water providers because DOM not only exerts a chlorine demand that can deteriorate a plant's pathogen inactivation capability, but it also favours the development of distribution system biofilms that have the potential to harbor pathogens (Government of Canada, 2020). To establish biological stability in distribution systems, health guidelines recommend a DOM-[C] level of less than 1.8 mg L^{-1} (Health Canada, 2020). Similar to DOM-[C], DBP-FPs did not increase drastically during storm events, with peak increases of 268 μg L^{-1} and 258 μg L^{-1} for TTHM-FP and THAA-FP,

respectively. Should concerns of DBP formation arise throughout storm events, the aforementioned filtration plant would ensure adequate and efficient disinfection. It should also be underscored that true DBP-FPs analysis involves hyperchlorination at doses that far exceed those applied in typical drinking water treatment plants (MWH, 2005). Thus, DBP formation under standard treatment conditions would almost certainly not be of concern in our study subwatersheds; this is further verified by the stream water DOM-[C] data, which remained fairly low overall.

Our findings corroborate other studies showing strong impacts of storm events on turbidity, DOM-[C], and DOM composition (e.g., Fellman et al., 2020, Hood et al., 2006, Vidon et al., 2008) and add to emerging research on storm DBP-FPs responses (e.g., Delpla and Rodriguez, 2017). During storm events, an increase in surficial flow activates new flow pathways that facilitate the transport of SS and DOM-[C] through shallow soil horizons (Coch et al., 2019, Fellman et al., 2020, Wagner et al., 2019). This results in a high degree of DOM leaching from recently produced soil organic matter, and also increases sediment entrainment (Delpla and Rodriguez, 2017, Hood et al., 2006, Oliver et al., 2017). Clockwise hysteresis patterns for DOM-[C] and turbidity indicate that surficial flow paths (1) rapidly transport near-stream DOM into the stream network upon reaching a critical soil saturation threshold (Birkel et al., 2017, Butturini et al., 2006), and (2) quickly deliver sediments from channel banks to streams while in-stream sediments remobilize (Smith and Dragovich, 2009). This consequently increases turbidity and DOM-[C] and the DOM pool shifts towards a more aromatic, high molecular weight composition that is indicative of fresher, plant-derived material (Coch et al., 2019, Delpla and Rodriguez, 2017). Hysteresis patterns further suggest that once shallower soil layers cease delivering water to streams, deeper flow pathways contribute more to stream flow (Birkel et al., 2017). With receding storm waters, flow travels through deeper soil horizons that are not major sources of sediment (Smith and Dragovich, 2009), but contain older, more processed DOM and less DOM-[C] (Kaiser and Kalbitz, 2012, Oliver et al., 2017, Werner et al., 2019). This loss of surficial flow paths therefore reduces stream water turbidity, DOM-[C], and DOM aromaticity and molecular weight (Werner et al., 2019). Importantly, all of these changes in water quality were noted across subwatershed sites. Given that storm events control the amount of DOM-[C] and DOM composition in stream water, DBP-FPs are also affected (Chow et al., 2011). An increase in DOM-[C] and more aromatic, high molecular weight DOM in stormflow typically

leads to greater TTHM-FP and THAA-FP following chlorination (Awad et al., 2018, Delpla and Rodriguez, 2017); this was also detected across all sites. Finally, hysteresis patterns also suggest a high level of responsiveness of SS, DOM, and DBP-FPs to small changes in stream flow.

The impacts of storm events on water quality and DBP-FPs observed here are consistent with other studies conducted in different forested landscapes. Previous research has reported increases in turbidity, DOM-[C], and aromatic DOM during storm events in forested tropical (Sánchez-Murillo et al., 2019), subtropical (Bao et al., 2019), temperate interior (Vidon et al., 2008), and coastal temperate (Fellman et al., 2020, Hood et al., 2006, Mistick and Johnson, 2020) watersheds. While few studies have documented storm DBP-FPs responses, those that have (e.g., Delpla and Rodriguez, 2017) report increased DBP-FPs in stormflow across forested watersheds in temperate regions. While our study subwatersheds experienced quick mobilization of SS and DOM during storm events, stream water quality and DBP-FPs responses were analogous across sites regardless of varying levels of forest harvest (further discussed in section 3.4.4) and soil characteristics. Rather than landscape differences driving variation in water quality and resultant DBP-FPs, hydrology was the dominant control (discussed in section 3.4.5). This highlights the importance of investigating the combined effect of forest harvest and flow conditions on stream water sources.

3.4.4 Joint effects of forest harvest and storm events on water quality and DBP-FPs

Despite harvest intensities ranging from 6.5 to 54.2% of watershed cover, and substantial differences in watershed soils, most subwatershed sites displayed similar increases in turbidity with stormflow. One site (HH-DS), however, had notably elevated storm turbidity relative to the three other sites. Prior studies have shown increased turbidity due to high-intensity forest harvesting (Erdogan et al., 2018) or the development, active use, and maintenance of resource roads (Jordan, 2006). While each of these activities accelerate soil surface erosion, enhanced turbidity at HH-DS was likely caused by natural erosion of fine silty-clay stream banks during high rainfall events (Barraclough et al., 2016).

Spatially-distinct subwatershed sites also showed analogous changes in DOM-[C] and DOM composition with increased flow during storm events, irrespective of the amount of harvested area or other catchment characteristics upstream. Forest harvest may have had a negligible effect on stream waters because logging slash, which is usually a major source of

DOM (Lee and Lajtha, 2016), was burned after harvest (personal observation, 19 October 2019). Slash (i.e., fine and coarse woody debris) is often left to decompose in harvested areas, which increases organic matter leaching and thus elevates DOM-[C] and aromatic, humic-like DOM in stream waters (Berkowitz et al., 2014, Dai et al., 2001). Prior research has indicated that, compared to harvested watersheds with little to no slash, forested watersheds have greater organic matter inputs (i.e., forest floor wood) that result in increased DOM-[C] and more aromatic, humic-like DOM in stream water (e.g., Lajtha and Jones, 2018, Lee and Lajtha, 2016). These studies thus suggest that old growth forest landscapes yield more aromatic, humic-like, and higher DOM-[C] than second growth (i.e., regenerating) forests. Given that our study subwatersheds largely consist of second growth forest, it is possible that DOM-[C] is reduced with a more aliphatic and protein-like composition (i.e., relative to what would have normally occurred in an old growth forest). The prevalence of second growth forests (i.e., past harvest in this region), coupled with slash removal, may explain the lack of effect of forest harvest on stream water DOM in Comox lake subwatersheds.

Our research, which did not show significant differences in storm water quality (and hence DBP-FPs) related to recent forest harvest, indicates that current landscape alteration has minimal impact on water quality in the Comox Lake watershed. These findings must be considered carefully, however, as this study was based on a limited sample size of four subwatersheds. Previous work in the Midwestern US similarly found that watersheds displayed comparable storm responses to one another, regardless of land use (Vidon et al., 2008). Here, the primary controls on water quality were precipitation and discharge (Vidon et al., 2008). Hydrology may therefore act as a key control on storm water quality and DBP-FPs in the Comox Lake watershed, with variation in the soil water table and hydrologic flow paths regulating stream dynamics during storms (Dai et al., 2001).

3.4.5 Importance of hydrologic connectivity in driving water quality and resultant DBP-FPs

Hydrologic shifts in turbidity, DOM-[C], DOM composition, and DBP-FPs, which are supported by our analysis of changing flow paths (via major cations, $\delta^{18}O$, and hysteresis), clearly overwhelm the effects of variation in recent forest harvest and soil characteristics. Given the over-riding importance of hydrology in controlling stream water quality and subsequent DBP formation in this region, it is critical that practitioners continue to consider the effects of

hydrologic connectivity on source waters. Hydrologic connectivity in Comox Lake subwatersheds may increase in the future with climate-driven changes in rainfall intensity, duration, and frequency (Chow et al., 2011, Parr et al., 2019). With enhanced hydrologic connectivity, new flow paths may be activated while water fluxes increase; not only would this result in elevated turbidity, DOM-[C], and more aromatic DOM, but it may also cause faster shifts in each of these metrics during storms in harvested areas (Erdogan et al., 2018, Mistick and Johnson, 2020). To further assess these relationships, future research should attempt to capture major storm events over additional watersheds. Continued evaluation of turbidity, DOM-[C], and DOM composition will also be essential for monitoring and adapting management strategies for effective drinking water treatment, especially as storm events become more prevalent in the future.

3.5 Tables

Table 3-1. Catchment characteristics (area, slope, elevation, soil thickness, clay content, and forest cover), harvested areas (1985-2019), and dates of the two storms at each of the four subwatershed sites in the Comox Lake watershed. Both rainfall amounts and corresponding stream water level increases are noted for the two storm events. Note that areas harvested between 1985 and 2019 were not included in percent forest cover.

Site	Area (km^2)	Mean slope (º Angle)	Mean elevation (m)	Mean soil thickness (m)	Mean clay content (% Soil)	Forest cover (% Area)	Harvest 1985-2019 (% Area)	Storm 1 Nov. 16–19, 2019		Storm 2 Dec. 5–9, 2019	
LH-DS	9.2	26.3	801.7	1.71	9.11	85.0	12.7	43.2*	43†	17.1*	19†
LH-SS	29.8	24.2	1083.4	1.29	4.20	72.4	6.5	25.4*	41†	14.2*	10†
HH-DS	6.9	11.4	379.2	1.81	14.66	45.8	54.2	53.8*	34†	20.4*	9†
HH-SS	3.6	24.7	952.3	1.10	4.07	67.3	32.7	82.2*	28†	35.2*	8†

* Denotes rainfall (mm).

† Denotes rise in stream water level (cm).

3.6 Figures

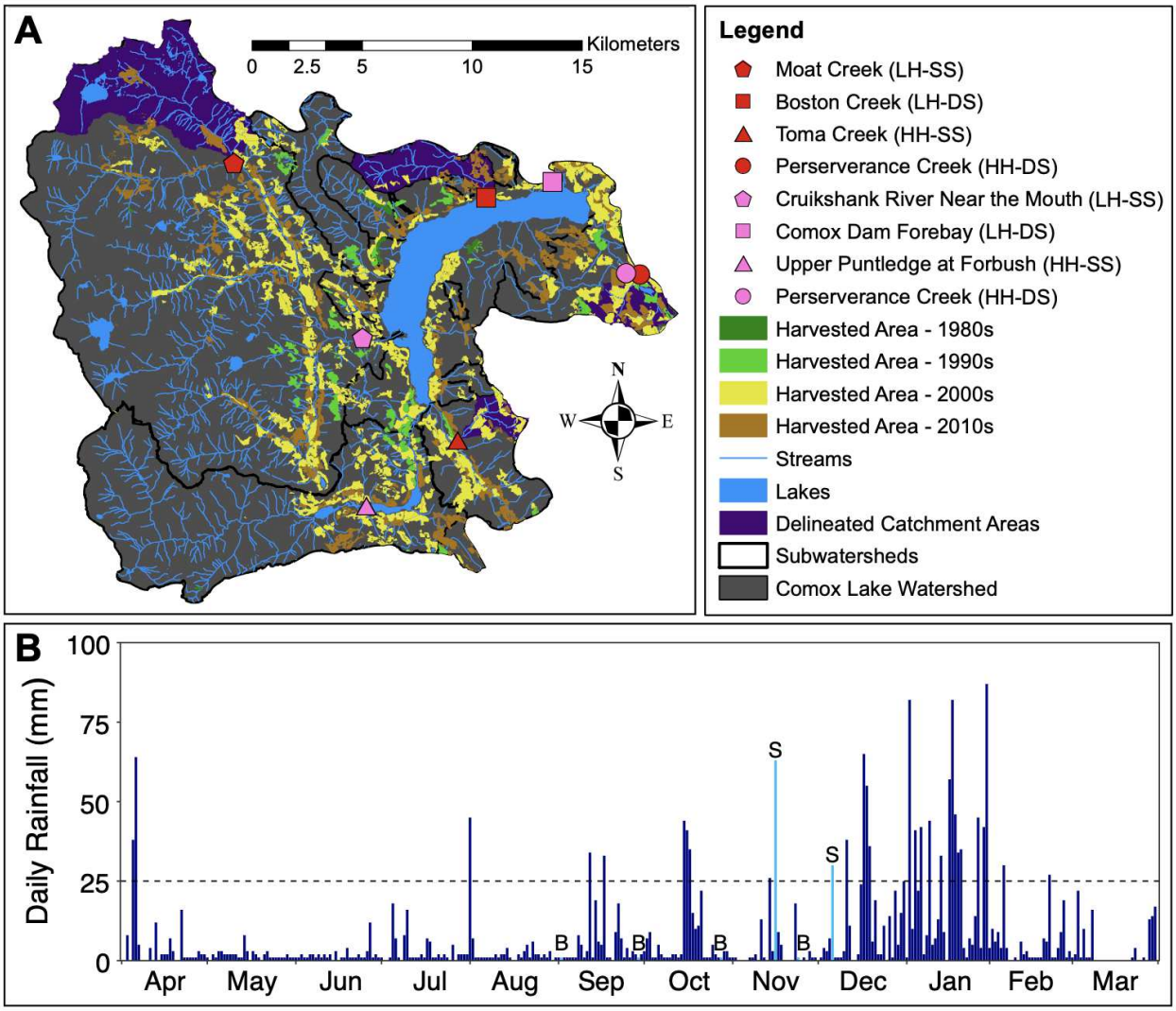

Figure 3-1. (A) The Comox Lake watershed. Streams and harvested areas are shown on the map in addition to other relevant features. Storm and baseflow sampling, and collection of water level data, were performed at four study sites (in red): Moat Creek (low harvest–shallow soil; LH-SS), Boston Creek (low harvest–deep soil; LH-DS), Toma Creek (high harvest–shallow soil; HH-SS), and Perserverance Creek (high harvest–deep soil; HH-DS). Rainfall data were collected from the nearest hydrometric station (in pink). (B) Total daily rainfall (mm) in the Comox Lake watershed from 1 April 2019 to 31 March 2020. Rainfall data were obtained from the "Cruikshank River Near the Mouth" hydrometric station. Light blue bars correspond to sample collection dates; B represents baseflow sample collection while S represents storm events captured during the study period.

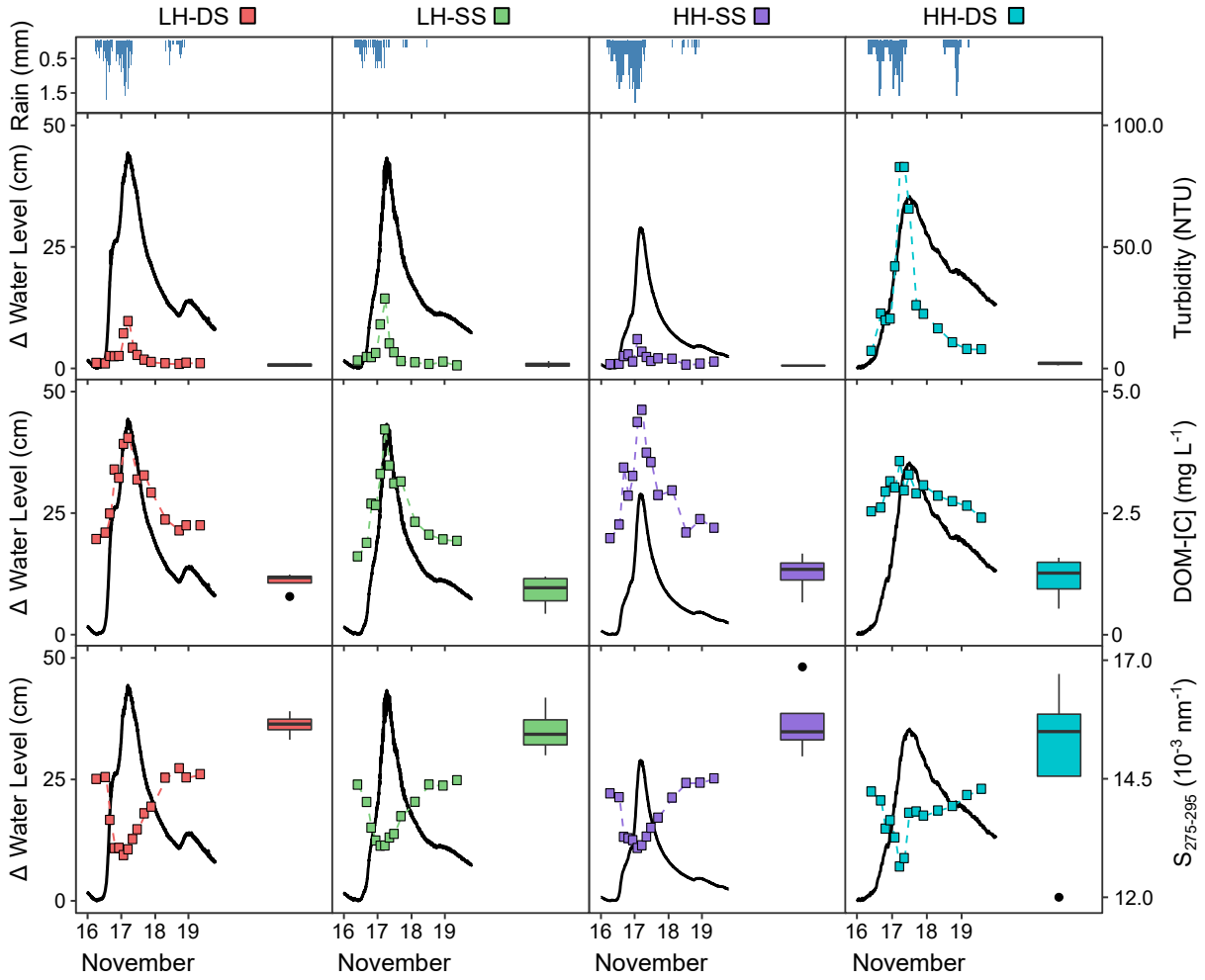

Figure 3-2. Rainfall (mm), stream water level (cm), and water quality (i.e., turbidity (NTU), DOM-[C] (mg L^{-1}), and $S_{275\text{-}295}$ (10^{-3} nm^{-1})) responses across subwatershed sites during the Nov. 16–19, 2019 storm event. Monthly baseflow samples collected during stable conditions are shown as box plots for comparison. Boxes comprise the 25th to 75th percentile, and whiskers represent the 5th and 95th percentile. Stream water level data were normalized to zero.

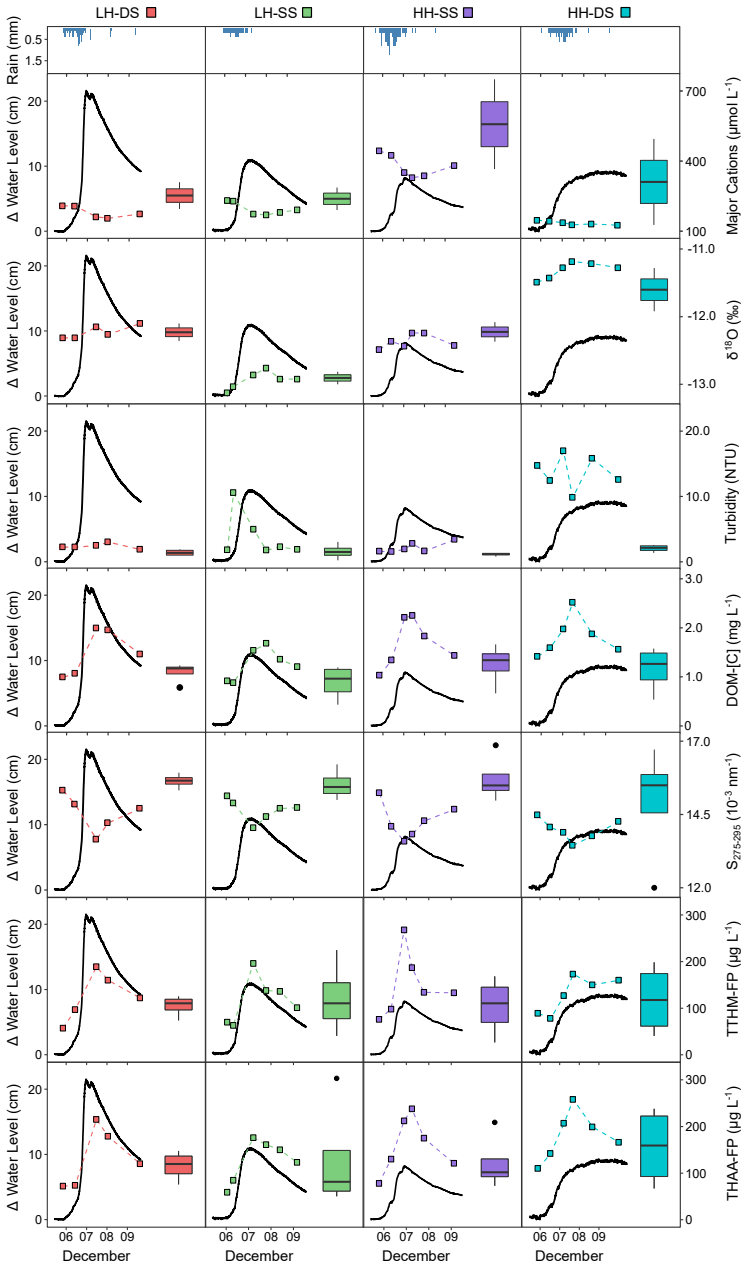

Figure 3-3. Rainfall (mm), stream water level (cm), water quality (i.e., major cations (µmol L^{-1}) $\delta^{18}O$ (‰), turbidity (NTU), DOM-[C] (mg L^{-1}), and $S_{275\text{-}295}$ (10^{-3} nm^{-1})), and DBP-FPs (i.e., TTHM-FP (µg L^{-1}) and THAA-FP (µg L^{-1})) responses across subwatershed sites during the Dec. 5–9, 2019 storm event. Monthly baseflow samples collected during stable conditions are shown as box plots for comparison. Boxes comprise the 25th to 75th percentile, and whiskers represent the 5th and 95th percentile. Stream water level data were normalized to zero and individual THM and HAA species FPs were summed to yield total FPs.

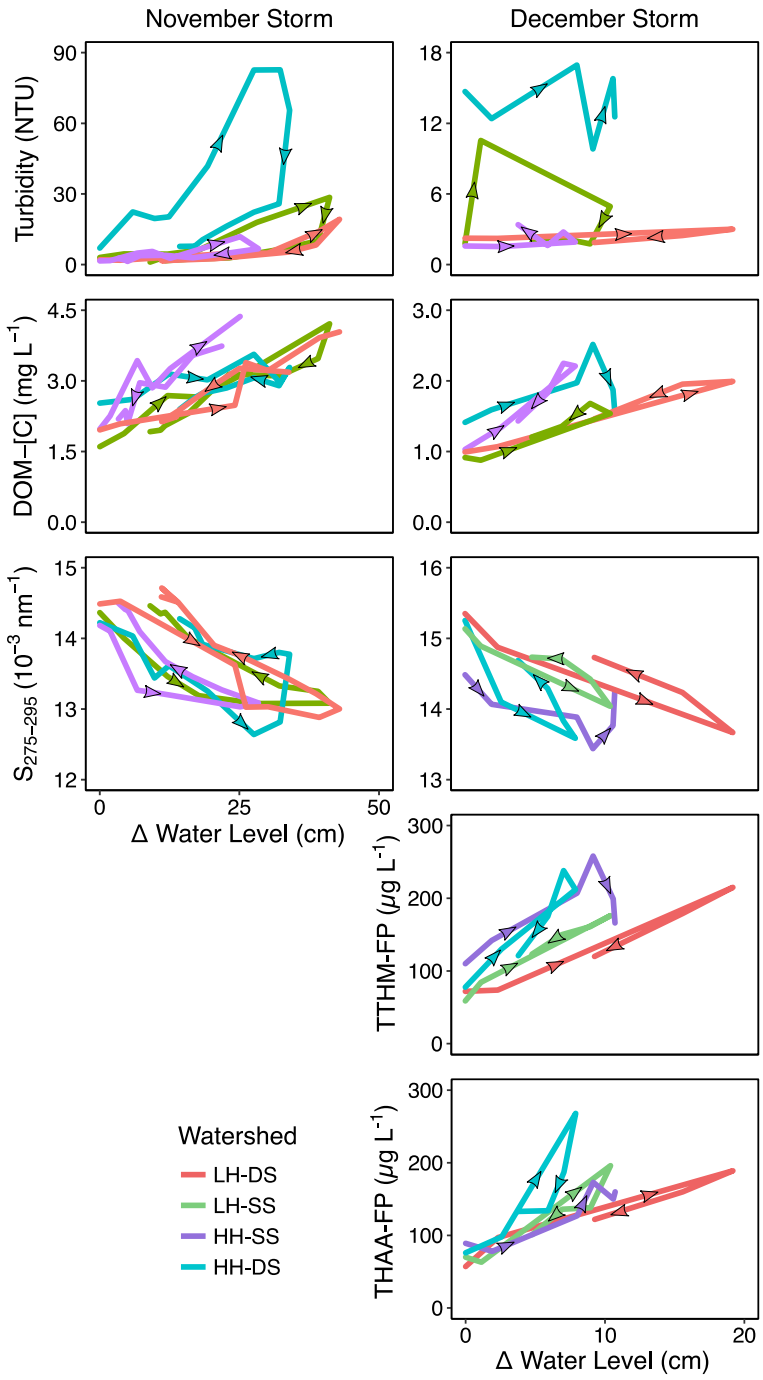

Figure 3-4. Turbidity (NTU), DOM-[C] (mg L^{-1}), $S_{275-295}$ (10^{-3} nm^{-1}), TTHM-FP (µg L^{-1}), and THAA-FP (µg L^{-1}) versus change in stream water level (cm) across subwatershed sites during the Nov. 16–19 and Dec. 5–9, 2019 storm events. The arrows represent the temporal direction of the storm from the rising to falling limb. Stream water level data were normalized to zero and individual THM and HAA species FPs were summed to yield total FPs.

CH4: General Conclusions

4.1 Research conclusions

4.1.1 Summary of findings

This study evaluated variation in stream water quality and disinfection by-product formation potentials (DBP-FPs) across different hydrologic conditions in forested subwatersheds with varying harvest intensities and catchment characteristics. Through my assessment of seasonal and spatial water quality dynamics in Chapter 2, I identified seasonality as a key factor regulating stream water quality. Although water quality did vary with forest harvest and natural catchment characteristics (e.g., topography, soil depth and clay content), seasonal variations in hydrology and temperature exerted a greater influence. Despite its importance, seasonal fluctuations in water quality did not appear to be amplified in subwatersheds with greater forest harvest. Considering the importance of seasonal hydrology in this region, I also investigated the effects of storm events and baseflow conditions on water quality and corresponding DBPs in Chapter 3. I found that water quality was directly linked to DBP-FPs, and that variation in each of these parameters was driven by storm event hydrology. During the events that were captured, forest harvest did not intensify changes in water quality or DBP-FPs. Together, these chapters revealed that the background spatiotemporal variation of suspended solids and dissolved organic matter (DOM) in a recovering landscape was not overwhelmed by recent forest harvest. Rather, changes in flow, either seasonally or during storm events, acted as a primary control on stream water quality and resultant DBP-FPs in the Comox Lake watershed. Long-term monitoring plans must thus be developed that consider water quality changes as hydroclimatic regimes shift in the future to exacerbate fluctuations in flow.

4.1.2 Limitations and improvements

No research is without limitations or improvements. This study could have benefitted from incorporating additional catchment characteristics into spatial analyses. Several other characteristics, including surficial geology, forest vegetation type, decomposition stage, and stand age, all have the potential to influence stream water quality but were not directly examined. While bedrock geology affects hydrologic pathways between streams and forested headwaters (Kreutzweiser et al., 2008), forest vegetation type, decomposition, and age influence the quality of DOM and total DOM exported in streams (Chow et al., 2011, Dai et al., 2001, Parry et al.,

2015). Unfortunately, I was unable to account for these characteristics in this research due to lack of data availability. Broadening the study region to include other watersheds with active harvesting in the Pacific Maritime ecozone could have also improved this work, as many subwatershed sites in the Comox Lake watershed were similar to one another. This is likely due to the steep terrain, thick bedrock, and thin soils that persist across the entire watershed (Valentine, 1978). Likewise, studying additional experimental watersheds would be useful to assess forest harvest effects against controls. This research could have additionally benefitted from long-term seasonal and storm sampling. The seasonal campaign offered a finite snapshot of stream water quality because only one wet and dry period were investigated. Results were similarly limited in the storm campaign, as no more than two storm events were captured during the autumn wet season. Sample collection over multiple wet and dry periods, as well as during the winter wet season and spring freshet, could thus improve this work. The use of automated sensors to continuously monitor stream water parameters may be particularly useful over the long-term (Bishop, 2020). This study also assumed that rainfall at each subwatershed site was identical to the nearest hydrometric station, regardless of the distance (< 10 km) between site and station. While this limitation has been encountered in other research (e.g., Mistick and Johnson, 2020), it is especially notable in this region because steep topographies result in various micro-climates across the Comox Lake watershed. Subwatershed sites may thus experience different weather than that at the nearest hydrometric station. Finally, the findings of this study could additionally be strengthened by considering the influence of Comox Lake and effects of hydrological factors (e.g., discharge, water table depth) on water quality and resultant DBP-FPs. It is important to note that while each of the aforementioned considerations may improve research, each has its own set of practical challenges in application.

4.2 Future research

This study recommends a few avenues for future research. First, given the inherent landscape differences present across Canadian ecozones, there is a need for additional studies conducted within Montane Cordillera, Boreal Plains, Taiga Plains, Boreal Shield, and Atlantic Maritime regions. Investigating the effects of forestry on source waters across these ecozones would enhance our understanding of how water quality and resultant DBPs are influenced by variation and changes in forest landscapes. Second, it is important to understand not only the

impacts of forest harvest on source waters now, but also in the future with changes in climate. Climatic shifts are predicted to increase extreme weather events in the Pacific Maritime ecozone (Wang et al., 2016), and this may alter the impacts of forestry on source water quality and DBP formation. A better understanding of how water quality and DBP-FPs vary with climate-driven shifts in hydrology could be obtained by conducting research over longer time scales and across different latitudes (i.e., to assess the northwards shift in climate). Finally, it is pertinent to study water quality in conjunction with water quantity, as the provision of flows is critical to sustaining high-quality source waters. Given that hydrology is a key factor determining water quality (and quantity) in the Pacific Maritime, it is imperative to bridge these two research domains. This will further our understanding of the interplay between water quantity and quality, while also ensuring stable, predictable, and clean water supplies in the future.

REFERENCES

APHA, AWWA, WEF. Standard methods for the examination of water and wastewater, 23rd edition. Washington, DC: American Public Health Association, American Water Works Association, Water Environment Federation; 2017:1504.

Awad, J., Fisk, C., W. Cox, J., Anderson, S., van Leeuwen, J. (2018). Modelling of THM formation potential and DOM removal based on drinking water catchment characteristics. *Science of The Total Environment*, 635, 761–8. doi:10.1016/j.scitotenv.2018.04.149

Baillie, B. R., Neary, D. G. (2015). Water quality in New Zealand's planted forests: a review. *New Zealand Journal of Forestry Science*, 45(1), 7. doi:10.1186/s40490-015-0040-0

Bao, H., Niggemann, J., Huang, D., Dittmar, T., Kao, S. (2019). Different responses of dissolved black carbon and dissolved lignin to seasonal hydrological changes and an extreme rain event. *Journal of Geophysical Research: Biogeosciences*, 0(ja), doi:10.1029/2018JG004822

Barraclough, C. L., Karkanis, S., Lucey, P., McDonald, L., Motyer, T. (2016). Comox Lake Watershed Protection Plan. Prepared for the Comox Valley Regional District by Aqua-Tex Scientific Consulting Ltd. Accessed at: https://www.comoxvalleyrd.ca/sites/default/files/docs/Projects-Initiatives/2-20160603_cvrd_wpp_final.pdf.

Bates, D., Maechler, M., Bolker, B., Walker, S. (2015). Fitting linear mixed-effects models using lme4. *Journal of Statistical Software*, 67(1), 1–48.

BC Hydro. (2020). History & hydroelectric operation: Power generation initially for mines in Cumberland area. Accessed at: https://www.bchydro.com/community/recreation_areas/puntledge.html.

Beck, H. E., Zimmermann, N. E., McVicar, T. R., Vergopolan, N., Berg, A., Wood, E. F. (2018). Present and future Köppen-Geiger climate classification maps at 1-km resolution. *Scientific Data*, 5(1), 180214. doi:10.1038/sdata.2018.214

Berkowitz, J. F., Summers, E. A., Noble, C. V., White, J. R., DeLaune, R. D. (2014). Investigation of biogeochemical functional proxies in headwater streams across a range of channel and catchment alterations. *Environmental Management*, 53, 534–48.

Birkel, C., Broder, T., Biester, H. (2017). Nonlinear and threshold-dominated runoff generation controls DOC export in a small peat catchment. *Journal of Geophysical Research: Biogeosciences*, 122(3), 498–513. doi:10.1002/2016JG003621

Bishop, A. (2020). Stream carbon flux in the Northern Pacific Coastal Temperate Rainforest: Seasonal DOC transport and CO2 and CH4 emissions. *Biological Sciences*, M.Sc., 1–116.

Bolker, B., Brooks, M., Clark, C., Geange, S., Poulsen, J., Stevens, H., White, J. (2009). Generalized linear mixed models: A practical guide for ecology and evolution. *Trends in Ecology & Evolution*, 24, 127–35. doi:10.1016/j.tree.2008.10.008

Bousfield, G. (2008). Peakflow prediction using an antecedent precipitation index in small forested watersheds of the Northern California coast range. *Natural Resources: Watershed Management*, M.Sc., 1–57.

Butturini, A., Gallart, F., Latron, J., Eusebi, V., Sabater, F. (2006). Cross-site comparison of variability of DOC and nitrate c–q hysteresis during the autumn–winter period in three Mediterranean headwater streams: A synthetic approach. *Biogeochemistry*, 77, 327–49. doi:10.1007/s10533-005-0711-7

Canadian Council of Forest Ministers. (2015). Satellite forest information for Canada. Accessed at: https://opendata.nfis.org/mapserver/nfis-change_eng.html. Accessed at: https://opendata.nfis.org/mapserver/nfis-change_eng.html.

Chang, M., McCullough, J. D., Granillo, A. B. (1983). Effects of land use and topography on some water quality variables in forested East Texas. *Journal of the American Water Resources Association*, 19(2), 191–6. doi:10.1111/j.1752-1688.1983.tb05313.x

Chow, A., O'Geen, A. T., Dahlgren, R. A., Peña, F. D., Wong, K., Wong, P. K. (2011). Reactivity of litter leachates from California oak woodlands in the formation of disinfection by-products. *Journal of Environmental Quality*, 40, 1607–16. doi:10.2134/jeq2010.0488

Chowdhury, S. (2018). Water quality degradation in the sources of drinking water: An assessment based on 18 years of data from 441 water supply systems. *Environmental Monitoring and Assessment*, 190(7), 379. doi:10.1007/s10661-018-6772-6

Coch, C., Juhls, B., Lamoureux, S. F., Lafrenière, M. J., Fritz, M., Heim, B., Lantuit, H. (2019). Comparisons of dissolved organic matter and its optical characteristics in small low and high Arctic catchments. *Biogeosciences*, 16(23), 4535–53. doi:10.5194/bg-16-4535-2019

Coch, C., Ramage, J. L., Lamoureux, S. F., Meyer, H., Knoblauch, C., Lantuit, H. (2020). Spatial variability of dissolved organic carbon, solutes and suspended sediment in disturbed low Arctic coastal watersheds. *Journal of Geophysical Research: Biogeosciences*, n/a, doi:10.1029/2019JG005505

Comox Valley Regional District. (2016a). Water quality for our future: Article 1 - sharing our watershed. Accessed at: https://www.comoxvalleyrd.ca/sites/default/files/docs/Services/5-cvrd_sharingourwatershed.pdf.

Comox Valley Regional District. (2016b). Water quality for our future: Article 2 - conserving our watershed. Accessed at: https://www.comoxvalleyrd.ca/sites/default/files/docs/Services/4-conservingourwater_sept2016.pdf.

Comox Valley Regional District. (2016c). Water quality for our future: Article 4 - monitoring water quality. Accessed at: https://www.comoxvalleyrd.ca/sites/default/files/docs/Services/2-cvrd_monitoring_water_quality_article_4.pdf.

Comox Valley Regional District. (2019a). Protecting our water: Water quality and management. Accessed at: https://www.comoxvalleyrd.ca/sites/default/files/docs/Projects-Initiatives/2wtp_backgrounder1.pdf.

Comox Valley Regional District. (2019b). Providing safe water: Constructing a new water treatment system. Accessed at: https://www.comoxvalleyrd.ca/sites/default/files/docs/Services/Water/cvrd_wtp_backgrounder2_may2019_final.pdf.

Cotruvo, J. A., Amato, H. (2019). National trends of bladder cancer and trihalomethanes in drinking water: A review and multicountry ecological study. *Dose-Response*, 17(1), doi:10.1177/1559325818807781

Coynel, A., Seyler, P., Etcheber, H., Meybeck, M., Orange, D. (2005). Spatial and seasonal dynamics of total suspended sediment and organic carbon species in the Congo River. *Global Biogeochemical Cycles*, 19(4), doi:10.1029/2004GB002335

Csank, A. Z., Czimczik, C. I., Xu, X., Welker, J. M. (2019). Seasonal patterns of riverine carbon sources and export in NW Greenland. *Journal of Geophysical Research: Biogeosciences*, 0(ja), doi:10.1029/2018JG004895

Dai, K. H., Johnson, C. E., Driscoll, C. T. (2001). Organic matter chemistry and dynamics in clear-cut and unmanaged hardwood forest ecosystems. *Biogeochemistry*, 54(1), 51–83.

Dawson, J. J. C., Soulsby, C., Tetzlaff, D., Hrachowitz, M., Dunn, S. M., Malcolm, I. A. (2008). Influence of hydrology and seasonality on DOC exports from three contrasting upland catchments. *Biogeochemistry*, 90(1), 93–113. doi:10.1007/s10533-008-9234-3

Delpla, I., Rodriguez, M. J. (2017). Variability of disinfection by-products at a full-scale treatment plant following rainfall events. *Chemosphere*, 166, 453–62. doi:10.1016/j.chemosphere.2016.09.096

Emelko, M. B., Silins, U., Bladon, K. D., Stone, M. (2011). Implications of land disturbance on drinking water treatability in a changing climate: Demonstrating the need for " source water supply and protection" strategies. *Water Research*, 45(2), 461–72. doi:10.1016/j.watres.2010.08.051

Epps, D. (2011). Water quality assessment and objectives for Comox Lake: overview report. Victoria: Ministry of Environment. Accessed at: https://www2.gov.bc.ca/assets/gov/environment/air-land-water/water/waterquality/water-quality-objectives/wqo_overview_comox_2011.pdf.

Erdogan, B. U., Gökbulak, F., Serengil, Y., Yurtseven, I., Özçelik, M. S. (2018). Changes in selected physical water quality characteristics after thinning in a forested watershed. *Catena*, 166, 220–8. doi:10.1016/j.catena.2018.04.010

Erdozain, M., Kidd, K., Kreutzweiser, D., Sibley, P. (2018). Linking stream ecosystem integrity to catchment and reach conditions in an intensively managed forest landscape. *Ecosphere*, 9(5), e02278. doi:10.1002/ecs2.2278

Fedora, M., Beschta, R. L. (1989). Storm runoff simulation using an antecedent precipitation index (API) model. *Journal of Hydrology*, 112, 121–33. doi:10.1016/0022-1694(89)90184-4

Fellman, J. B., Buma, B., Hood, E., Edwards, R. T., D'Amore, D. V. (2016). Linking LiDAR with streamwater biogeochemistry in coastal temperate rainforest watersheds. *Canadian Journal of Fisheries and Aquatic Sciences*, 74(6), 801–11. doi:10.1139/cjfas-2016-0130

Fellman, J. B., Hood, E., Behnke, M. I., Welker, J. M., Spencer, R. G. M. (2020). Stormflows drive stream carbon concentration, speciation and dissolved organic matter composition in coastal temperate rainforest watersheds. *Journal of Geophysical Research: Biogeosciences*, n/a, e2020JG005804. doi:10.1029/2020JG005804

Fellman, J. B., Hood, E., Spencer, R. G. M. (2010). Fluorescence spectroscopy opens new windows into dissolved organic matter dynamics in freshwater ecosystems: A review. *Limnology and Oceanography*, 55(6), 2452–62. doi:10.4319/lo.2010.55.6.2452

Fong, E. (2019). Provincial forest inventory 2019: Provincial age class map. Accessed at: https://www2.gov.bc.ca/gov/content/industry/forestry/managing-our-forest-resources/forest-inventory/data-management-and-access/spatial-ready-data.
García, P. E., Queimaliños, C., Diéguez, M. C. (2019). Natural levels and photo-production rates of hydrogen peroxide (H2O2) in Andean Patagonian aquatic systems: Influence of the dissolved organic matter pool. *Chemosphere*, 217, 550–7. doi:10.1016/j.chemosphere.2018.10.179
Gartner, T., Mehan III, G. T., Mulligan, J., Roberson, J. A., Stangel, P., Qin, Y. (2014). Protecting forested watersheds is smart economics for water utilities. *American Water Works Association*, 106(9), 54–64.
GeoBC. (2020). Freshwater atlas stream network. Accessed at: https://www2.gov.bc.ca/gov/content/data/geographic-dataservices/topographic-data/freshwater.
Gonsior, M., Schmitt-Kopplin, P., Stavklint, H., Richardson, S. D., Hertkorn, N., Bastviken, D. (2014). Changes in dissolved organic matter during the treatment processes of a drinking water plant in Sweden and formation of previously unknown disinfection byproducts. *Environmental Science & Technology*, 48(21), 12714–22. doi:10.1021/es504349p
Government of British Columbia. (1996). Community watershed guidebook. Accessed at: https://www.for.gov.bc.ca/ftp/hfp/external/!publish/FPC%20archive/old%20web%20site%20contents/fpc/fpcguide/WATRSHED/Watertoc.htm.
Government of British Columbia. (2001). Ambient water quality guidelines (criteria) for turbidity, suspended and benthic sediments: Overview report. Accessed at: https://www2.gov.bc.ca/assets/gov/environment/air-land-water/water/waterquality/water-quality-guidelines/approved-wqgs/turbitity-or.pdf.
Government of British Columbia. (2003). British Columbia's forests: a geographical snapshot. Accessed at: https://www.for.gov.bc.ca/hfd/pubs/Docs/Mr/Mr112.htm.
Government of British Columbia. (2012). Drinking water treatment objectives (microbiological) for surface water supplies in British Columbia. Accessed at: https://www2.gov.bc.ca/assets/gov/environment/air-land-water/water/waterquality/how-drinking-water-is-protected-in-bc/part_b_-_5_surface_water_treatment_objectives.pdf.
Government of British Columbia. (2019). British Columbia approved water quality guidelines: Aquatic life, wildlife & agriculture. Accessed at: https://www2.gov.bc.ca/assets/gov/environment/air-land-water/water/waterquality/water-quality-guidelines/approved-wqgs/wqg_summary_aquaticlife_wildlife_agri.pdf.
Government of British Columbia. (2020a). BEC map. Accessed at: https://catalogue.data.gov.bc.ca/dataset/bec-map.
Government of British Columbia. (2020b). Soil survey spatial view. Accessed at: https://catalogue.data.gov.bc.ca/dataset/soil-survey-spatial-view.
Government of Canada. (1980). Description of soils for northern Vancouver Island. Accessed at: http://sis.agr.gc.ca/cansis/publications/surveys/bc/bc45/index.html.
Government of Canada. (1985). Soils of southern Vancouver Island. Accessed at: http://sis.agr.gc.ca/cansis/publications/surveys/bc/bc44/index.html.
Government of Canada. (2013). Soils of British Columbia. Accessed at: http://sis.agr.gc.ca/cansis/soils/bc/soils.html.
Government of Canada. (2017). Geospatial data extraction. Accessed at: https://maps.canada.ca/czs/index-en.html.
Government of Canada. (2020). Guidance on natural organic matter in drinking water. Accessed at: https://www.canada.ca/en/health-canada/services/publications/healthy-living/guidance-natural-organic-matter-drinking-water.html.
Groeneveld, M., Catalán, N., Attermeyer, K., Hawkes, J., Einarsdóttir, K., Kothawala, D., Bergquist, J., Tranvik, L. (2020). Selective adsorption of terrestrial dissolved organic matter to inorganic surfaces along a boreal inland water continuum. *Journal of Geophysical Research: Biogeosciences*, n/a, e2019JG005236. doi:10.1029/2019JG005236
Hansen, A. M., Kraus, T. E. C., Pellerin, B. A., Fleck, J. A., Downing, B. D., Bergamaschi, B. A. (2016). Optical properties of dissolved organic matter (DOM): Effects of biological and photolytic degradation. *Limnology and Oceanography*, 61(3), 1015–32. doi:10.1002/lno.10270
Hansen, M. C., Potapov, P., Moore, R., Hancher, M., Turubanova, S., Tyukavina, A., Thau, D., Stehman, S., Goetz, S., Loveland, T., Kommareddy, A., Egorov, A., Chini, L., Justice, C. O., Townshend, J. (2013). High-resolution global maps of 21st-century forest cover change. *Science (New York, NY)*, 342, 850–3. doi:10.1126/science.1244693

Health Canada. (2020). Guidelines for Canadian drinking water quality. Accessed at: https://www.canada.ca/en/health-canada/services/environmental-workplace-health/reports-publications/water-quality/guidelines-canadian-drinking-water-quality-summary-table.html.

Helms, J. R., Stubbins, A., Ritchie, J. D., Minor, E. C., Kieber, D. J., Mopper, K. (2008). Absorption spectral slopes and slope ratios as indicators of molecular weight, source, and photobleaching of chromophoric dissolved organic matter. *Limnology and Oceanography*, 53(3), 955–69. doi:10.4319/lo.2008.53.3.0955

Hengl, T., Mendes de Jesus, J., Heuvelink, G. B. M., Ruiperez Gonzalez, M., Kilibarda, M., Blagotić, A., Shangguan, W., Wright, M. N., Geng, X., Bauer-Marschallinger, B., Guevara, M. A., Vargas, R., MacMillan, R. A., Batjes, N. H., Leenaars, J. G. B., Ribeiro, E., Wheeler, I., Mantel, S., Kempen, B. (2017). SoilGrids250m: Global gridded soil information based on machine learning. *PLOS One*, 12(2), e0169748. doi:10.1371/journal.pone.0169748

Hood, E., Gooseff, M. N., Johnson, S. L. (2006). Changes in the character of stream water dissolved organic carbon during flushing in three small watersheds, Oregon. *Journal of Geophysical Research: Biogeosciences*, 111(G1), doi:10.1029/2005JG000082

Hrudey, S. E. Chlorination disinfection by-products (DBPs) in drinking water and public health in Canada: A primer for public health practitioners reviewing evidence from over 30 years of research. A knowledge translation review for the National Collaborating Centre on Environmental Health. 2008:167.

Hur, J., Jung, M. C. (2008). The effects of soil properties on the turbidity of catchment soils from the Yongdam dam basin in Korea. *Environmental Geochemistry and Health*, 31(3), 365. doi:10.1007/s10653-008-9176-7

Hutchins, R. H. S., Prairie, Y. T., del Giorgio, P. A. (2019). Large-scale landscape drivers of CO2, CH4, DOC, and DIC in Boreal river networks. *Global Biogeochemical Cycles*, 33(2), 125–42. doi:10.1029/2018GB006106

Jacobs, S. R., Breuer, L., Butterback-Bahl, K., Pelster, D. E., Rufino, M. C. (2017). Land use affects total dissolved nitrogen and nitrate concentrations in tropical montane streams in Kenya. *Science of the Total Environment*, 603, 519–32. doi:https://doi.org/10.1016/j.scitotenv.2017.06.100

Jones, M. W., de Aragão, L. E. O. C., Dittmar, T., de Rezende, C. E., Almeida, M. G., Johnson, B. T., Marques, J. S. J., Niggemann, J., Rangel, T. P., Quine, T. A. (2019). Environmental controls on the riverine export of dissolved black carbon. *Global Biogeochemical Cycles*, 0(ja), doi:10.1029/2018GB006140

Jordan, P. (2006). The use of sediment budget concepts to assess the impact on watersheds of forestry operations in the southern interior of British Columbia. *Geomorphology*, 79(1), 27–44. doi:10.1016/j.geomorph.2005.09.019

Kaiser, K., Kalbitz, K. (2012). Cycling downwards – Dissolved organic matter in soils. *Soil Biology and Biochemistry*, 52, 29–32. doi:10.1016/j.soilbio.2012.04.002

Kassambara, A., Mundt, F. (2020). factoextra: Extract and visualize the results of multivariate data analyses. R package version 1.0.7. Accessed at: https://CRAN.R-project.org/package=factoextra.

Kreutzweiser, D. P., Hazlett, P. W., Gunn, J. M. (2008). Logging impacts on the biogeochemistry of boreal forest soils and nutrient export to aquatic systems: A review. *Environmental Reviews*, 16, 157–79. doi:10.1139/A08-006

Lajtha, K., Jones, J. (2018). Forest harvest legacies control dissolved organic carbon export in small watersheds, western Oregon. *Biogeochemistry*, 140(3), 299–315. doi:10.1007/s10533-018-0493-3

Lechevallier, M. W., Evans, T. M., Seidler, R. J. (1981). Effect of turbidity on chlorination efficiency and bacterial persistence in drinking water. *Applied and Environmental Microbiology*, 42, 159–67. doi:10.1128/AEM.42.1.159-167.1981

Lee, B. J., Kim, J., Hur, J., Choi, I. H., Toorman, E., Fettweis, M., Choi, J. W. (2019). Seasonal dynamics of organic matter composition and its effects on suspended sediment flocculation in river water. *Water Resources Research*, 0(ja), doi:10.1029/2018WR024486

Lee, B. S., Lajtha, K. (2016). Hydrologic and forest management controls on dissolved organic matter characteristics in headwater streams of old-growth forests in the Oregon Cascades. *Forest Ecology and Management*, 380, 11–22. doi:10.1016/j.foreco.2016.08.029

Lee, B. S., Lajtha, K., Jones, J. A., White, A. E. (2018). Fluorescent DOC characteristics are related to streamflow and pasture cover in streams of a mixed landscape. *Biogeochemistry*, 140(3), 317–40. doi:10.1007/s10533-018-0494-2

Legendre, P., Legendre, L. F. (2012). Canonical ordination. Numerical Ecology with R, 153–225.

Levia, D., Carlyle-Moses, D., Tanaka, T. (2011). Digital terrain analysis approaches for tracking hydrological and biogeochemical pathways and processes in forested landscapes. Forest Hydrology and Biogeochemistry: Synthesis of Past Research and Future Directions, 69-100. doi:10.1007/978-94-007-1363-5

Li, A., Zhao, X., Mao, R., Liu, H., Qu, J. (2014). Characterization of dissolved organic matter from surface waters with low to high dissolved organic carbon and the related disinfection byproduct formation potential. *Journal of Hazardous Materials*, 271, 228–35. doi:10.1016/j.jhazmat.2014.02.009

MacKinnon, A., Meidinger, D., Klinka, K. (1992). Use of the biogeoclimatic ecosystem classification system in British Columbia. *The Forestry Chronicle*, 68(1), 100–20. doi:10.5558/tfc68100-1

Mbonimpa, E. G., Yuan, Y., Nash, M. S., Mehaffey, M. H. (2014). Sediment and total phosphorous contributors in Rock River watershed. *Journal of Environmental Management*, 133, 214–21.

McKitrick, R., Aliakbari, E., Stedman, A. (2018). Evaluating the state of fresh water in Canada. Fraser Institute. Accessed at: https://www.fraserinstitute.org/sites/default/files/evaluating-the-state-of-fresh-water-in-canada.pdf.

McSorley, H. J. (2020). Spatial and temporal variation in natural organic matter quantity and quality across a second growth forested drinking water supply area on Vancouver Island, BC. *Geological Sciences*, M.Sc., 1–187.

Meidinger, D., Pojar, J. Ecosystems of British Columbia. BC Ministry of Forests, Victoria, BC. 1991:330.

Mistick, E., Johnson, M. S. (2020). High-frequency analysis of dissolved organic carbon storm responses in headwater streams of contrasting forest harvest history. *Journal of Hydrology*, 590, 125371. doi:10.1016/j.jhydrol.2020.125371

Muller, J. E., Carson, J. T., Gunning, H. C., Jeffery, W. G. (1965). Geology, Comox Lake area, British Columbia. Geological Survey of Canada, Preliminary Map 2-1965, 1 sheet. Accessed at: https://doi.org/10.4095/107728.

Murphy, K. R., Stedmon, C. A., Graeber, D., Bro, R. (2013). Fluorescence spectroscopy and multi-way techniques. PARAFAC. *Analytical Methods*, 5(23), 6557–66. doi:10.1039/C3AY41160E

MWH. Water Treatment: Principles and Design, 2nd Edition. John Wiley & Sons Inc; 2005:1968.

Mzobe, P., Yan, Y., Berggren, M., Pilesjö, P., Olefeldt, D., Lundin, E., Roulet, N., Persson, A. (2020). Morphometric control on dissolved organic carbon in subarctic streams. *Journal of Geophysical Research: Biogeosciences*, n/a, e2019JG005348. doi:10.1029/2019JG005348

Nakagawa, S., Schielzeth, H. (2013). A general and simple method for obtaining R2 from generalized linear mixed-effects models. *Methods in Ecology and Evolution*, 4(2), 133–42. doi:10.1111/j.2041-210x.2012.00261.x

National Academies of Sciences, Engineering, and Medicine. Review of the New York City Department of Environmental Protection Operations Support Tool for Water Supply. Washington, DC: The National Academies Press; 2018:174.

Natural Resources Canada. (1957). Bedrock Geology of Canada. Atlas of Canada, 3rd edition. Accessed at: https://geoscan.nrcan.gc.ca/starweb/geoscan/servlet.starweb?path=geoscan/fulle.web&search1=R=294165.

Natural Resources Canada. (2020a). Threats to forest water resources. Accessed at: https://www.nrcan.gc.ca/our-natural-resources/forests-forestry/sustainable-forest-management/conservation-protection-canadas/threats-forest-water-resources/15082.

Natural Resources Canada. (2020b). Water. Accessed at: https://www.nrcan.gc.ca/our-natural-resources/forests-forestry/sustainable-forest-management/conservation-protection-canadas/water/13207.

Nkambule, T. I., Krause, R. W. M., Haarhoff, J., Mamba, B. (2011). Natural organic matter (NOM) in South African waters: NOM characterisation using combined assessment techniques. *Water SA*, 38, 697–706. doi:10.4314/wsa.v38i5.7

Ohte, N., Tokuchi, N. (2011). Hydrology and biogeochemistry of temperate forests. Forest Hydrology and Biogeochemistry: Synthesis of Past Research and Future Directions, 261–84. doi:10.1007/978-94-007-1363-5

Oksanen, J., Blanchet, G. F., Friendly, M., Kindt, R., P., McGlinn, D., Minchin, P. R., O'Hara, R. B., Simpson, G. L., Solymos, P. M., Stevens, H. H., Szoecs, E., Wagner, H. (2019). vegan: Community ecology package. R package version 2.5-6. Accessed at: https://CRAN.R-project.org/package=vegan.

Oliver, A., Tank, S., Giesbrecht, I., Korver, M. C., Floyd, W. C., Sanborn, P., Bulmer, C., Lertzman, K. (2017). A global hotspot for dissolved organic carbon in hypermaritime watersheds of coastal British Columbia. *Biogeosciences*, 14, 3743–62. doi:10.5194/bg-14-3743-2017

Osburn, C. L., Oviedo-Vargas, D., Barnett, E., Dierick, D., Oberbauer, S. F., Genereux, D. P. (2018). Regional groundwater and storms are hydrologic controls on the quality and export of dissolved organic matter in two tropical rainforest streams, Costa Rica. *Journal of Geophysical Research: Biogeosciences*, 123(3), 850–66. doi:10.1002/2017JG003960

Pacific Climate Impacts Consortium. (2019). Seasonal Anomaly Maps. Prepared by the University of Victoria. Accessed at: https://www.pacificclimate.org/analysis-tools/seasonal-anomaly-maps.

Parr, T. B., Inamdar, S. P., Miller, M. J. (2019). Overlapping anthropogenic effects on hydrologic and seasonal trends in DOC in a surface water dependent water utility. *Water Research*, 148, 407–15. doi:10.1016/j.watres.2018.10.065

Parry, L. E., Chapman, P. J., Palmer, S. M., Wallage, Z. E., Wynne, H., Holden, J. (2015). The influence of slope and peatland vegetation type on riverine dissolved organic carbon and water colour at different scales. *Science of The Total Environment*, 527-528, 530–9. doi:10.1016/j.scitotenv.2015.03.036

Pike, R. G., Feller, M. C., Stednick, J. D., Rieberger, K. J., Carver, M. (2010). Water Quality and Forest Management. Compendium of Forest Hydrology and Geomorphology in British Columbia, 401–40.

Poulin, B. A., Ryan, J. N., Aiken, G. R. (2014). Effects of iron on optical properties of dissolved organic matter. *Environmental Science & Technology*, 48(17), 10098–106. doi:10.1021/es502670r

R Core Team. (2020). R: A language and environment for statistical computing. R Foundation for Statistical Computing, Vienna, Austria. Accessed at: http://www.R-project.org/.

Reid, D. A., Hassan, M. A., Floyd, W. (2016). Reach-scale contributions of road-surface sediment to the Honna River, Haida Gwaii, BC. *Hydrological Processes*, 30(19), 3450–65. doi:10.1002/hyp.10874

Richardson, S. D., Ternes, T. A. (2018). Water analysis: emerging contaminants and current issues. *Analytical Chemistry*, 90(1), 398–428. doi:10.1021/acs.analchem.7b04577

Ritson, J. P., Graham, N. J. D., Templeton, M. R., Clark, J. M., Gough, R., Freeman, C. (2014). The impact of climate change on the treatability of dissolved organic matter (DOM) in upland water supplies: A UK perspective. *Science of The Total Environment*, 473, 714–30. doi:10.1016/j.scitotenv.2013.12.095

Roberts, C. M., Inniss, E. C. (2014). Implementing Treatment Sequences to Promote Reduction of DBPs in Small Drinking Water Systems. *Water Resources Management*, 28(6), 1631–43. doi:10.1007/s11269-014-0570-x

Sánchez-Murillo, R., Romero-Esquivel, L. G., Jiménez-Antillón, J., Salas-Navarro, J., Corrales-Salazar, L., Álvarez-Carvajal, J., Álvarez-McInerney, S., Bonilla-Barrantes, D., Gutiérrez-Sibaja, N., Martínez-Arroyo, M., Ortiz-Apuy, E., Salgado-Lobo, J., Villalobos-Morales, J., Esquivel-Hernández, G., Rojas-Jiménez, L. D., Gómez-Castro, C., Jiménez-Madrigal, Q., Vargas-Gutiérrez, O., Birkel, C. (2019). DOC transport and export in a dynamic tropical catchment. *Journal of Geophysical Research: Biogeosciences*, 0(ja), doi:10.1029/2018JG004897

Schelker, J., Eklöf, K., Bishop, K., Laudon, H. (2012). Effects of forestry operations on dissolved organic carbon concentrations and export in boreal first-order streams. *Journal of Geophysical Research*, 117, doi:https://doi.org/10.1029/2011JG001827

Schelker, J., Öhman, K., Löfgren, S., Laudon, H. (2014). Scaling of increased dissolved organic carbon inputs by forest clear-cutting – What arrives downstream? *Journal of Hydrology*, 508, 299–306. doi:10.1016/j.jhydrol.2013.09.056

Schloerke, B., Cook, D., Larmarange, J., Briatte, F., M., _Thoen, E., Elberg, A., Crowley, J. (2020). GGally: Extension to 'ggplot2'. R package version 2.0.0. Accessed at: https://CRAN.R-project.org/package=GGally.

Schnorbus, M. A. (2018). Climate change impacts on hydrology for the Comox Lake watershed: Final report.

Sharma, A. R., Déry, S. J. (2020a). Contribution of atmospheric rivers to annual, seasonal, and extreme precipitation across British Columbia and Southeastern Alaska. *Journal of Geophysical Research: Atmospheres*, 125(9), e2019JD031823. doi:10.1029/2019JD031823

Sharma, A. R., Déry, S. J. (2020b). Variability and trends of landfalling atmospheric rivers along the Pacific Coast of northwestern North America. *International Journal of Climatology*, 40(1), 544–58. doi:10.1002/joc.6227

Smith, H. G., Dragovich, D. (2009). Interpreting sediment delivery processes using suspended sediment-discharge hysteresis patterns from nested upland catchments, south-eastern Australia. *Hydrological Processes*, 23(17), 2415–26. doi:10.1002/hyp.7357

Stubbins, A., Lapierre, J.-F., Berggren, M., Prairie, Y. T., Dittmar, T., del Giorgio, P. A. (2014). What's in an EEM? Molecular signatures associated with dissolved organic fluorescence in Boreal Canada. *Environmental Science & Technology*, 48(18), 10598–606. doi:10.1021/es502086e

Stubbins, A., Spencer, R. G. M., Chen, H., Hatcher, P. G., Mopper, K., Hernes, P. J., Mwamba, V. L., Mangangu, A. M., Wabakanghanzi, J. N., Six, J. (2010). Illuminated darkness: Molecular signatures of Congo River dissolved organic matter and its photochemical alteration as revealed by ultrahigh precision mass spectrometry. *Limnology and Oceanography*, 55(4), 1467–77. doi:10.4319/lo.2010.55.4.1467

Summers, R. S., Hooper, S. M., Shukairy, H. M., Solarik, G., Owen, D. (1996). Assessing DBP yield: Uniform formation conditions. *American Water Works Association*, 88(6), 80–93. doi:10.1002/j.1551-8833.1996.tb06573.x

Tremblay, Y., Rousseau, A. N., Plamondon, A. P., Lévesque, D., Prévost, M. (2009). Changes in stream water quality due to logging of the boreal forest in the Montmorency Forest, Québec. *Hydrological Processes*, 23, 764–76.

U.S. Environmental Protection Agency. Guidance for data quality assessment: practical methods for data analysis (No. EPA QA/G-9 QA00 Version). Accessed at: https://www.epa.gov/sites/production/files/2015-06/documents/g9-final.pdf. U.S. Environmental Protection Agency; 2000.

Valentine, K. W. G. (1978). The soil landscapes of British Columbia. Victoria: Ministry of Environment and Agriculture Canada. Accessed at: http://www.env.gov.bc.ca/esd/distdata/ecosystems/Soils_Reports/Soil_Landscapes_of_BC_1986.pdf.

van Meerveld, H. J., Baird, E. J., Floyd, W. C. (2014). Controls on sediment production from an unpaved resource road in a Pacific maritime watershed. *Water Resources Research*, 50(6), 4803–20. doi:10.1002/2013WR014605

Vidon, P., Wagner, L. E., Soyeux, E. (2008). Changes in the character of DOC in streams during storms in two Midwestern watersheds with contrasting land uses. *Biogeochemistry*, 88(3), 257–70. doi:10.1007/s10533-008-9207-6

Vonk, J. E., Tank, S. E., Mann, P. J., Spencer, R. G. M., Treat, C. C., Striegl, R. G., Abbott, B. W., Wickland, K. P. (2015). Biodegradability of dissolved organic carbon in permafrost soils and aquatic systems: a meta-analysis. *Biogeosciences*, 12(23), 6915–30. doi:10.5194/bg-12-6915-2015

Wagner, S., Fair, J. H., Matt, S., Hosen, J., Raymond, P., Saiers, J., Shanley, J., Dittmar, T., Stubbins, A. (2019). Molecular hysteresis: Hydrologically-driven changes in riverine dissolved organic matter chemistry during a storm event. *Journal of Geophysical Research: Biogeosciences*, 0(ja), doi:10.1029/2018JG004817

Wang, T., Hamann, A., Spittlehouse, D., Carroll, C. (2016). Locally downscaled and spatially customizable climate data for historical and future periods for North America. *PLOS One*, 11, e0156720. doi:10.1371/journal.pone.0156720

Warner, K. A., Saros, J. E. (2019). Variable responses of dissolved organic carbon to precipitation events in boreal drinking water lakes. *Water Research*, 156, 315–26. doi:10.1016/j.watres.2019.03.036

Wei, T., Simko, V. (2017). R package "corrplot": Visualization of a Correlation Matrix (Version 0.84). Accessed at: https://github.com/taiyun/corrplot.

Weiler, M., Spittlehouse, D. L., Pike, R. G., Winkler, R. D., Carlyle-Moses, D. E., Jost, G., Hutchinson, D., Hamilton, S., Marquis, P., Quilty, E., Moore, R. D., Richardson, J., Jordan, P., Hogan, D., Teti, P., Coops, N. (2010). Watershed Measurement Methods and Data Limitations. Compendium of forest hydrology and geomorphology in British Columbia, 553–637.

Weishaar, J. L., Aiken, G. R., Bergamaschi, B. A., Fram, M. S., Fujii, R., Mopper, K. (2003). Evaluation of specific ultraviolet absorbance as an indicator of the chemical composition and reactivity of dissolved organic carbon. *Environmental Science & Technology*, 37(20), 4702–8. doi:10.1021/es030360x

Werner, B. J., Musolff, A., Lechtenfeld, O. J., de Rooij, G. H., Oosterwoud, M. R., Fleckenstein, J. H. (2019). High-frequency measurements of dissolved organic carbon quantity and quality in a headwater catchment. *Biogeosciences Discussion*, 2019, 1–30. doi:10.5194/bg-2019-188

Wickham, H. (2016). ggplot2: Elegant graphics for data analysis. Springer-Verlag, New York.

Winkler, R. D., Moore, R. D., Redding, T. E., Spittlehouse, D. L., Carlyle-Moses, D. E., Smerdon, B. D. (2010). Hydrologic Processes and Watershed Response. Compendium of Forest Hydrology and Geomorphology in British Columbia, 133–77.

Wright, K. A., Sendek, K. H., Rice, R. M., Thomas, R. B. (1990). Logging effects on streamflow: Storm runoff at Caspar Creek in northwestern California. *Water Resources Research*, 26(7), 1657–67. doi:10.1029/WR026i007p01657

Wu, H., Xu, X., Fu, P., Cheng, W., Fu, C. (2020). Responses of soil WEOM quantity and quality to freeze–thaw and litter manipulation with contrasting soil water content: A laboratory experiment. *Catena*, 105058. doi:10.1016/j.catena.2020.105058

Yamashita, Y., Kloeppel, B. D., Knoepp, J., Zausen, G. L., Jaffe', R. (2011). Effects of watershed history on dissolved organic matter characteristics in headwater streams. *Ecosystems*, 14, 1110–22. doi:10.1007/s10021-011-9469-z

Zhai, H., He, X., Zhang, Y., Tingting, D., Adeleye, A., Li, Y. (2017). Disinfection byproduct formation in drinking water sources: A case study of Yuqiao reservoir. *Chemosphere*, 181, doi:10.1016/j.chemosphere.2017.04.028

Zheng, Y., Waldron, S., Flowers, H. (2018). Fluvial dissolved organic carbon composition varies spatially and seasonally in a small catchment draining a wind farm and felled forestry. *Science of The Total Environment*, 626, 785–94. doi:10.1016/j.scitotenv.2018.01.001

Zuur, A. F., Ieno, E. N., Smith, G. M. (2007). Linear regression. Analyzing ecological data, 49–77.

APPENDICES

Appendix 1: Supporting Information for Chapter 2.

Table A1-1. Percent land use in the Comox Lake watershed.

Land use	Area (%)
Municipal land holdings	1.18
Privately owned lands	0.55
Crown provincial	0.07
Forestry	67.07
Provincial parkland	31.13

Table A1-2. Descriptive statistics (mean ± standard deviation) of conductivity (μS cm^{-1}), major cations (μmol L^{-1}), $\delta^{18}O$ (‰), turbidity (NTU), DOM-[C] (mg L^{-1}), $SUVA_{254}$ (L mg^{-1} m^{-1}), $S_{275\text{-}295}$ (nm^{-1} x 10^3), and the number (n) of samples collected at each of the 30 synoptic sites during the synoptic sampling campaign. The final row represents values across all sites.

Site	Conductivity (μS cm^{-1})	Major Cations (μmol L^{-1})	$\delta^{18}O$ (‰)	Turbidity (NTU)	DOM-[C] (mg L^{-1})	$SUVA_{254}$ (L mg^{-1} m^{-1})	$S_{275\text{-}295}$ (nm^{-1} x 10^3)	*n**
BAU	72.6 ± 3.7	367 ± 38	-12.31 ± 0.34	1.55 ± 0.80	1.46 ± 0.16	3.51 ± 0.86	18.9 ± 5.4	2
BEC	30.3 ± 3.3	164 ± 47	-12.23 ± 0.35	1.29 ± 0.64	1.40 ± 0.23	3.40 ± 1.21	20.1 ± 8.6	4
BOC	45.5 ± 5.2	252 ± 81	-12.23 ± 0.18	1.42 ± 0.46	1.09 ± 0.46	3.26 ± 0.84	18.5 ± 3.1	4
CCC	57.6 ± 4.2	287 ± 34	-12.64 ± 0.28	0.80 ± 0.01	1.27 ± 0.16	2.94 ± 0.33	18.3 ± 2.2	2
CK2	42.7 ± 1.9	219 ± 38	-13.22 ± 0.28	1.14 ± 0.36	0.76 ± 0.36	3.22 ± 0.11	17.8 ± 4.3	4
CKR	36.4 ± 4.7	195 ± 18	-13.11 ± 0.34	0.89 ± 0.42	0.39 ± 0.42	3.12 ± 0.87	15.8 ± 4.2	4
COC	41.9 ± 6.5	196 ± 11	-12.90 ± 0.24	0.80 ± 0.27	0.24 ± 0.49	2.53 ± 0.44	16.9 ± 1.2	4
CPC	48.5 ± 4.5	239 ± 7	-12.74 ± 0.35	0.90 ± 0.13	0.34 ± 0.27	2.98 ± 0.75	20.1 ± 4.1	4
CRC	22.6 ± 2.7	124 ± 32	-11.76 ± 0.39	1.12 ± 0.47	2.23 ± 1.01	4.04 ± 0.48	19.0 ± 3.9	4
DAC	51.6 ± 2.7	273 ± 45	-12.87 ± 0.25	1.31 ± 0.10	0.32 ± 0.25	2.45 ± 0.39	18.4 ± 2.0	4
ERC	40.9 ± 2.1	209 ± 40	-13.26 ± 0.36	1.18 ± 0.67	0.76 ± 0.67	3.19 ± 0.54	17.5 ± 1.9	4
GGC	45.5 ± 4.8	234 ± 52	-12.02 ± 0.02	0.82 ± 0.19	1.00 ± 0.39	2.92 ± 0.18	16.8 ± 0.8	3
HAC	129.7 ± 3.5	663 ± 25	-12.68 ± 0.15	1.18 ± 0.07	0.70 ± 0.27	2.98 ± 0.16	15.8 ± 1.2	2
HEC	111.4 ± 22.8	615 ± 252	-12.17 ± 0.37	1.57 ± 0.22	0.36 ± 0.48	2.96 ± 0.45	16.8 ± 1.1	4
HTC	17.8 ± 0.8	87 ± 31	-11.13 ± 0.20	0.98 ± 0.21	1.53 ± 0.16	2.93 ± 0.18	16.0 ± 0.7	2
IDC	30.0 ± 0.7	152 ± 22	-13.34 ± 0.33	0.87 ± 0.11	0.26 ± 0.33	3.19 ± 0.52	17.7 ± 1.7	4
MOC	43.9 ± 6.1	239 ± 68	-13.04 ± 0.14	1.58 ± 1.17	0.89 ± 0.98	3.52 ± 1.12	16.2 ± 1.8	4
PC2	61.2 ± 4.3	330 ± 55	-12.91 ± 0.08	1.30 ± 0.48	0.39 ± 0.29	2.32 ± 0.28	16.3 ± 1.8	4
PEC	66.3 ± 4.1	361 ± 61	-12.86 ± 0.03	0.72 ± 0.14	0.37 ± 0.53	2.96 ± 0.73	16.3 ± 0.7	4
PV2	47.9 ± 25.7	311 ± 260	-11.60 ± 0.45	2.07 ± 0.55	1.16 ± 0.33	3.82 ± 0.29	16.1 ± 1.6	4
PVC	53.4 ± 6.6	254 ± 89	-11.76 ± 0.48	2.37 ± 1.21	1.06 ± 0.27	3.45 ± 0.77	15.5 ± 0.3	3
REC	25.5 ± 0.4	128 ± 16	-13.41 ± 0.29	1.12 ± 0.23	0.21 ± 0.35	3.03 ± 0.47	15.7 ± 1.5	4
TMT	49.9 ± 11.2	275 ± 147	-12.06 ± 0.88	0.92 ± 0.55	0.79 ± 0.57	2.73 ± 0.07	16.9 ± 1.8	4
TO2	95.0 ± 25.9	561 ± 274	-12.23 ± 0.21	1.13 ± 0.23	1.25 ± 0.33	3.21 ± 0.38	19.4 ± 2.8	4
TOC	69.2 ± 2.4	348 ± 19	-12.68 ± 0.40	1.28 ± 0.44	0.60 ± 1.40	3.27 ± 0.72	17.4 ± 4.5	3
TRC	32.8 ± 5.2	168 ± 54	-11.39 ± 0.48	0.93 ± 0.15	1.38 ± 0.23	3.21 ± 0.15	18.5 ± 0.7	3
UPR	51.3 ± 0.4	262 ± 28	-12.58 ± 0.22	0.97 ± 0.56	0.65 ± 0.29	2.61 ± 0.35	15.7 ± 0.3	4
UT1	70.6 ± 16.5	431 ± 215	-12.00 ± 0.25	0.94 ± 0.15	1.48 ± 0.47	3.57 ± 0.71	18.7 ± 2.3	4
WAC	116.4 ± 1.8	619 ± 29	-12.85 ± 0.21	1.35 ± 0.31	0.39 ± 0.45	3.51 ± 0.61	16.3 ± 0.8	4
WHC	27.2 ± 1.0	132 ± 14	-13.40 ± 0.06	1.42 ± 0.51	0.73 ± 0.14	3.42 ± 0.56	15.8 ± 0.7	3
	53.8 ± 27.5	287 ± 167	-12.51 ± 0.65	1.20 ± 0.55	0.81 ± 0.55	3.14 ± 0.71	17.3 ± 2.8	107

* At each site, only 2 samples were collected for major cations and $\delta^{18}O$, while up to 4 samples were collected for all other parameters.

Table A1-3. Descriptive statistics (mean ± standard deviation) of conductivity (µS cm^{-1}), major cations (µmol L^{-1}), $\delta^{18}O$ (‰), turbidity (NTU), DOM-[C] (mg L^{-1}), $SUVA_{254}$ (L mg^{-1} m^{-1}), $S_{275\text{-}295}$ (nm^{-1} x 10^3), and the number (n) of samples collected at each of the 10 seasonal sites during the seasonal sampling campaign. The final row represents values across all sites.

Site	Conductivity (µS cm^{-1})	Major Cations (µmol L^{-1})	$\delta^{18}O$ (‰)	Turbidity (NTU)	DOM-[C] (mg L^{-1})	$SUVA_{254}$ (L mg^{-1} m^{-1})	$S_{275\text{-}295}$ (nm^{-1} x 10^3)	*n**
BEC	26.0 ± 11.3	121 ± 43	-12.67 ± 0.48	0.86 ± 0.62	1.63 ± 0.43	3.82 ± 0.52	15.1 ± 1.0	10
BOC	36.0 ± 8.8	187 ± 67	-12.64 ± 0.42	0.85 ± 0.59	1.31 ± 0.32	3.55 ± 0.37	15.1 ± 1.0	10
CKR	36.1 ± 11.4	172 ± 36	-13.30 ± 0.42	0.63 ± 0.40	0.57 ± 0.25	3.27 ± 0.66	16.8 ± 2.0	10
GGC	46.9 ± 8.8	252 ± 55	-12.26 ± 0.20	0.55 ± 0.29	0.93 ± 0.35	3.33 ± 0.59	15.4 ± 1.2	9
PEC	61.3 ± 7.8	323 ± 52	-12.79 ± 0.22	0.70 ± 0.63	0.58 ± 0.36	3.05 ± 0.60	17.3 ± 2.6	10
PVC	64.4 ± 38.7	352 ± 223	-11.91 ± 0.38	3.38 ± 4.25	1.17 ± 0.57	3.72 ± 0.90	14.1 ± 2.4	9
TMT	44.4 ± 14.0	278 ± 99	-12.21 ± 0.57	0.64 ± 0.49	0.91 ± 0.37	2.81 ± 0.73	14.7 ± 5.5	10
TOC	61.6 ± 7.5	295 ± 66	-12.52 ± 0.45	0.75 ± 0.57	0.55 ± 0.21	2.91 ± 0.46	17.0 ± 2.8	7
UPR	53.9 ± 14.7	252 ± 20	-12.60 ± 0.31	0.63 ± 0.46	0.57 ± 0.20	3.10 ± 1.03	20.2 ± 4.2	10
UT1	56.1 ± 14.1	335 ± 133	-12.34 ± 0.35	0.78 ± 0.44	2.03 ± 0.89	3.73 ± 0.35	14.3 ± 1.0	10
	46.5 ± 20.0	255 ± 118	-12.55 ± 0.50	0.96 ± 1.54	1.02 ± 0.62	3.32 ± 0.69	16.2 ± 3.2	95

* At each site, 6–8 samples were collected for major ions and $\delta^{18}O$, while up to 10 samples were collected for all other parameters.

Table A1-4. Results of partial redundancy analysis (partial RDA) models used to identify dominant landscape attributes driving variation in stream water quality. Significant attributes ($p < 0.1$), variance partitioning, R^2, adjusted R^2 (Adj-R^2), sampling period and the number (n) of samples analyzed are shown for each model.

Partial RDA	Significant attributes	Variance partitioning	R^2	Adj-R^2	Sampling period	*n**
Model A	Clay content (F=2.96, p=0.013)	Conditioned: 38% Constrained: 1% Unconstrained: 61%	0.01	0.01	Synoptic & seasonal	152
Model B	Clay content (F=2.62, p=0.036) BGZ^4 † (F=2.37, p=0.048)	Conditioned: 26% Constrained: 4% Unconstrained: 70%	0.04	0.03	Synoptic	102
Model C	Clay content (F=2.32, p=0.041) Elevation (F=2.35, p=0.051) BGZ^4 † (F=2.05, p=0.082)	Conditioned: 47% Constrained: 5% Unconstrained: 48%	0.05	0.04	Seasonal	86

† BGZ^4 represents the mountain hemlock moist maritime windward biogeoclimatic zone.

* 36 samples overlap between the synoptic and seasonal campaigns; these samples were used in all models.

Table A1-5. Results of linear mixed effects models (LMMs) used to assess the influence of air temperature (Air Temp) and the antecedent precipitation index (API) on conductivity, major cations, $\delta^{18}O$, turbidity, DOM-[C], and DOM compositional metrics (i.e., $SUVA_{254}$, $S_{275-295}$, and PARAFAC components). Degrees of freedom (df), root mean square error (RMSE), intercept (Int), fixed effects (Air Temp and API), conditional R^2 (Con-R^2), and marginal R^2 (Mar-R^2) are indicated for each model. Random effects are shown as "R(1|Watershed)", and p-values above the 90% confidence threshold are shown in bold.

Variable	Model	df	RMSE	Int	Fixed Effects		Con-R^2	Mar-R^2
					Air Temp (ºC)	API (mm)		
Conduct-ivity	*b1*(Temp) + *b2*(API) + R(1|Watershed)	5	0.414	3.837	*b1*= -0.013 t= -0.261 p= 0.7937	*b2*= -0.005 t= -0.105 p= 0.9165	0.16	0.00
Major Cations	*b1*(Temp) + *b2*(API) + R(1|Watershed)	5	0.288	5.480	*b1*= 0.114 t= 2.996 **p< 0.001**	*b2*= -0.084 t= -2.161 **p< 0.05**	0.42	0.17
$\delta^{18}O$	*b1*(Temp) + *b2*(API) + R(1|Watershed)	5	0.308	-12.530	*b1*= -0.185 t= -4.139 **p< 0.001**	*b2*= 0.028 t= 0.628 p= 0.5301	0.60	0.15
Turbidity	*b1*(Temp) + *b2*(API) + R(1|Watershed)	5	0.743	-0.456	*b1*= -0.092 t= -0.991 p= 0.3215	*b2*= -0.114 t= -1.225 p= 0.2207	0.12	0.02
DOM-[C]	*b1*(Temp) + *b2*(API) + R(1|Watershed)	5	0.398	-0.164	*b1*= -0.092 t= -1.743 **p< 0.1**	*b2*= -0.031 t= -0.581 p= 0.5612	0.55	0.02
$SUVA_{254}$	*b1*(Temp) + *b2*(API) + R(1|Watershed)	5	0.188	1.202	*b1*= 0.055 t= 2.391 **p< 0.05**	*b2*= 0.018 t= 0.779 p= 0.4362	0.14	0.02
$S_{275-295}$	*b1*(Temp) + *b2*(API) + R(1|Watershed)	5	0.118	-4.121	*b1*= 0.009 t= 0.628 p= 0.5303	*b2*= -0.004 t= -0.252 p= 0.8014	0.23	0.01

(continued)

Table A1-5 continued.

C1	*b1*(Temp) + *b2*(API) + R(1|Watershed)	5	0.299	-0.872	*b1*= 0.027 t= 0.752 p= 0.4522	*b2*= -0.108 t= -3.037 **p< 0.01**	0.16	0.15
C2	*b1*(Temp) + *b2*(API) + R(1|Watershed)	5	0.402	-1.565	*b1*= 0.014 t= 0.278 p= 0.7808	*b2*= -0.155 t= -3.270 **p< 0.01**	0.15	0.14
C3	*b1*(Temp) + *b2*(API) + R(1|Watershed)	5	0.510	-1.677	*b1*= -0.042 t= -0.705 p= 0.4809	*b2*= 0.147 t= 2.370 **p< 0.05**	0.11	0.08
C4*	*b1*(Temp) + *b2*(API)	83	0.133	0.177	*b1*= -0.005 t= -0.303 p= 0.7624	*b2*= 0.034 t= 2.130 **p< 0.05**	--	0.04

* C4 is a simple linear model containing only fixed effects. R(1|Watershed) was removed to avoid boundary (singular) fit issues, as these typically result in type 1 errors.

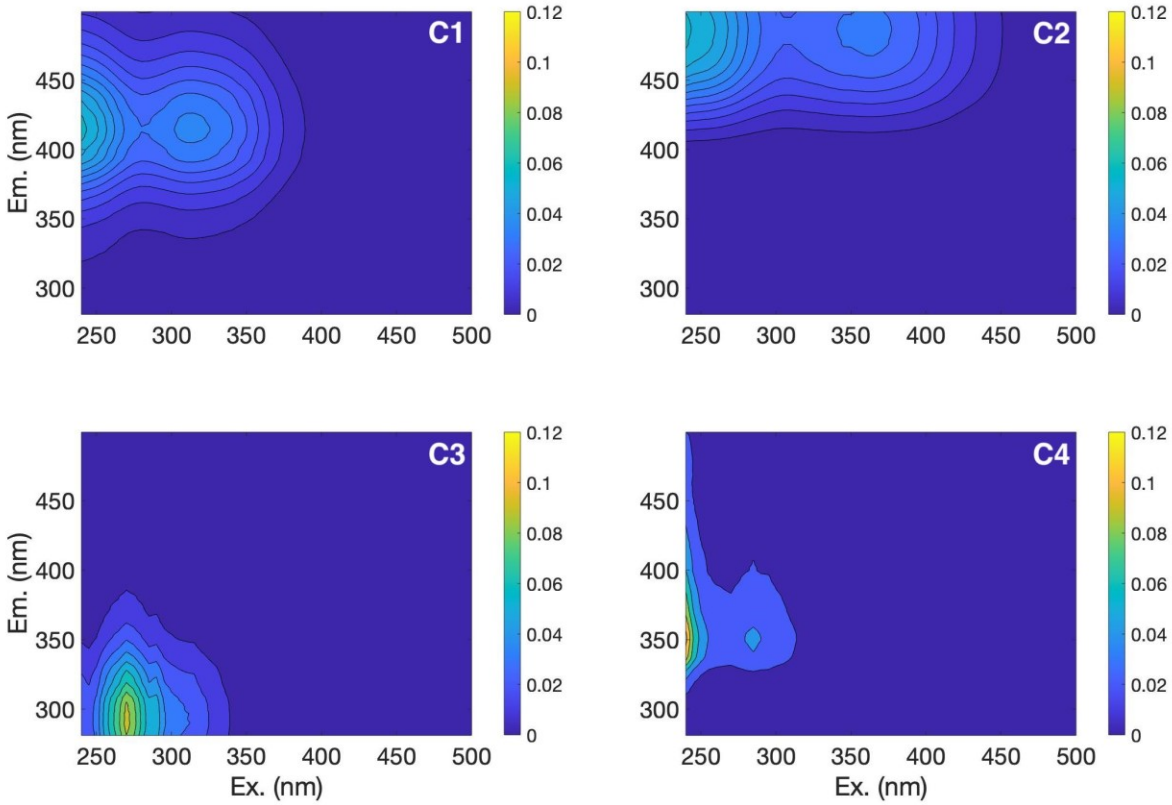

Figure A1-1. PARAFAC components of excitation-emission matrices (EEMs) measured in samples collected across Comox Lake subwatersheds. Four fluorescence peaks (C1–C4) were identified and displayed in optical space. The colour gradient indicates fluorescence intensity in Raman units.

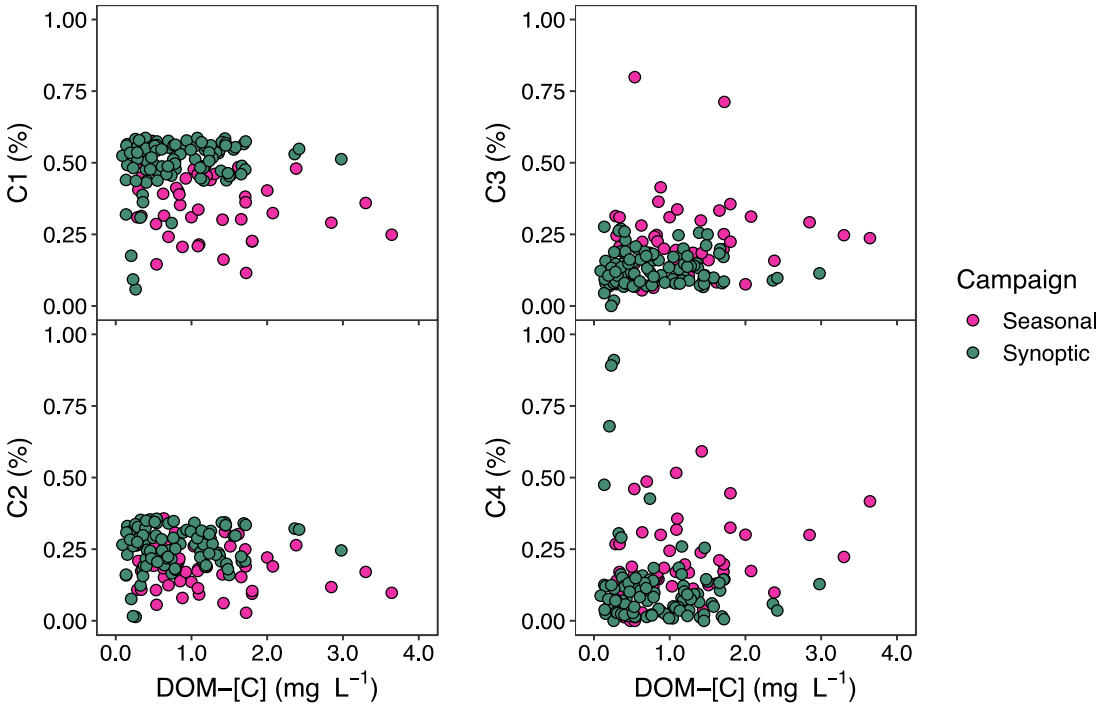

Figure A1-2. Biplots showing DOM-[C] (mg L^{-1}) versus PARAFAC components (%) for stream water collected across Comox Lake subwatersheds during the seasonal and synoptic sampling campaigns. Note that 36 samples overlap between the two campaigns; these samples were all coded as “synoptic”.

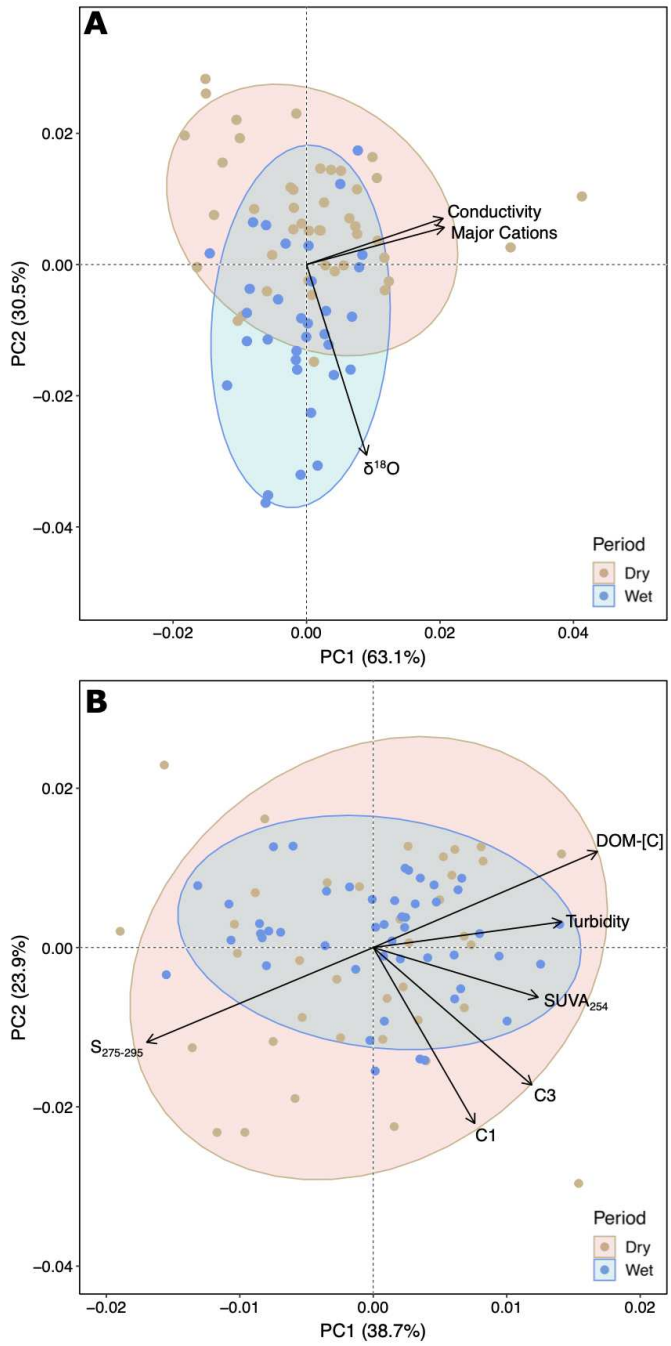

Figure A1-3. Principal components analysis (PCA) biplot of (A) conductivity, major cations, and $\delta^{18}O$, and (B) turbidity, DOM-[C], and DOM compositional indices (i.e., $S_{275\text{-}295}$, $SUVA_{254}$, C1, and C3) for samples collected across Comox Lake subwatersheds during the seasonal campaign. Ellipses show sample groupings associated with wet and dry periods and highlight seasonal variability. While wet and dry samples show separation in (A), the two seasonal periods completely overlap in (B).

Appendix 2: Supporting Information for Chapter 3.

Table A2-1. Climate (1981–2019) comparisons between Comox Lake (49°36'N, 125°10'W; elevation: 314 m) and a mountain peak on the western ridge of the watershed (49°34'N, 125°24'W; elevation: 2020 m). While mean annual temperature, total annual precipitation, and precipitation as snow differ between sites, the percentage of precipitation (shown in parentheses) occurring in each season is largely consistent. Note that different microclimates arise across the watershed due to variable topography. All data were obtained from Wang et al. (2016) (http://www.climatewna.com).

Site	Mean annual temperature (ºC)	Total annual precipitation (mm yr^{-1})	Precipitation as snow (mm)	Autumn precipitation (Oct–Dec; mm)	Winter precipitation (Jan–Mar; mm)	Spring precipitation (Apr–Jun; mm)	Summer precipitation (Jul–Sep; mm)
Lake	9.4	2193	132 (6%)	965 (44%)	833 (38%)	241 (11%)	154 (7%)
Mountain	1.7	4036	2341 (58%)	1803 (45%)	1450 (36%)	535 (13%)	248 (6%)

Table A2-2. Water quality (major cations (µmol L^{-1}), $\delta^{18}O$ (‰), turbidity (NTU), TSS (mg L^{-1}), DOM-[C] (mg L^{-1}), $SUVA_{254}$ (L mg^{-1} m^{-1}), and $S_{275-295}$ (10^{-3} nm^{-1})) and DBP-FPs (i.e., TTHM-FP (µg L^{-1}) and THAA-FP (µg L^{-1})) data for samples collected across sites during stable baseflow conditions in autumn 2019. Note that collection dates differ for water quality and DBP-FPs samples; the latter were collected up to five days earlier. ND indicates no data.

Watershed	Date	Cations (µmol L^{-1})	$\delta^{18}O$ (‰)	Turbidity (NTU)	TSS (mg L^{-1})	DOM-[C] (mg L^{-1})	$SUVA_{254}$ (L mg^{-1} m^{-1})	$S_{275-295}$ (10^{-3} nm^{-1})	Date	TTHM-FP (µg L^{-1})	THAA-FP (µg L^{-1})
LH-DS	09-06	310	-12.36	1.72	0.40	0.78	3.32	15.62	09-02	75	77
LH-DS	10-01	ND	ND	1.91	0	1.23	3.24	15.94	09-29	118	107
LH-DS	11-01	ND	ND	1.05	0	1.16	3.19	15.33	10-28	105	133
LH-DS	11-28	195	-12.10	1.02	0	1.18	3.28	15.71	11-24	126	148
LH-SS	09-04	287	-13.14	0.24	0.30	0.43	4.09	15.30	09-02	42	51
LH-SS	10-01	ND	ND	1.73	0	0.79	3.59	16.22	09-29	91	66
LH-SS	10-31	ND	ND	3.06	0.10	1.13	2.83	15.00	10-28	132	98
LH-SS	11-27	191	-12.94	1.30	0	1.19	3.58	15.59	11-24	225	302
HH-DS	09-06	495	-11.92	1.38	0.60	0.53	4.17	11.47	09-02	42	68
HH-DS	10-02	ND	ND	2.41	1.30	1.08	3.05	16.63	09-29	70	102
HH-DS	11-01	ND	ND	1.89	0.60	1.58	3.73	15.21	10-28	199	217
HH-DS	11-29	127	-11.28	2.60	0.50	1.45	4.33	15.38	11-24	167	238
HH-SS	09-03	755	-12.08	0.80	0.30	0.66	3.26	15.55	09-02	28	74
HH-SS	09-29	ND	ND	1.31	0.10	1.28	3.24	16.88	09-29	85	100
HH-SS	10-29	ND	ND	1.28	0	1.40	3.01	15.45	10-28	138	105
HH-SS	11-25	368	-12.37	1.15	0	1.67	3.33	14.98	11-24	169	208

Table A2-3. Date and time of sample collection, stream water level (cm), and water quality (major cations (μmol L^{-1}), $\delta^{18}O$ (‰), turbidity (NTU), TSS (mg L^{-1}), DOM-[C] (mg L^{-1}), $SUVA_{254}$ (L mg^{-1} m^{-1}), and $S_{275\text{-}295}$ (10^{-3} nm^{-1})) and DBP-FPs (i.e., TTHM-FP (μg L^{-1}) and THAA-FP (μg L^{-1})) data for samples collected across sites during the Dec. 5–9, 2019 storm event.

Watershed	Date	Time (PST)	Level (cm)	Cations (μmol L^{-1})	$\delta^{18}O$ (‰)	Turbidity (NTU)	TSS (mg L^{-1})	DOM-[C] (mg L^{-1})	$SUVA_{254}$ (L mg^{-1} m^{-1})	$S_{275\text{-}295}$ (10^{-3} nm^{-1})	TTHM-FP (μg L^{-1})	THAA-FP (μg L^{-1})
LH-DS	12-05	20:10	12.7	204	-12.29	2.24	0.2	0.99	3.17	15.35	57	72
LH-DS	12-06	10:10	15.1	203	-12.29	2.23	1.0	1.07	3.33	14.87	97	74
LH-DS	12-07	10:45	31.9	157	-12.13	3.01	0.6	1.99	4.26	13.67	189	215
LH-DS	12-08	0:10	28.3	151	-12.24	2.47	0.2	1.95	3.74	14.23	160	179
LH-DS	12-09	13:15	22.0	170	-12.08	1.87	0.3	1.46	3.59	14.73	122	120
LH-SS	12-06	3:00	2.4	231	-13.09	1.80	0.2	0.91	3.23	15.14	70	59
LH-SS	12-06	10:00	3.6	229	-13.00	10.55	0.4	0.88	3.73	14.89	63	85
LH-SS	12-07	9:15	12.8	173	-12.83	4.94	0.6	1.54	4.27	14.04	196	176
LH-SS	12-08	0:00	11.4	170	-12.73	1.76	0.7	1.68	3.59	14.42	138	161
LH-SS	12-08	16:00	9.4	180	-12.89	2.26	0.2	1.36	3.77	14.71	136	150
LH-SS	12-09	11:50	7.2	191	-12.89	1.86	0.2	1.20	3.64	14.73	101	123
HH-DS	12-05	20:05	45.9	147	-11.48	14.70	11.8	1.41	3.89	14.49	89	110
HH-DS	12-06	10:05	47.8	143	-11.42	12.40	7.6	1.59	3.75	14.07	78	142
HH-DS	12-07	1:05	52.4	136	-11.27	16.95	11.4	1.97	4.02	13.89	127	207
HH-DS	12-07	11:15	53.6	127	-11.18	9.82	6.2	2.52	3.63	13.44	173	258
HH-DS	12-08	9:05	54.5	131	-11.21	15.80	8.8	1.87	4.35	13.77	150	199
HH-DS	12-09	14:35	54.8	126	-11.27	12.55	6.4	1.56	4.74	14.26	160	166
HH-SS	12-05	20:00	45.7	442	-12.46	1.59	0.3	1.03	3.21	15.25	76	78
HH-SS	12-06	10:00	48.2	422	-12.34	1.53	0.3	1.34	3.71	14.10	98	130
HH-SS	12-07	1:00	53.6	350	-12.41	1.92	6.3	2.21	4.34	13.59	268	212
HH-SS	12-07	10:05	52.7	328	-12.22	2.77	3.0	2.25	3.91	13.83	187	238
HH-SS	12-08	0:00	51.6	336	-12.22	1.62	1.3	1.83	3.93	14.29	134	175
HH-SS	12-09	10:40	49.5	379	-12.40	3.40	0.8	1.43	3.62	14.69	133	121

Table A2-4. Date and time of sample collection, stream water level (cm), and water quality (turbidity (NTU), TSS (mg L^{-1}), DOM-[C] (mg L^{-1}), $SUVA_{254}$ (L mg^{-1} m^{-1}), and $S_{275-295}$ (10^{-3} nm^{-1})) data for samples collected across sites during the Nov. 16–19, 2019 storm event. ND indicates no data.

Watershed	Date	Time (PST)	Level (cm)	Turbidity (NTU)	TSS (mg L^{-1})	DOM-[C] (mg L^{-1})	$SUVA_{254}$ (L mg^{-1} m^{-1})	$S_{275-295}$ (10^{-3} nm^{-1})
LH-DS	11-16	6:50	25.7	2.06	10.8	1.96	4.04	14.49
LH-DS	11-16	13:20	29.4	1.86	0.7	2.09	3.78	14.53
LH-DS	11-16	16:35	49.9	4.91	2.9	2.48	4.52	13.62
LH-DS	11-16	19:50	51.9	4.78	1.8	3.39	5.20	13.03
LH-DS	11-16	23:05	55.9	4.91	3.2	3.22	5.35	13.03
LH-DS	11-17	2:20	65.1	14.20	23.3	3.92	5.37	12.88
LH-DS	11-17	5:35	68.7	19.25	23.0	4.04	5.35	13.00
LH-DS	11-17	8:50	64.5	8.32	6.6	ND	ND	13.22
LH-DS	11-17	12:05	59.6	5.33	4.3	3.18	5.26	13.43
LH-DS	11-17	17:05	50.8	3.42	2.0	3.27	4.16	13.76
LH-DS	11-17	22:05	46.2	2.48	0.5	2.91	4.02	13.90
LH-DS	11-18	8:05	39.8	1.94	0.3	2.36	4.00	14.51
LH-DS	11-18	18:05	36.8	1.64	0.6	2.13	4.00	14.71
LH-DS	11-18	23:05	39.5	2.17	0.3	2.24	3.93	14.52
LH-DS	11-19	9:05	36.8	1.92	0	2.18	4.06	14.59
LH-SS	11-16	10:00	12.6	3.06	0.3	1.60	4.16	14.37
LH-SS	11-16	16:30	17.0	4.55	1.8	1.88	4.28	14.00
LH-SS	11-16	19:45	24.8	4.46	3.2	2.69	4.28	13.46
LH-SS	11-16	23:00	30.4	6.17	4.2	2.66	5.61	13.19
LH-SS	11-17	2:15	40.8	17.95	15.3	3.30	5.68	13.08
LH-SS	11-17	5:30	53.8	28.55	20.9	4.21	5.30	13.08
LH-SS	11-17	8:45	51.7	10.08	10.0	3.47	5.62	13.25
LH-SS	11-17	12:00	44.8	6.45	5.0	3.10	5.34	13.33
LH-SS	11-17	17:00	35.8	2.86	2.4	3.14	4.31	13.70
LH-SS	11-18	3:00	28.5	2.34	1.0	2.31	4.31	14.00
LH-SS	11-18	13:00	24.3	1.66	0.8	2.05	4.06	14.37
LH-SS	11-18	23:00	23.5	2.62	0.2	1.95	4.11	14.35

(continued)

Table A2-4 continued.

LH-SS	11-19	9:00	21.6	1.05	0.7	1.92	3.87	14.46
HH-DS	11-16	10:00	54.8	7.04	4.4	2.53	3.58	14.22
HH-DS	11-16	16:30	60.7	22.40	15.0	2.61	4.05	14.03
HH-DS	11-16	19:45	64.6	19.55	14.6	2.94	4.19	13.44
HH-DS	11-16	23:00	67.2	20.30	16.8	3.15	3.97	13.62
HH-DS	11-17	2:15	74.1	41.80	35.3	3.02	5.02	13.25
HH-DS	11-17	5:30	82.4	82.65	105.7	3.56	5.60	12.64
HH-DS	11-17	8:45	87.1	82.70	95.3	2.96	6.08	12.82
HH-DS	11-17	12:00	88.8	65.55	120.3	3.29	4.12	13.77
HH-DS	11-17	17:00	86.9	25.80	56.4	2.90	4.22	13.80
HH-DS	11-17	22:00	82.4	22.25	44.6	3.06	4.02	13.71
HH-DS	11-18	8:00	77.5	16.30	47.6	2.85	4.08	13.82
HH-DS	11-18	18:00	73.2	10.57	16.5	2.74	4.16	13.92
HH-DS	11-19	4:00	71.8	7.82	10.4	2.64	4.15	14.15
HH-DS	11-19	14:00	69.1	7.74	9.4	2.40	4.41	14.28
HH-SS	11-16	6:45	51.9	1.58	0.3	1.98	4.29	14.18
HH-SS	11-16	13:15	53.4	1.70	0.7	2.26	3.88	14.10
HH-SS	11-16	16:30	58.3	4.87	0.7	3.43	3.88	13.27
HH-SS	11-16	19:45	61.0	5.60	1.6	2.85	5.10	13.24
HH-SS	11-16	23:00	64.2	2.65	3.2	3.26	4.97	13.20
HH-SS	11-17	2:15	76.7	11.85	19.4	4.37	4.94	13.03
HH-SS	11-17	5:30	80.0	6.71	3.8	4.62	4.93	13.09
HH-SS	11-17	8:45	73.4	4.52	1.6	3.74	5.30	13.27
HH-SS	11-17	12:00	68.2	2.87	0.7	3.54	4.82	13.46
HH-SS	11-17	17:00	63.3	3.97	0.5	2.87	4.99	13.67
HH-SS	11-18	3:00	58.7	3.78	0.1	2.96	3.75	14.10
HH-SS	11-18	13:00	56.6	1.38	0.2	2.09	4.49	14.40
HH-SS	11-18	23:00	56.2	1.82	0.2	2.37	3.77	14.41
HH-SS	11-19	9:00	54.9	2.61	0	2.19	3.96	14.50

Table A2-5. Results of Mann–Whitney U tests used to investigate water quality and DBP-FPs differences between baseflow and stormflow at each subwatershed site. U-values represent the sum of ranks for baseflow samples. P-values at the 5% significance level are shown in bold, while p-values at the 10% significance level are italicized.

Variable	Site			
	LH-SS	LH-DS	HH-SS	HH-DS
Turbidity	U= 36 p= 0.1925	U= 17 **p= 0.0076**	U= 3 **p< 0.001**	U= 9 **p< 0.001**
TSS	U= 43 p= 0.3846	U= 56 p= 0.8488	U= 70 p= 0.5446	U= 8 **p< 0.001**
DOM-[C]	U= 3 **p< 0.001**	U= 2 **p< 0.001**	U= 3 **p< 0.001**	U= 7 **p< 0.001**
$SUVA_{254}$	U= 41 p= 0.3411	U= 22 **p= 0.0225**	U= 30 *p= 0.0646*	U= 50 p= 0.5761
$S_{275-295}$	U= 107 **p< 0.001**	U= 110 **p< 0.001**	U= 108 **p= 0.0011**	U= 97 **p= 0.0188**
TTHM-FP	U= 5 p= 0.1714	U= 1 **p= 0.0476**	U= 4 p= 0.1143	U= 7 p= 0.3524
THAA-FP	U= 4 p= 0.1143	U= 2 *p= 0.0952*	U= 3 *p= 0.0667*	U= 6 p= 0.2571

Table A2-6. Results of multiple linear regression (MLR) models used to assess the influence of water quality (i.e., DOM-[C] (mg L^{-1}), $SUVA_{254}$ (L mg^{-1} m^{-1}), and $S_{275-295}$ (10^{-3} nm^{-1})) on DBP-FPs (i.e., TTHM-FP (µg L^{-1}) and THAA-FP (µg L^{-1})). Degrees of freedom (df), root mean square error (RMSE), intercept, water quality indicator coefficient outputs, the coefficient of multiple determination (Mult-R^2), and the adjusted coefficient of multiple determination (Adj-R^2) are indicated for each model. P-values at the 5% significance level are shown in bold, while p-values at the 10% significance level are italicized. All models were statistically significant ($p < 0.01$). Note that baseflow and stormflow samples were incorporated into all models.

DBP-FPs	Model	df	RMSE	Intercept	Coefficients			Mult-R^2	Adj-R^2
					DOM-[C] (mg L^{-1})	$SUVA_{254}$ (L mg^{-1} m^{-1})	$S_{275-295}$ (10^{-3} nm^{-1})		
TTHM-FP	*b1*(DOM-[C]) + *b2*($SUVA_{254}$) + *b3*($S_{275-295}$)	35	0.287	4.710	*b1*= 0.405 t= 7.433 **p< 0.001**	*b2*= 0.085 t= 1.345 p= 0.187	*b3*= 0.133 t= 2.087 **p= 0.044**	0.654	0.624
THAA-FP	*b1*(DOM-[C]) + *b2*($SUVA_{254}$) + *b3*($S_{275-295}$)	35	0.236	4.856	*b1*= 0.380 t= 8.470 **p< 0.001**	*b2*= 0.105 t= 2.024 *p= 0.051*	*b3*= 0.082 t= 1.570 p= 0.125	0.734	0.711

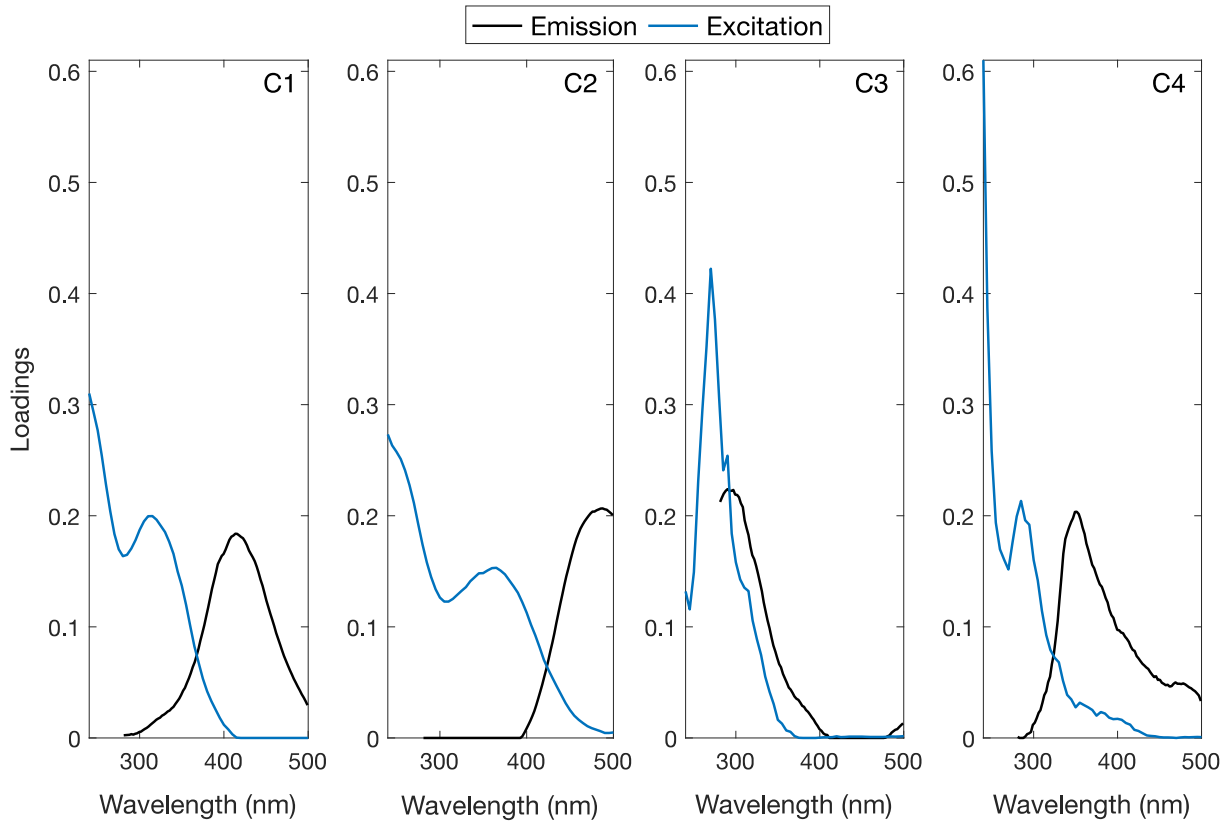

Figure A2-1. Spectral comparison of excitation and emission loadings for each PARAFAC component. Four components (C1–C4) were identified from excitation-emission matrices (EEMs) in samples collected across Comox Lake subwatersheds.

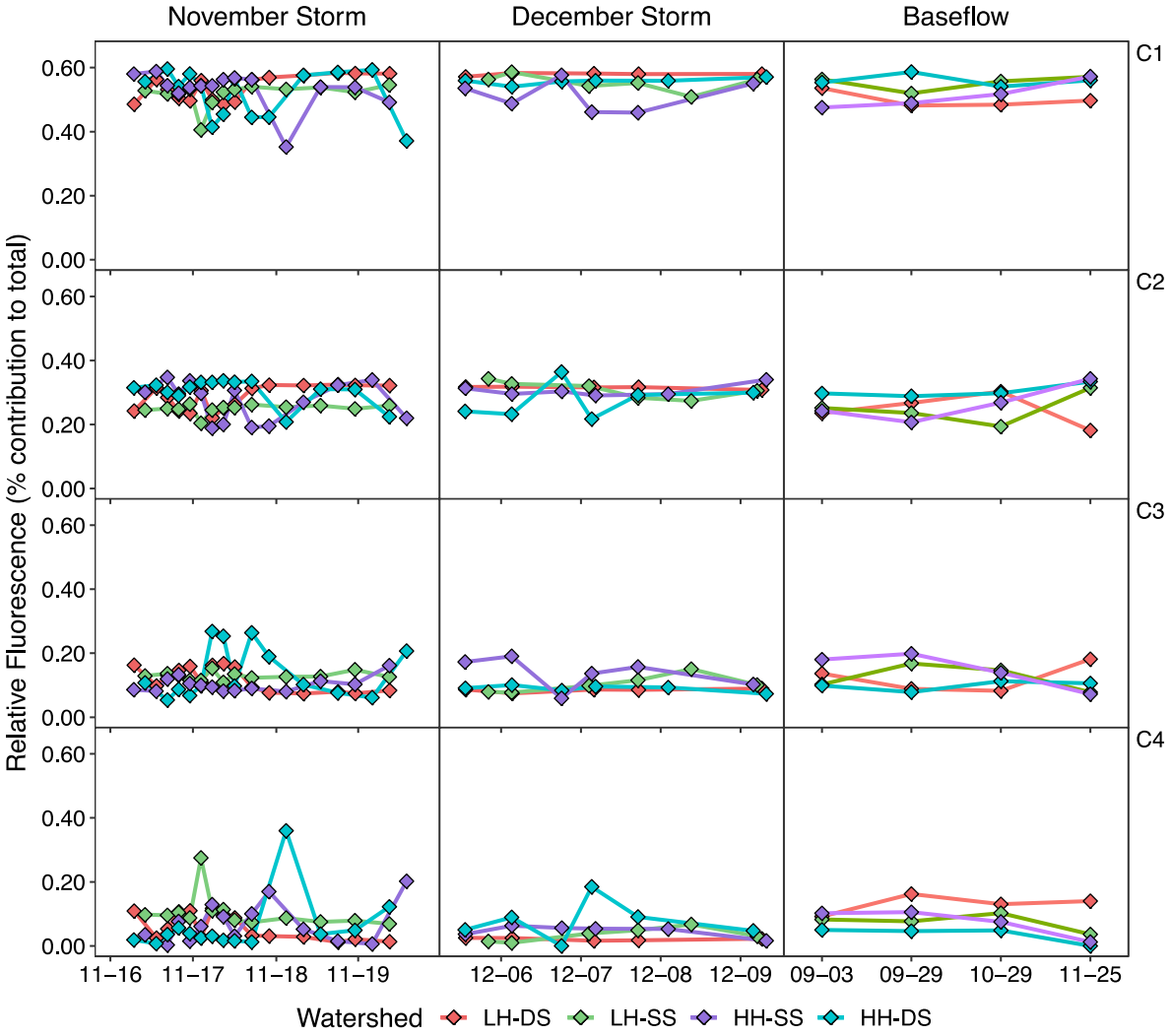

Figure A2-2. Relative fluorescence (percent contribution) of the four DOM components (C1–C4) determined by parallel factor (PARAFAC) analysis for storm and baseflow samples. Minimal changes in components occurred across the four subwatershed sites during baseflow and the Nov. 16–19 and Dec. 5–9, 2019 storm events.

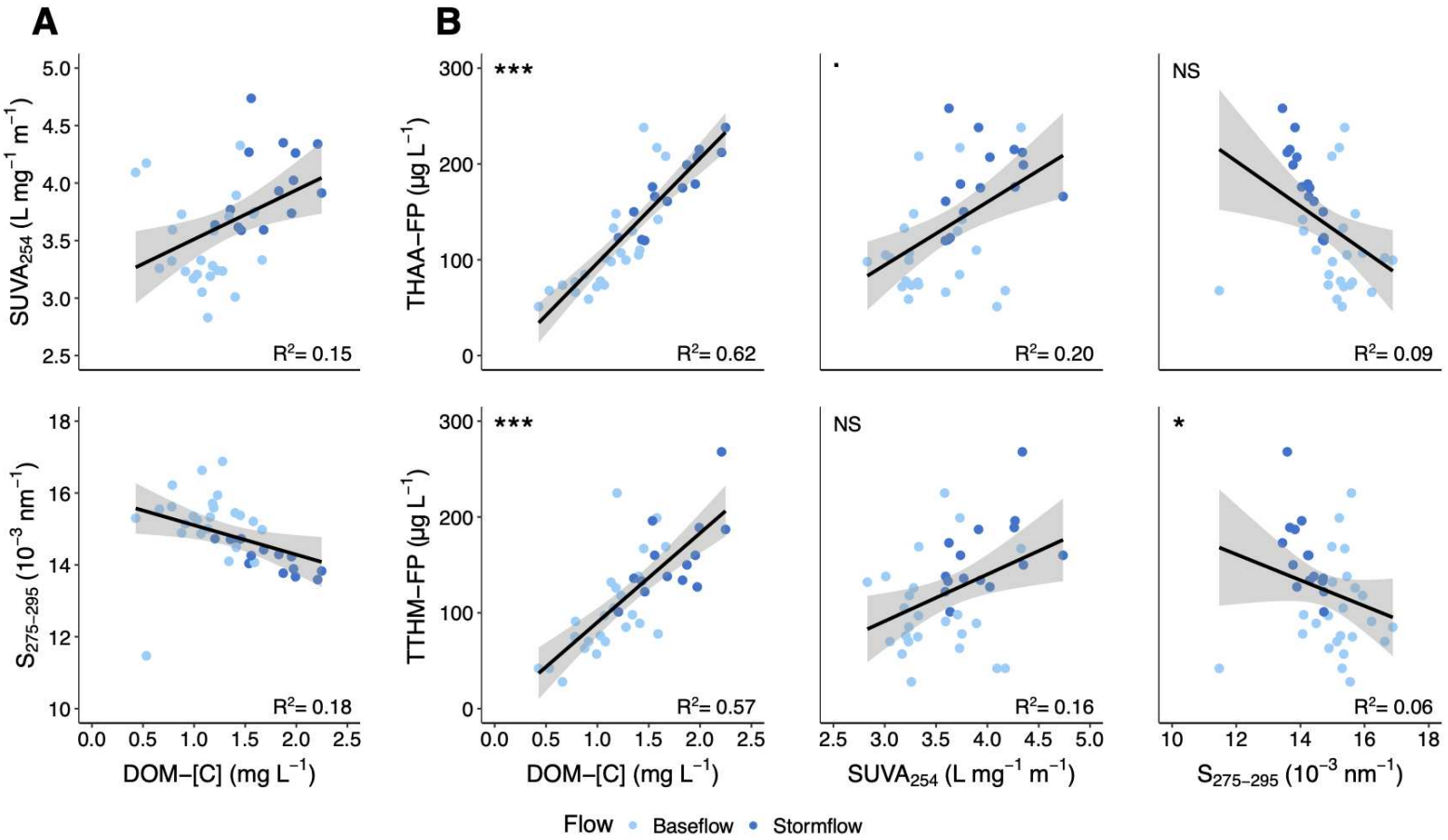

Figure A2-3. Biplots showing (A) $SUVA_{254}$ (L mg^{-1} m^{-1}) and $S_{275-295}$ (10^{-3} nm^{-1}) versus DOM-[C] (mg L^{-1}), and (B) TTHM-FP (µg L^{-1}) and THAA-FP (µg L^{-1}) versus DOM-[C] (mg L^{-1}), $SUVA_{254}$ (L mg^{-1} m^{-1}), and $S_{275-295}$ (10^{-3} nm^{-1}) for stream water collected across subwatershed sites during stormflow and baseflow conditions. Individual THM and HAA species FPs were summed to yield total FPs. Baseflow samples include those collected monthly during stable conditions and the first two samples of the Dec. 5–9 event, while stormflow samples include those remaining from the event. Significance levels are indicated by stars: <0.001 = ***, <0.01 = **, <0.05 = *, <0.1 = ., NS = not significant. Detailed results for (B) can be found in Table A2-6.